DYNAMICS AND REMODELING OF THE ENTEROCYTE BRUSH BORDER DURING BACTERIAL INFECTION: IMPLICATIONS FOR INTESTINAL HOST DEFENSE

By

David A. Shifrin, Jr.

Dissertation

Submitted to the Faculty of the

Graduate School of Vanderbilt University

In partial fulfillment of the requirements

For the degree of

DOCTOR OF PHILOSOPHY

In

Cell and Developmental Biology

August, 2013

Nashville, Tennessee

Professor Robert J. Coffey

Professor Ryoma Ohi

Professor David W. Piston

Professor Matthew J. Tyska

ACKNOWLEDGEMENTS

I first want to thank my mentor, Matt Tyska, for his guidance and patience during the last several years. His infectious enthusiasm for science was apparent from our first conversation, and despite the inevitable ups and downs of basic research, this trait has always been a constant. He has taught me to think carefully about the questions that should be asked, and encouraged me to never be constrained by the current paradigm. With ruthless but careful editing, he has taught me much about how to write well. Matt has constantly pushed me to learn and to get better, something that applied to work at the bench, sitting in front of a microscope, and learning to ride a bike. Many thanks for accepting me into the lab as a graduate student and for providing me with tools invaluable for my future.

The members of the Tyska lab, past and present, have been great friends and outstanding colleagues. I am very grateful for the assistance and insight they have provided. Everyone in the lab is committed to doing the best science possible, and the quality of work they produce has motivated and challenged me to do the same. Beyond the science, I am especially thankful for the friendships that have developed. Coming in every day and dealing with the challenges of bench work is a lot of fun when it's done with good friends.

Many thanks to my committee members, Drs. Bob Coffey, Dave Piston, Puck Ohi, and Lance Prince. Their advice and support has been critical during graduate school, not only for the scientific training, but also for guidance in looking forward to the next step. Members of the Epithelial Biology Center, Microtubules and Motors Club, and CDB staff and administration have provided valuable time, resources, training and

feedback. I also want to acknowledge members of Lynn Matrisian's lab, who trained me during my first two years at the bench as a technician and encouraged me to pursue graduate school.

I have been blessed with an amazing family, without whom graduate school, or much of anything else, would not have happened. My parents have always pushed me to finish the job and to do it well, and though a slow learner I've tried to apply that lesson to the lab. Thanks to my siblings and wonderful in-laws for their support and understanding. Finally, and most importantly, I cannot fully express the extent of my gratitude to and love for my wife Megan. Her partnership in this little adventure has meant everything.

TABLE OF CONTENTS

Page

LIST OF FIGURES

LIST OF TABLES

Table Page

LIST OF ABBREVIATIONS

A13	Annexin-13
A/E	Attaching/effacing
AMP	Anti-microbial peptides
AP	Alkaline phosphatase
BB	Brush border
BFP	Bundle forming pilus
CFU	Colony forming unit
DN	Dominant negative
ECV	Extracellular vesicle
EPEC	Enteropathogenic *E. coli*
ESCRT	Edosomal sorting complex required for transport
FAVS	Fluorescence-activated vesicle sorting
GPI	Glycosylphosphatidylinositol
IAP	Intestinal alkaline phosphatase
IEL	Intraepithelial lymphocytes
KD	Knockdown
KO	Knockout
LEE	Locus of enterocyte effacement
LPS	Lipopolysaccharide
LSCM	Laser scanning confocal microscopy
LV	Lumenal vesicle
MLP	Microvillus-like process

MLPCDH	Mucin-like protocadherin
MVB	Multi-vesicular body
Myo1a	Myosin-1a
Myo1d	Myosin-1d
Myo2	Myosin-2
NGL	NF-kB-GFP-Luciferase
OMV	Outer membrane vesicle
PAS	Periodic acid-Schiff
PCDH24	Protocadherin 24
PLAP	Placental alkaline phosphatase
SEM	Scanning electron microscopy
SFB	Segmented filamentous bacteria
SI	Sucrase isomaltase
T3SS	Type III secretion system
TEM	Transmission electron microscopy
TH1	Tail homology-1
TLR	Toll-like receptor
TNAP	Tissue non-specific alkaline phosphatase
WT	Wild type

CHAPTER I

INTRODUCTION

Intestinal epithelium structure

The mammalian small intestine is a polarized organ with an inner layer facing the lumen and its contents, and an outer layer anchored by mesentery in the abdominal cavity. Because the lumen of the digestive tract is essentially open to the external environment, intestinal tissue must function not only as an absorptive surface but also as a defense against external insults, blocking translocation of harmful substances into circulation or the abdominal cavity. Structurally, the small intestine is comprised of four primary layers, with the mucosa at the interface between lumen and tissue, followed by the submucosa, muscularis propria, and the serosa. The mucosa is subdivided into an epithelium, lamina propria, and muscularis mucosa (Fig. 1-1A) (Rao and Wang, 2010). Folds in the epithelium form crypts and villi, which provide increased surface area for absorption. Stem cells reside at the base of the crypt and divide asymmetrically, maintaining the epithelium through daughter cell differentiation into absorptive enterocytes, mucus-secreting goblet cells, hormone-secreting enteroendocrine cells, and anti-microbial paneth cells (Fig. 1-1B) (Barker *et al.*, 2008).

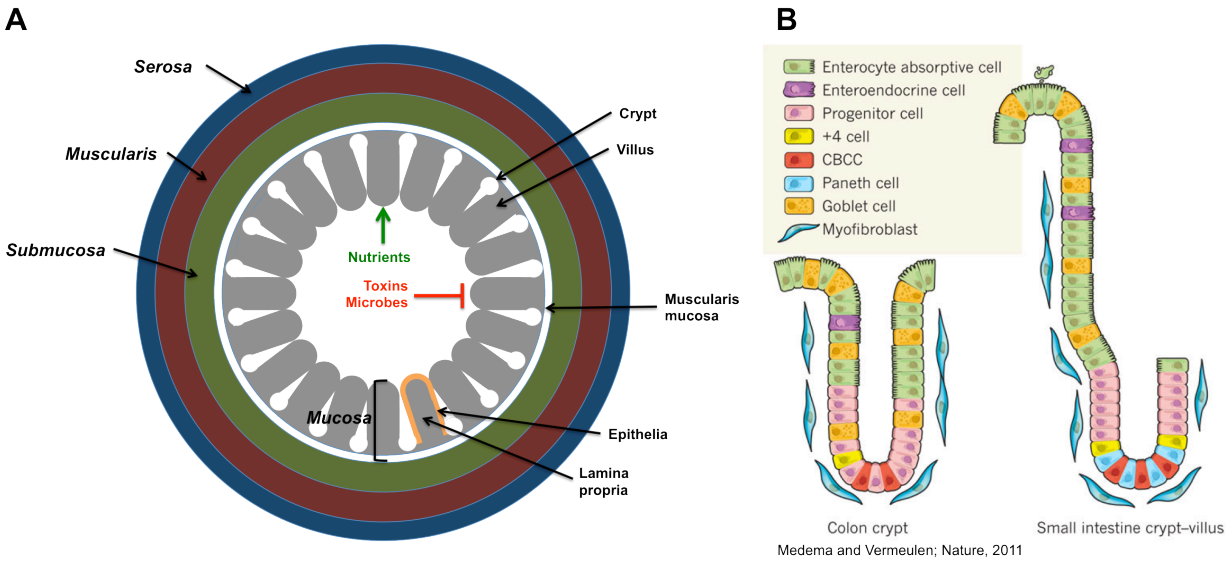

Figure 1-1: Intestinal architecture and epithelial cell types

Immune functions of the intestinal epithelial layer

Because the intestinal epithelium is in direct contact with the lumenal environment, it forms a barrier that allows for selective absorption of nutrients while preventing entry of pathogens and toxins into systemic circulation. Most immune cells, such as dendritic cells, are primarily found in the lamina propria. Dendritic cells extend protrusions through the epithelium to reach the lumenal surface and sample bacteria (Rescigno *et al.*, 2001). They also form tight junctions to maintain continuity with surrounding enterocytes and prevent unwanted bacterial translocation to the underlying tissue (Rescigno *et al.*, 2001). Intraepithelial lymphocytes (IEL) are integrated with the epithelium. These cells include specialized T-cells, and mediate downstream immune responses via cytokine secretion and indirect activation of B-Cells (Cheroutre, 2005).

Non-immune cells within the epithelium, some of which are significantly more abundant than IELs, also play a notable role in host defense. Mucus produced by goblet

cells provides a coating across the epithelium to help inhibit bacterial interaction with the epithelial surface (McGuckin *et al.*, 2011). Under normal conditions microbes are almost entirely excluded from reaching the inner of two mucus layers, providing spatial separation between potential pathogens and host tissue (Johansson *et al.*, 2008; Johansson *et al.*, 2011). Additionally, anti-microbial peptides (AMP) secreted by Paneth cells in the crypts help maintain crypt sterility (Ouellette, 1999). AMPs are also integrated into the mucus layer along the length of the villus, where they prevent enteric infection and regulate the gut bacterial population (Meyer-Hoffert *et al.*, 2008; Salzman *et al.*, 2010). Enterocytes also play several roles in immunity, discussed further below.

Enterocytes and the brush border in host defense

Enterocytes are the majority cell type of the intestinal epithelium and play a significant role in immune function. The apical and basolateral surfaces of these polarized cells are separated by tight junctions, which, along with adherens junctions and desmosomes, link each enterocyte to its neighbor near the apex of the cell. Junctions are comprised of four groups of proteins (occludin, claudins, junction-adhesion molecules, and Coxsackievirus and Adenovirus Receptor proteins), and are critical for maintaining the integrity of the intestinal epithelial layer. Any disruptions in the tight junctions can lead to aberrant water flux or translocation of toxic molecules or organisms (Guttman and Finlay, 2009). Such disruptions frequently occur during intestinal infection; pathogen-induced separation of several junctional proteins from the lateral cell membrane leads to fluid efflux and severe diarrhea (Guttman and Finlay, 2009). Injection of certain bacterial effectors leads to altered dynamics of junctional

actin, which allows for redistribution of tight junction proteins to the sites of bacterial attachment on the apical surface (Peralta-Ramirez *et al.*, 2008).

Apical to tight junctions of the enterocytes is an array of actin-based protrusions called microvilli (Mooseker, 1985). Tightly packed in a hexagonal array called the brush border, these organelles are enriched in enzymes, transporters, and host defense molecules. Importantly, they significantly increase available absorptive surface area (Louvard *et al.*, 1992). Each microvillus is comprised of 20-30 parallel actin filaments supporting the overlying plasma membrane (Mooseker and Tilney, 1975). The core microvillar actin bundles are anchored in the terminal web, a sub-apical meshwork of keratin, spectrin, myosin-2, and plastin (Bretscher and Weber, 1978; Grimm-Gunter *et al.*, 2009). Heteromeric complexes of protocadherin-24 (PCDH24) and mucin-like protocadherin (MLPCDH) link the distal tips of microvilli; this interaction is critical for normal development of a brush border and for regulating microvillar packing and length (Fig. 1-2) (Crawley *et al*, unpublished data).

Within the microvillus, core actin filaments are bundled by villin, fimbrin, and, to a lesser extent, espin (Fig. 1-2) (Bretscher and Weber, 1979, 1980; Bretscher, 1981; Bartles *et al.*, 1998). Espin cross-linking induces significant elongation of microvillar actin filaments by slightly altering the rate of plus-end polymerization (Loomis *et al.*, 2003). In cell culture models, espin-stabilized actin can be leveraged for microscopy studies, providing improved visualization by elongating microvilli (Loomis *et al.*, 2003). Villin both severs and bundles actin, in a Ca^{2+} and phospho-dependent manner, making it an important molecule for remodeling of the brush border following damage to the enterocyte (Ferrary *et al.*, 1999; Khurana and George, 2008). Fimbrin, also known as

plastin-1, cross-links microvillar actin bundles within the microvillus and anchors them to the terminal web (Bretscher and Weber, 1980; Grimm-Gunter *et al.*, 2009).

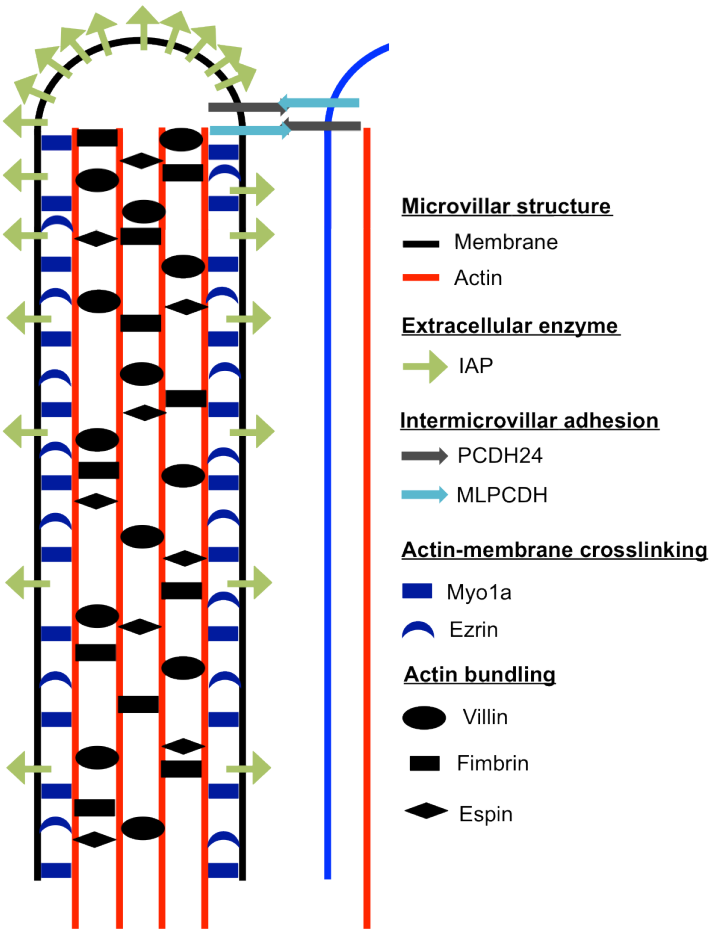

Figure 1-2: Protein composition of the enterocyte microvillus
*Not all components shown

Linking the parallel actin bundles to the overlying plasma membrane are lateral bridges comprised of the motor protein myosin-1a (myo1a) and the actin-bundling protein ezrin (Fig. 1-2) (Mooseker and Tilney, 1975; Matsudaira and Burgess, 1979; Sato *et al.*, 1992; Tyska *et al.*, 2005). myo1a is comprised of an N-terminal motor domain that binds actin and hydrolyzes ATP, an alpha helical, force-transducing neck

domain that is rigidified by binding calmodulin molecules in a Ca^{2+}-dependent manner, and a C-terminal tail domain that binds plasma membrane (Mooseker and Cheney, 1995). Studies on other class-I myosins has demonstrated load sensitivity; duty ratio - the proportion of the total ATP cycle a motor spends bound to actin - increases when the molecule is under mechanical strain (Laakso *et al.*, 2008). It is possible that myo1a could exhibit similar force sensitivity, which would increase the time each molecule spends as a rigid cross-linker in the microvillus. Additionally, by acting in ensemble myo1a molecules effectively increase the population duty ratio (De La Cruz and Ostap, 2004). Work in our lab has clarified the importance of myo1a for maintaining microvillar structure. In myo1a knockout (KO) brush borders membrane tension decreases significantly, a result which explains herniations observed *in vivo* (Tyska *et al.*, 2005; Nambiar *et al.*, 2009). Other characteristics and functions of myo1a are discussed below.

Enterocytes also express several transmembrane mucins that localize to microvilli and form a glycocalyx that aids in defense against pathogens (McGuckin *et al.*, 2011). Additionally, low levels of toll-like receptors (TLRs) on the apical membrane allow enterocytes to activate immune signaling pathways. TLRs constitute one of the primary receptor families used by host cells to respond to environmental and pathogen-derived toxins. Eleven mammalian TLRs have been identified, and at least six respond to bacterial molecules (Akira and Takeda, 2004). In particular, TLR-4 acts as a receptor for lipopolysaccharide (LPS), a toxic compound produced by Gram-negative bacteria (Poltorak *et al.*, 1998; Tapping *et al.*, 2000). LPS binds TLR-4 and its co-receptor MD-2. Upon LPS binding, TLR-4 then binds the intracellular adaptor protein MyD88. In the

absence of TLR-4 activation, the NF-kB transcriptional complex is sequestered in the cytoplasm by the inhibitor of nuclear factor-kB (IkB) complex. Upon initiation of LPS-induced signaling, a series steps involving the recruitment, phosphorylation/activation, and degradation of several intermediate proteins and complexes lead to the phosphorylation of IkB and subsequent targeting for its ubiquitylation and degradation. NF-kB is then released, translocates to the nucleus, and transcribes its target genes (Fig. 1-3) (Akira and Takeda, 2004; Ghosh and Hayden, 2008). In inflamed tissues, NF-kB activation is correlated with increased levels of interleukins and tumor necrosis factor (TNF) and recruitment of immune cells (Li and Verma, 2002; Akira and Takeda, 2004; Wullaert *et al.*, 2011).

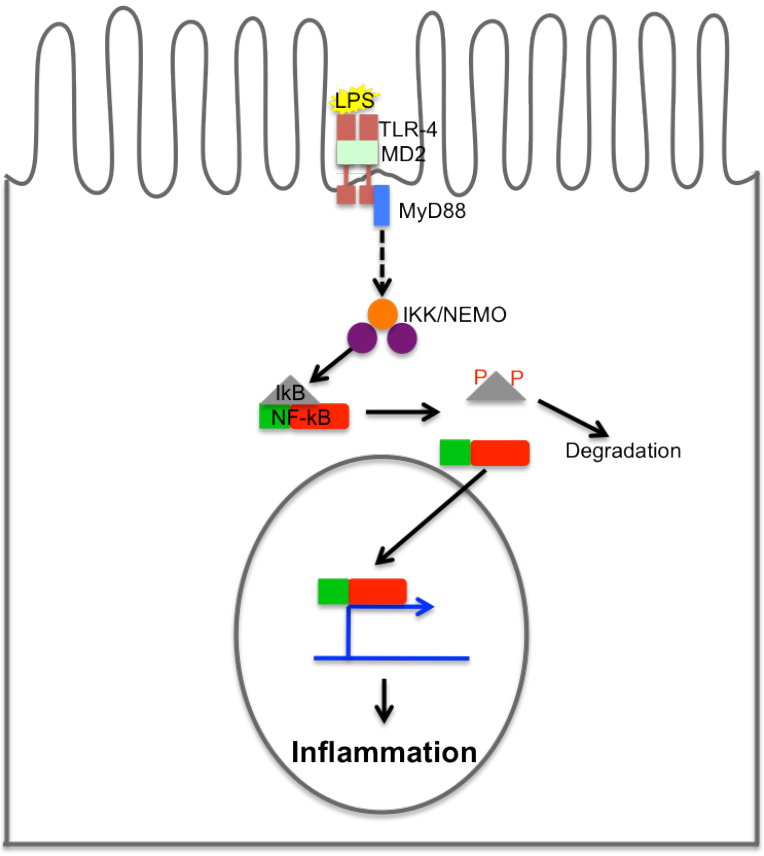

Figure 1-3: TLR-4 mediated activation of the NF-kB inflammatory pathway

Activation of NF-kB has the potential to become a positive feedback loop: cytokines controlled by NF-kB are expressed and released, leading to further TLR-mediated NF-kB signaling. Therefore, the pathways involved must be tightly regulated to prevent unchecked inflammatory responses, such as the infamous “cytokine storm” associated with some viral and bacterial infections (Tisoncik *et al.*, 2012). Investigators have found that under homeostasis, intestinal epithelial cells in culture express very low levels of TLR-4 on their apical surfaces, which likely prevents excessive inflammatory signaling (Abreu *et al.*, 2001).

Microvillar vesicle shedding

Myo1a is not simply a static linker in microvilli. In the absence of nucleotide, the motor exhibits a high affinity for actin, whereas ATP binding releases the motor (Howard, 2001). In a two-step process, hydrolysis of ATP and release of P_i, then release of ADP, conformational changes occur that displaces the motor relative to the rest of the molecule (Veigel *et al.*, 1999; Howard, 2001). In isolated brush borders, addition of 1mM ATP induced the rapid translocation of membrane towards the tips of microvilli, i.e. towards the plus ends of the parallel actin bundles. (McConnell and Tyska, 2007). In contrast, brush borders isolated from myo1a KO mice do not exhibit membrane translocation, demonstrating that this motor is capable of exerting force on microvillar membrane (McConnell and Tyska, 2007).

As microvillar membrane reaches the distal ends of the underlying actin bundles, it is released as small vesicles into solution (McConnell and Tyska, 2007). Remarkably,

these vesicles can be isolated from small intestine lumenal contents *in vivo*; the number of vesicles found in myo1a KO mice is greatly reduced and the variability in size increases (McConnell *et al.*, 2009). The finding that lumenal vesicle (LV) shedding is dependent on myo1a motor activity suggests these organelles are released in a controlled manner, indicating a regulated physiological function for LVs. Further proteomic and biochemical analysis revealed that LVs are enriched in a subset of microvillar proteins, including intestinal alkaline phosphatase (IAP) and the membrane binding protein annexin-13 (A13), this specific enrichment is lost in myo1a KO LVs (McConnell *et al.*, 2009). Although the exact mechanism of LV shedding remains unclear, it is likely due in large part to translocation of membrane by myo1a. A sub-population of the motor protein may also help to segregate microvillar proteins. FRAP studies in microvilli showed that ~20% of the intra-microvillar myo1a population has a slow rate of turnover, approximately the same percentage as that bound to microvillar lipid rafts containing the digestive enzyme sucrase isomaltase (SI) (Tyska and Mooseker, 2002, 2004). This population of myo1a may immobilize SI-containing rafts, allowing for enrichment of IAP at distal tips.

LV shedding is regulated by myo1a, but is also likely supported by the composition and curvature of microvillar membrane. Microvillar plasma membrane is unique in that it consists of largely stable lipid rafts, sometimes referred to as “super rafts” (Danielsen and Hansen, 2003). Distinct raft populations exist at the base and tip of a microvillus, but in general the high concentrations of cholesterol and sphingolipids may promote and help stabilize the extreme membrane curvature found at both ends of the protrusion (Danielsen and Hansen, 2003). Furthermore, maintaining this high

curvature is conducive for membrane scission events in the form of budding (from the tips) or endocytosis (at the base). Lipid microdomains recruit GPI-anchored proteins including IAP, as well as some transmembrane proteins such as SI (Tyska and Mooseker, 2004). Cholesterol concentration increases along the length of a microvillus, which likely promotes a similar gradient of raft associated proteins (Fig. 1-4). Further sorting at the distal tips of microvilli must be involved in producing the unique protein composition of LVs, where IAP and A13 are highly enriched, and myo1a and SI are excluded. A population of myo1a associates with SI-containing lipid rafts along the microvillar axis (Tyska and Mooseker, 2004); differences between the membrane lipid composition along the axis and the highly curved microvillar tip might exclude SI and the motor while providing an environment conducive to GPI-anchored IAP.

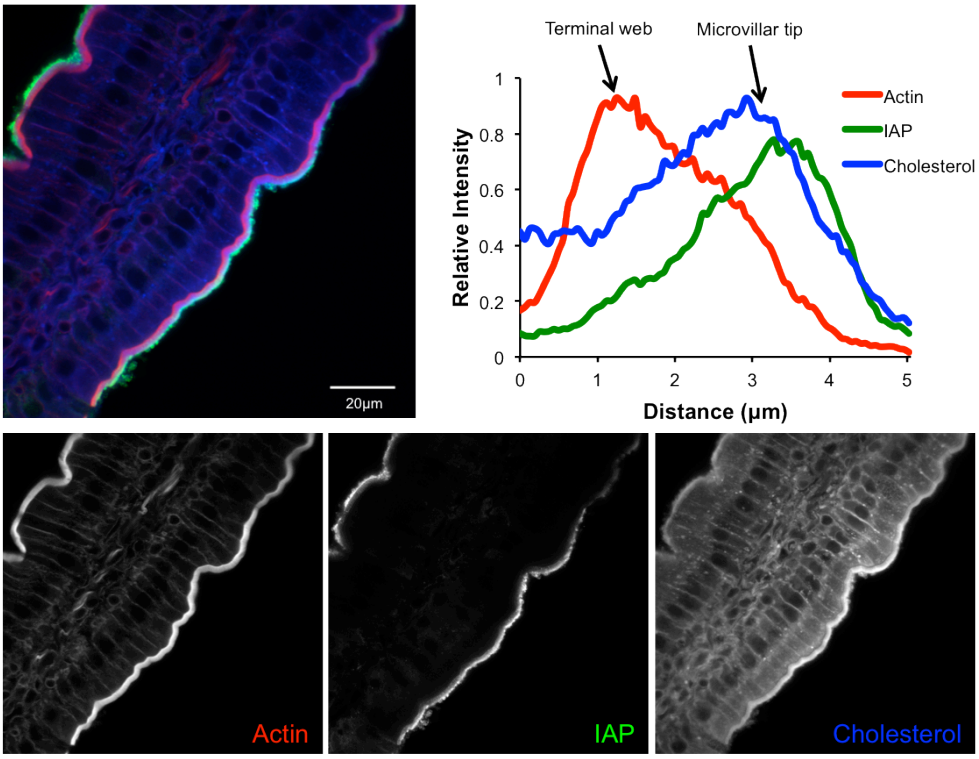

Figure 1-4: Gradient of lipid raft-associated molecules along the microvillar axis

Immunofluorescence of mouse small intestinal tissue shows that IAP is enriched at the distal tips of microvilli. This is likely regulated by cholesterol, which is a key component of lipid rafts and forms a gradient along the microvillar axis. The chart shows the gradients of IAP and cholesterol signal, increasing from just above the terminal web to pre-LV buds distal to the ends of the actin bundles.

Intestinal Alkaline Phosphatase

IAP is one of four alkaline phosphatase isozymes expressed in humans, along with liver/bone/kidney, or tissue non-specific AP (TNAP), placental AP (PLAP), and a minor form called placental-like AP (McKenna *et al.*, 1979; Harris, 1990). Collectively, these enzymes dephosphorylate a wide range of substrates, with known function in processes ranging from bone formation, to fat absorption, to detoxification of bacterial products. APs function as dimers (Hoylaerts *et al.*, 1997), each monomer requiring two Zn^{2+} and one Mg^{2+} ion (Millan, 2006). A glycosylphosphatidylinositol (GPI) anchor tethers the enzymatic ectodomain to the membrane and helps localize IAP to lipid rafts, a feature which likely leads to enrichment at the distal tips of microvilli (Lowe *et al.*, 1990; McConnell *et al.*, 2009).

Biochemical studies revealed that purified IAP, as its name suggests, functions most effectively at high pH in experimental conditions. *In vitro* analysis of both purified soluble enzyme and IAP bound to isolated membrane vesicles demonstrated a maximal activity above pH 9.5 (Chappelet-Tordo *et al.*, 1974). Though intestinal pH increases along the length of the small bowel, from < 6.5 in the duodenum to > 7.4 in the distal ileum, it never reaches the apparent optimum for IAP activity (Fallingborg, 1999). Intriguingly, Chappelet-Tordo *et al* pointed out that V_m of the membrane-bound form of IAP is reached at a lower pH than that of the soluble enzyme (1974). The authors also find that IAP has a relatively low K_m of IAP at pH < 8.0 (such as that found in the distal small intestine), which when taken together with high concentrations of phosphate-containing substrates in the intestinal lumen, IAP “most probably works in V_m conditions *in vivo*” (Chappelet-Tordo *et al.*, 1974). Despite this analysis, along with later work

showing alkaline phosphatase to be an incredibly efficient enzyme *in vitro* (Simopoulos and Jencks, 1994), the field was unable to conclusively determine the *in vivo* function for IAP for another twenty years.

A physiological function for IAP was elucidated in 1997, when Poelstra *et al*. tested bacterial lipopolysaccharide (LPS, or endotoxin), a molecule with multiple phosphate groups, as a substrate for IAP (Poelstra *et al.*, 1997). This work revealed that IAP not only liberates phosphate from LPS, but it does so at physiological pH. Although this document will focus on LPS, other recent work has expanded the catalogue of known IAP substrates to include bacterial toxins such as flagellin and CpG DNA (Chen *et al.*, 2010b).

On a molecular level, LPS binds TLR-4, initiating the signaling cascade described above (Fig. 1-3) (Tapping *et al.*, 2000; Akira and Takeda, 2004). Dephosphorlyation of LPS by IAP prevents activation of the NF-kB pathway (Goldberg *et al.*, 2008). Inhibition of endogenous IAP increases serum LPS levels and mortality in rats infected with *E. coli* or orally administered LPS (Poelstra *et al.*, 1997; Koyama *et al.*, 2002). Studies in zebrafish showed that IAP expression is turned on in the larval stage three days post-fertilization; this time point corresponds with the opening of the mouth and resultant introduction of bacteria into the digestive tract (Bates *et al.*, 2006). Similarly, administration of LPS is sufficient to induce IAP expression, and inhibition or morpholino-mediated knockdown of endogenously expressed IAP led to hypersensitivity to LPS (Bates *et al.*, 2006; Bates *et al.*, 2007). IAP KO mice are actually less susceptible to treatment with soluble LPS than WT, and although these animals have no overt phenotype under normal conditions, pathogenic bacteria more readily translocate

when compared to WT animals (Goldberg *et al.*, 2008). Furthermore, the composition of the IAP-KO intestinal bacterial population is altered relative to that of WT (Chen *et al.*, 2010a; Malo *et al.*, 2010).

Together, these studies led to a model where the introduction of intestinal bacteria stimulates the expression of IAP, which functions as a host defense factor to dephosphorylate (and thereby detoxify) LPS. Detoxification, in turn, reduces the proinflammatory potential of the intestinal microbiome, reducing inflammatory signaling and immune responses (Bates *et al.*, 2007). In IAP KO animals, the chronically high levels of proinflammatory molecules that retain their toxicity is thought to lead to overstimulation of inflammatory signaling cascades and subsequent downregulation of TLR-4 as a tolerance mechanism (Chen *et al.*, 2010a). Not only does IAP detoxify bacterial products, but it also helps prevent acute overgrowth of pathogens by aiding in maintenance of a healthy bacterial population (Malo *et al.*, 2010). In this finely balanced system, intestinal bacteria induce the host-defense enzyme IAP, which in turn regulates the microbiome. Disease states such as colitis have been correlated with perturbations on either side of the equation [(Mazmanian *et al.*, 2008; Tuin *et al.*, 2009), reviewed by (Packey and Sartor, 2009)]. Although most IAP studies focus on the soluble enzyme, work showing its enrichment on LVs raises the intriguing possibility that vesicles serve to deliver IAP to the intestinal lumen, concentrating its activity as a host defense factor (McConnell *et al.*, 2009).

Intestinal Microbiome

Due to the enormous surface area presented by the small intestine, as well as its exclusive role in nutrient absorption, it is important to understand the interplay between this organ and the microbiome. “Microbiome” refers to the collective genome of resident microbes, “microbiota” refers to the microbial population. A stunning ~15,000 species of bacteria reside in the human intestine, with a total bacterial load of ~10^{14} bacterial cells (although it should be noted that most studies have put the number of bacterial species much lower, closer to 1,000) (Savage, 1977; Frank *et al.*, 2007; Claesson *et al.*, 2009). The vast majority of these are found in the large bowel, where the concentration approaches 10^{12} bacteria per gram of intestinal contents (Sartor, 2008). However, we have estimated that at least 10^{8} bacteria are present in the small intestine (Shifrin and Tyska, 2012). Bacteria in the small intestine are required both to aid in digestion and to protect against infection from pathogens acquired from the environment as well as native, opportunistic pathogens already in the gut (Backhed *et al.*, 2004; Backhed *et al.*, 2005). The entire relationship between host and microbiome is one of finely tuned cross-talk; bacteria and bacterial genes are so integral to the normal functioning of the human body that some investigators suggest that humans are “supraorganisms” comprised of *homo sapiens* and its resident microbes (Gill *et al.*, 2006). Significant variation exists between the microbiota of individuals at the level of genus and species. However, under normal conditions the core bacterial population is relatively consistent at the higher phylogenetic levels, consisting of ~30-50% *Bacteroidetes*, ~50-70% *Firmicutes*, and small contributions from other phyla including *Actinobacteria* and *Proteobacteria* (Eckburg *et al.*, 2005; Peterson *et al.*, 2008). Furthermore, the functional

conservation of the microbiome is quite high; i.e. healthy individuals exhibit similar microbial genetic profiles, even when the microbial species carrying those genes vary (Qin *et al.*, 2010; Consortium, 2012).

Gut bacteria are necessary for normal development of intestinal architecture; the intestines of germ-free zebrafish remain in an immature state with impaired epithelial differentiation. These animals have minimal IAP activity and reduced numbers of goblet and enteroendocrine secretory cells, defects which can be reversed by the introduction of a normal microbiota (Bates *et al.*, 2006). Intestinal bacteria also play a critical role in stimulating development of the host immune system (Falk *et al.*, 1998; Hooper *et al.*, 1998; Round and Mazmanian, 2009; Sommer and Backhed, 2013). Differentiation of T_H17 helper T-cells is regulated by an unusual microbe called segmented filamentous bacteria (SFB), which under normal conditions is the only bacterial species in direct contact with host epithelia (Ivanov *et al.*, 2009). More generally, isolated lymphoid follicles, tertiary lymphoid structures that serve as “outposts” of immune defense in the intestinal tract, show lower levels of maturation in germ-free mice. Similarly, these animals have reduced numbers of Peyer’s patches (Round and Mazmanian, 2009). These studies show that a normal gut microbiome is important for inducing maturation of the mammalian immune system, which in turn allows the host to regulate the microbiome and prevent overgrowth of species that could be harmful to both the host and the commensal bacterial population.

While the microbial population helps to regulate the host physiology, the reverse is also true. For example, secretion of α-defensin by Paneth cells is important not only for preventing pathogenic infection, but also for maintaining normal gut bacterial

populations (Salzman *et al.*, 2010). Expression of the human α-defensin gene *DEFA5* in mice causes inversion of the ratio between *Firmicutes* and *Bacteroidetes* and reduction in the number of SFB. In turn, shifts in the microbiome alter the mucosal inflammatory response, measured by a drop in the number of T_H17 T-cells (Salzman *et al.*, 2010). IAP KO mice have decreased overall numbers of colonic bacteria, and while the relative abundance of both *Firmicutes* and *Bacteroidetes* remains statistically similar, shifts at lower phylogenetic levels are observed in the form of an increase in the class *Clostridia* (phylum *Firmicutes*) and the family *Helicobacteraceae* (phylum *Proteobacteria*) (Malo *et al.*, 2010). Though outside the scope of this discussion, it is important to note that factors such as diet, environment, and genetics are all factors in determining an individual's specific microbiota (Lozupone *et al.*, 2012).

Perturbations to intestinal physiology, such as infection, inflammatory bowel disease, and obesity, are also correlated with significant shifts in the microbiota (Ley *et al.*, 2005; Peterson *et al.*, 2008; Turnbaugh *et al.*, 2009). In mice infected with the enteric pathogen *Citrobacter rodentium*, relative abundance of *Bacteroidetes* in the colon decreases dramatically (Lupp *et al.*, 2007). In the same study, investigators demonstrated that a genetic predisposition towards inflammation allows for significant increases in the percentage of the family *Enterobacteriaceae*, part of the phylum *Proteobacteria,* which includes *E. coli* species (Lupp *et al.*, 2007). Consistent with this, Crohn's disease patients also exhibit increased colonization by the *E. coli* population, including the pathogenic adherent/invasive *E. coli* (Packey and Sartor, 2009). In human patients with bacterial translocation to mesenteric lymph nodes and systemic circulation following laparotomy, *E. coli* accounts for the majority (67%) of bacterial species

cultured (O'Boyle *et al.*, 1998). This study was carried out prior to the common application of culture-independent methods for investigating bacterial populations, and therefore does not take into account what is now known to be a huge population of nonculturable bacteria. However, it is consistent with later analyses using molecular tools and points to *E. coli* as both a marker of defective barrier function as well as an opportunistic pathogen with the capacity to perturb intestinal homeostasis. Furthermore, within this species, several strains that are primary enteric pathogens cause disease in otherwise healthy individuals.

Enteropathogenic *E. coli*

Over 750,000 children under the age of five die of diarrhea-related dehydration each year (World Health Organization). Most common in developing regions, several types of bacteria, including a group of virulent *E. coli* strains found in contaminated food or water, lead to outbreaks of diarrheal diseases (Evans and Evans, 1996). Among these is Enteropathogenic *E. Coli* (EPEC), which attaches to the apical surface of enterocytes. EPEC infection ultimately results in severe disruption of tight junctions, which causes massive fluid and ion imbalances across the intestinal epithelial barrier, and subsequent diarrhea (Guttman and Finlay, 2009).

EPEC is called an attaching/effacing (A/E) pathogen. It remains on the extracellular surface of a host cell, co-opting host cell machinery to produce an actin-rich pedestal that anchors the bacterium while allowing it to move laterally across the cell surface (Stevens *et al.*, 2006). Many of the highly conserved bacterial factors involved in this process are encoded by a pathogenicity island called the locus of enterocyte effacement (LEE), while several more non-LEE proteins involved in

pathogenicity vary between bacterial strains (Wong *et al.*, 2011). Initial attachment of EPEC to the apical surface of an enterocyte is mediated primarily by the bundle forming pilus (BFP), with a partially redundant role played by a component of the type III secretion system (T3SS) called EspA (Cleary *et al.*, 2004). BFP are also critical for inter-bacterial adhesion, helping EPEC form characteristic microcolonies, where multiple bacterial cells auto-aggregate on the cell surface in a process called localized adherence (Hicks *et al.*, 1998). Upon contact, BFP filaments retract, bringing the bacterium closer to the host cell surface and allowing the attachment process to proceed (Zahavi *et al.*, 2011). Once the BFP has retracted, EPEC utilize the T3SS, a specialized “needle,” to inject virulence factors into a host cell. It has been noted that direct injection of bacterial proteins allows an EPEC cell to gain direct access to the host cytosol without having to utilize host cell endocytic pathways and retrotranslocation (Viswanathan *et al.*, 2009). Multiple virulence factors are involved in this process; however, the primary pathway for intimate attachment and pedestal formation involves insertion of the bacterial protein Translocated Intimin Receptor (Tir) into the host cell membrane (Deibel *et al.*, 1998). The outer membrane protein intimin (eae), a critical mediator of EPEC attachment and virulence, then binds and clusters Tir on the host cell surface and promotes phosphorylation of Tir at Y474 (Donnenberg *et al.*, 1993; Kenny, 1999; Liu *et al.*, 1999). In fact, a short sequence of 12 C-terminal residues, including Y474, is sufficient to induce the next step: binding of Tir to Nck (Campellone *et al.*, 2002). Nck binds N-WASP, activates the Arp2/3 actin nucleation complex, and results in the rapid polymerization of a dense, branched actin network under the bacterium (Campellone, 2010; Wong *et al.*, 2011). Recent work has shown in HeLa cells that in

addition to branched actin, pedestals also contain a spectrin “cage” around the periphery (Ruetz *et al.*, 2011; Ruetz *et al.*, 2012). Spectrin may help to stabilize the actin network and link it to the plasma membrane (Ruetz *et al.*, 2012). Ultimately, a pedestal comprised of a robust cytoskeletal network overlaid by the plasma membrane surrounds the bacterium on three sides, holding it in place on the extracellular surface and providing a secure attachment to allow for division and, over time, the formation of a microcolony of multiple EPEC cells. Microvilli surrounding the microcolony are destroyed during this process, leaving an area around the bacteria devoid of brush border and giving rise to a cellular morphology termed the A/E lesion (Fig. 1-5).

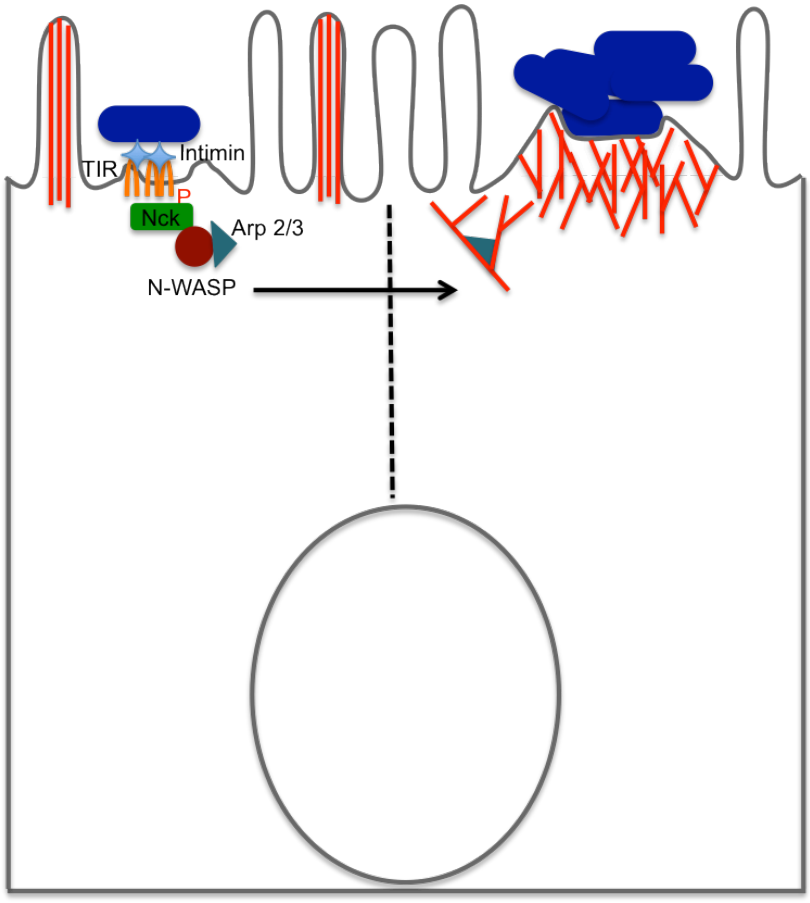

Figure 1-5: Tir and intimin mediate EPEC pedestal formation via the Arp2/3 pathway

As the process of intimate EPEC attachment progresses, microvilli surrounding the bacteria elongate and orient toward the pathogen (Dean *et al.*, 2006). Microvillar elongation has long been observed as part of the normal A/E process during EPEC infection (Bernet-Camard *et al.*, 1996; Phillips *et al.*, 2000; Cleary *et al.*, 2004; Shaw *et al.*, 2005; Dean *et al.*, 2013). The extended protrusions, often called microvillus-like processes (MLP), are thought to depend upon the LEE-encoded effector protein espF, and though not intimin-dependent, develop more slowly in Δintimin EPEC mutants (Frankel *et al.*, 1998; Phillips *et al.*, 2000; Shaw *et al.*, 2005). EspF putatively binds actin, N-WASP, and the actin-sequestering protein profilin (Weflen *et al.*, 2009; Wong *et al.*, 2011); consequently, EspF injected by EPEC disrupts tight junctions, most likely by sequestering actin-profilin complexes, thereby altering actin dynamics and endocytosis (Peralta-Ramirez *et al.*, 2008). At the same time, an *in vitro* study showed that EspF promotes actin polymerization through its interaction with N-WASP and a membrane-cytoskeleton adaptor protein SNX9; this function is likely used at sites of bacterial attachment to advance pedestal formation (Alto *et al.*, 2007; Peralta-Ramirez *et al.*, 2008).

Summary

Infection by enteric pathogens can be viewed as a tug-of-war. The innate immune system deploys constitutively active processes to prevent infection and maintain homeostasis. For example, mucins produce by goblet cells forms a thick layer to inhibit bacteria from reaching the epithelial surface, paneth cells in the crypt secrete antimicrobial peptides (McGuckin *et al.*, 2011), and tight junctions between cells in the epithelial layer prevent microbial translocation. Leukocytes in the gut recognize and

destroy pathogens and toxins, and when necessary activate signaling cascades to initiate a larger inflammatory response. As discussed above, the microbiota itself can be considered a defense mechanism by self-regulating and working in conjunction with the host to prevent overgrowth of opportunistic pathogens and/or invasion from primary pathogens normally excluded from the intestinal tract. Upon sensing the presence of a pathogen, host cells activate immune responses in order to clear the microbial threat and prevent systemic infection. Likewise, bacteria have developed mechanisms to subvert host immune function. Secreted EPEC toxins activate pro-inflammatory signaling by enterocytes and other cell types, while active infection by live EPEC to a certain extent actually leads to an attenuation of this process (Sharma *et al.*, 2006). That is, the enterocyte responds defensively to bacterial toxins, but the bacteria itself can manipulate a host cell into limiting its response. Beyond attenuating inflammation, pathogens alter other host cell processes, including limiting apoptosis as a mechanism to clear infected cells (Hausmann, 2010), and hijacking cytoskeletal pathways during intimate attachment.

Because the brush border is the first contact point for pathogenic bacteria, I have chosen to focus on the role of this domain during the early infection process. Several aspects of host defense mediated by enterocytes have been discussed above. Our lab has demonstrated the presence of IAP-enriched vesicles in the intestinal lumen. Membrane-bound IAP at distal tips of microvilli, the enrichment of this enzyme in LVs, and the highly regulated nature of LV shedding by the motor protein myo1a led us to investigate a possible novel role for these extracellular organelles in host defense. In the work described in Chapter IV, we characterize this novel function of LVs. We find

that LV-bound IAP is catalytically active, and robustly dephosphorylates LPS from numerous bacterial sources. Removal of phosphate from LPS reduces the molecule's toxicity; indeed, in cell culture, treatment of LPS from pathogenic *E. coli* reduces activation of the NF-kB pathway. Using two human intestinal epithelial cell lines, we show that LVs inhibit EPEC attachment to host cells, reducing the ability of the bacteria to form intimate attachment. LVs also have a bactericidal effect; EPEC population growth is inhibited in overnight cultures in the presence of LVs. Finally, LV shedding is a constitutive process, but can be increased in response to the presence of pathogens. Using western blot analysis, we show an increase in LV protein markers following addition of EPEC to intestinal epithelial cell culture. Consistent with previously published work showing that myo1a is critical for LV shedding (McConnell and Tyska, 2007; McConnell *et al.*, 2009), we find that pathogen-stimulated LV shedding is dependent upon the functional motor protein. Together, this work demonstrates that LVs constitute a previously unknown aspect of innate immunity, potentially functioning *in vivo* in a multi-faceted manner to limit the proinflammatory potential of intestinal contents and inhibit bacterial infection.

In the second part of my research, I focused on the effect a pathogenic bacteria has on the brush border by investigating how cellular actin is used by EPEC to form a pedestal. Although the signaling pathways and host cytoskeletal rearrangements that occur during intimate EPEC infection are well characterized, a significant gap in knowledge exists at the point of initial contact between bacterium and host cell. Tantalizing hints have been published previously, most notably the presence of MLPs relatively early in the infection process. These studies, though informative, have been

limited by the use of static readouts. To date, we are unaware of a true kinetic analysis of microvillar dynamics and pedestal formation utilizing live cell microscopy. We have attempted to address this gap with a combination of live cell deconvolution imaging and scanning electron microscopy (SEM) of EPEC attachment to Caco-2_{BBE} cells. We have found that during pedestal formation, apical “flow” appears to draw microvilli into the region of attachment, and that this process is at least in part dependent upon PCDH24. Consistent with previous work, we see microvillar elongation (i.e. the formation of MLPs) occuring during this process; MLPs are induced by EPEC and elongate towards the bacterial cell in a directed manner, cluster at their distal tips, and adhere to the bacterium. In cells expressing espin, a parallel actin bundling protein, we observe microvilli being incorporated into nascent pedestals, a finding that strongly suggests pedestals can be built by recycling of pre-formed actin structures. We therefore hypothesize that EPEC not only hijack Arp2/3 actin polymerization machinery, but also utilize the large pool of F-actin in the apical domain to form intimate attachments. In this model microvilli provide actin to the bacteria early in attachment; as the bundles are repurposed into pedestals, the microvilli are disassembled, leading to effacement at later stages. Our model is further supported by the observation that upon inhibition of the Arp2/3 complex, EPEC still induce the formation of pedestals. We believe this data represents a previously uncharacterized pathway by which EPEC subverts the apical domain of enterocytes in order to intimately adhere to the host cell.

The studies described here provide a number of exciting new insights into interactions between host epithelia and pathogenic microbes, and give rise to new models of host defense in the mammalian gut mucosa.

CHAPTER II

MATERIALS AND METHODS

Chapters III, IV

Isolation of native LVs

All procedures involving animals were carried out under the auspices of the Vanderbilt University Medical Center Institutional Animal Care and Use Committee. Lumenal vesicles were isolated from rat small intestines as described previously (McConnell *et al.*, 2009), with the addition of ampicillin (50 μg/ml), kanamycin (30 μg/ml), and tetracycline (50 μg/ml) to the 500 x *g* supernatants, the resuspended 100,000 x *g* pellet, and the LV-containing sucrose gradient fractions, to eliminate contaminating bacteria from native material. LV protein concentrations were determined by BCA assay. An average rat LV preparation produces 100-150 μg LVs/ml intestinal contents. However, this range likely represents a low end estimate for the physiological concentration of LVs in the lumen for two reasons: (i) SEM of native rat small intestine shows that large numbers of LVs are caught in the mucous layer (unpublished observations), and (ii) LVs are likely cleared from the lumen via their direct interactions with lumenal bacteria (Fig. 3-1). Vesicles in either of these two populations are not likely to be recovered during typical preparations. Thus, experiments were carried out using a maximum of 200 μg LVs/ml media (attachment, RelA translocation, and enzymatic assays). For growth assays, LVs were used at a concentration of 50 μg LVs/ml as higher concentrations impacted baseline OD_{600} readings.

Phosphate release assays

Malachite green (Sigma, St. Louis, MO) at 0.56 mM in ddH_2O was mixed in a 3:1 ratio with 4.2% ammonium molybdate (Sigma) in 4 N HCL (MG:AM solution). For LPS dephosphorylation assays, 100 µg/ml phenol-purified LPS (Sigma) ± 10 µg LVs or 0.1U IAP (Sigma) were incubated in 50 µl LV reaction buffer (1x TBS pH 8.1, 1 mM $MgCl_2$, 0.1 mM ZnCl) for 30 min at 37° C. A 500 µl volume of MG:AM solution was added to the reaction, and allowed to sit at room temperature for 1 min, after which the phosphate-MG:AM reaction was quenched with 50 µl 34% sodium-citrate (Sigma) in ddH_2O. 200 µl reactions were loaded into clear 96-well plates and absorbance read on a BioTek plate reader at 650 nm. For kinetic assays, reaction volumes were increased to 400 µl, 25 µl samples were removed at 2 min intervals and added to 250 µl of MG:AM, and reactions were quenched at 1 min with 25 µl 34% Na-citrate.

FAVS analysis

Intestinal flushate was passed through a coarse wire filter, followed by a 40 µm filter to remove large particulate matter. The resulting material was used for labeling and sorting. Material was blocked for 1 hr at 4° C with 2 % bovine serum albumin (BSA), and LVs were labeled with anti-IAP antibody (1:400; Sigma-Aldrich) and DiD (1:400; Invitrogen) for 1 hr at 4° C, pelleted at 100,000 *g* for 1 hr, washed in PBS, pelleted again, resuspended in PBS, and Alexa Fluor 488-conjugated goat anti–rabbit secondary antibody was added (1:400) for 1 hr at 4° C (Invitrogen). Bacteria were stained using DAPI (1:2000). FAVS was performed as previously described (Cao *et al.*, 2008) using a FACSAria II (BD) customized with forward scatter photomultiplier tube assembly, which

was initially calibrated using CS&T beads. Unstained and single-stained (anti-IAP only, DiD only, or DAPI only) vesicles were used to compensate spectral overlap, which in all cases was nominal. Multicolor stained particles were gated for both IAP and DAPI, and signals pulse processed for doublet discrimination.

Cell culture and bacterial strains

HT-29 and Caco-2_{BBE} were grown in DMEM (Gibco) supplemented with 10% defined fetal bovine serum and 1 mM L-glutamine (Gibco) at 37° C, 5% CO_2. Caco-2_{BBE} cells were transfected with GFP-tagged myo1a-TH1 (Tyska and Mooseker, 2004) and maintained in selection media (growth media with 500 μg/ml G418). For RelA translocation assays, HT-29 cells were plated on coverslips and simultaneously transfected (Effectene, Qiagen) with GFP-RelA (Chen *et al.*, 2001). Media was changed after 24 hrs and cells serum-starved in DMEM overnight prior to use. EPEC were grown overnight in Luria-Bertani broth with kanamycin, shaking at 225 rpm, 37° C. *Shigella* strains were grown similarly. Prior to use in attachment assays, overnight EPEC cultures were diluted and grown for 2 hrs in recovery media as described (Sharma *et al.*, 2006).

Bacteria attachment and microvillar vesicle shedding assays

For bacterial attachment assays, cells were seeded on acid-washed coverslips in 6-well dishes (TRP) or polycarbonate Transwell filters (Costar) differentiate for five-days post-confluency. Approximately $2x10^5$ CFU EPEC ± i) 200 μg/ml LV, ii) 200 μg/ml fixed LV (15 min fixation in 4% paraformaldehyde [EMS]-PBS, then washed 3x by centrifugation at 100,000 x *g* in 1x TBS, resuspended to original volume in 1x TBS), iii) 2 U/ml IAP, or iv) 200 μg/ml LV + 10 mM L-phe were added to coverslips in serum-free

DMEM. 6-well plates were centrifuged for 5 min at 50 x *g* to accelerate contact between bacteria and the cell monolayer, then incubated for 3 hr at 37° C, 5% CO^2. For RelA translocation assays, EPEC were used at ~$2x10^7$ CFU. Shedding assays were carried out by seeding Caco-2_{BBE} cells or Caco-2_{BBE} cells stably expressing EGFP-myo1a-TH1 in T75 flasks, and growing until 7 days post-confluency. Prior to treatment, monolayers were washed with sterile PBS, then incubated with ~$2x10^6$ CFU live EPEC, EPEC heated at 95° C for 15 min, *Shigella*, or 10 µg/ml *E. coli* O55:B5 LPS diluted in serum-free DMEM for 6 hr. Media was removed and centrifuged at 5,000 x *g*, 20,000 x *g*, and 100,000 x *g*, with pellets from each step being resuspended in 1/100 the original volume to concentrate cellular material.

Western blots

Samples were diluted with Laemmli sample buffer, heated at 100 C° for 5 min, and equal volumes loaded on a 4-12% Nu-Page gradient gel (Invitrogen). Proteins were transferred to nitrocellulose, which was subsequently blocked for 1 hr in 5% milk-PBS. Primary antibodies against IAP (Sigma), Annexin A13b (R&D) and actin (Sigma) were diluted 1:1000 in PBS containing 0.1% Tween-20 (PBS-T), and incubated with the membranes at room temperature for 1 hr. Membranes were washed in PBS-T, then incubated with donkey-anti-rabbit 800 or donkey-anti-goat 680 IRdye (Li-Cor) at 1:10,000 for 30 min. Membranes were again washed with PBS-T and imaged using a Li-Cor Odyssey infrared imaging system. Images of membrane scans were cropped and contrast adjusted using ImageJ version 1.45d (NIH).

Electron microscopy

Sample preparation and imaging for negative-stain TEM and SEM was carried out as described previously (McConnell *et al.*, 2009). Negative-stain samples were imaged on a Phillips CM12 TEM. Samples for SEM were imaged on a Hitachi S-4200 cold field emission SEM.

Immunofluorescence labeling and confocal imaging

Coverslips were fixed with 4% paraformaldehyde/PBS for 15 min, washed, and blocked for 1 hr in 5% BSA/PBS. For EPEC attachment assays, rabbit polyclonal anti-IAP (Sigma) was diluted 1:200 and incubated on sample coverslips for 1 hr. Coverslips were then washed (3 x PBS) and treated for 30 min with goat-anti-rabbit secondary antibody (1:200) and phalloidin (1:200) to delineate pedestals and cell morphology. Because IAP was enriched at sites of bacterial attachment even at very early stages of adherence, this marker and DAPI were used to count EPEC on the surface of monolayers. Clusters of five or more EPEC organisms were counted as microcolonies. For RelA translocation assays, cells were only stained with phalloidin. Coverslips were again washed (3 x PBS) and mounted on slides using ProLong Gold with DAPI (Invitrogen). Images were acquired using a Leica SP5 laser scanning confocal microscope (LSCM), and cropped and contrast adjusted using ImageJ version 1.45d. For RelA translocation assays, samples were imaged using a Nikon TiE inverted widefield microscope with Nikon Elements v.3.2. Mean intensities from the nucleus and cytoplasm in raw images were acquired using the “oval selection” and “measure” tools in ImageJ. Cytoplasmic:nuclear ratio was calculated and cells with a ratio of ≤1.1 were counted as having nuclear translocation.

Bacterial growth assays

Native Gram-negative bacteria were isolated by streaking out serial dilutions of rat intestinal contents onto MacConkey agar; colonies were selected and grown in liquid culture overnight using LB media. Bacteria were grown in recovery medium (Sharma *et al.*, 2006) for 2 hr and added at a concentration of ~2.5x10^4 CFU/ml, determined by streaking serial dilutions onto LB agar plates, into LB broth (for EPEC, including 50 µl ampicillin to prevent contamination). LVs were added at a concentration of 50 µl, or IAP at 5 U/ml. Reaction mixtures of 200 µl were seeded in replicate in 96-well plates. OD_{600} was determined by incubating plates at 37° C in a Synergy HT plate reader, shaking for 60 sec prior to each reading at 10 min intervals. To determine viable CFU following overnight growth, samples were diluted 1:100 and sonicated in a Branson 1510 water bath sonicator for 2 x 30 sec, then serially diluted to 1:100,000 and plated on LB agar plates with ampicillin. Plates were incubated overnight at 37° C then scanned and colonies counted on a GelCount system (Oxford Optronix). For stationary phase assays in depleted media, LVs were added to overnight EPEC cultures without changing media. For stationary phase assays in replenished media, overnight cultures were pelleted at 800 x *g* for 3 min, then resuspended in the original volume of fresh LB.

16S rDNA analysis

Diluted rat small intestine contents were streaked out on MacConkey agar plates and incubated at 37° C overnight. Colonies were picked and samples of each added to 25 µl endotoxin-free H_2O. Samples were heated at 95° C for 2 min to lyse bacteria, then centrifuged at 16,000 x *g* for 2 min. Supernatant was used as template for PCR, with Platinum PCR Supermix (Invitrogen) and the highly conserved primers 8F/1492R (Eden

et al., 1991; Schmidt and Relman, 1994). PCR reactions used a Eppendorf MasterCycler according to the following parameters: initial denaturing at 94° C for 3 min, then 30 cycles of 94° for 30 sec, 48° for 45 sec, 72° for 30 sec, and a final extension at 72° for 10 min. Sequencing was carried out at the Vanderbilt University Medical Center DNA sequencing core, using the 907R primer (Wen *et al.*, 2008); sequences were uploaded to the Ribosomal Database Project (RDP) and identification was made to the genus level (Wang *et al.*, 2007).

Tissue preparation and analysis

Small intestines from WT and myo1a KO 129 SVJ1 or FVB mice were collected, flushed with warm saline (0.9% W/V NaCl, 0.2% Na-Azide, 2mM Imidazole pH 7.2), filled with 4% PFA (EMS), and the ends were clamped and fixed at room temperature for 15 min. Intestines were opened longitudinally and rolled. For frozen embedding, rolls were fixed 4% PFA for 2 hr, and incubated in 1 M sucrose in TBS (150 mM NaCl and 50 mM Tris, pH 8.0) overnight at 4° C. Tissue was embedded in OCT, frozen, and 20 µm-thick transverse sections were cut on a cryostat (Leica). Sections were stained using anti-IAP (1:200; Sigma-Aldrich) and Alexa Fluor 488 secondary (1:200), 568 phalloidin (1:200; Invitrogen). Fillipin was used at 50 µg/ml. Images were acquired with a Leica TCS SP5 LSCM or an Olympus FV1000 LSCM and processed using ImageJ. Villar length measurements were taken using the freehand line tool in ImageJ, and the number of IAP-enriched puncta counted. For IAP and fillipin gradients, 5 µm lines were drawn from just below the terminal web to just past the end of the brush border, and intensity profiles were plotted for each channel.

For histological analysis, rolls were fixed in 10% formalin overnight and submitted to the Vanderbilt Immunohistochemistry Core for paraffin embedding, sectioning, and staining. Sections were stained with hematoxylin & eosin for general histological analysis, or Periodic acid-Schiff and Alcian blue staining to label goblet cells. Images were acquired with a QImaging Micropublisher 3.3 RTV, and enhanced and cropped using ImageJ 1.45d. Goblet cells were counted manually on a per villus basis along the length of the intestine.

ELISA assays

WT and myo1a KO small intestines were removed and flushed with saline. The ileum was then cut longitudinally and the mucosa scraped into RIPA buffer with Pefabloc. Samples were homogenized in a glass dounce and centrifuged at 15,000 x *g*. Cytokine levels in the resulting supernatant was probed using R&D Quantikine kits for IL-6 and TNF-α.

Chapters VI, VII

Cell culture and shRNA knockdown

Caco-2_{BBE} cells were grown as described above; HeLa cells were grown in DMEM (Gibco) supplemented with 10% defined fetal bovine serum. EPEC cultures were grown as described above. For PCDH24 knockdown, shRNA plasmids (OpenBiosystems) were expressed in DH5-α bacterial cells and purified using Qiagen maxiprep kits. HEK293FT cells were grown in DMEM with 10% FBS, 2mM L-Glutamine, and 1% MEM non-essential amino acids solution. Cells were transfected 6 hrs after plating with PCDH24 or scramble shRNA using FuGene6, according to manufacturers

instructions (Promega). Virus was harvested two days after transfection, concentrated, and stored overnight. Concentrated virus was centrifuged and resuspended in DMEM, mixed with Polybrene, and added to Caco-2_{BBE} cells. Transfected cells were selected for using puromycin, and knockdown was confirmed by western blotting.

Attachment assays and sample processing for confocal and SEM imaging

For attachment assays, Caco-2_{BBE} cells were grown on glass coverslips or collagen-coated Transwell filters as described above for 14 days post-confluency. Bacteria at $2x10^5$ CFU/ml were added to monolayers and incubated for 1 or 3 hrs. To accelerate bacterial contact in order to investigate the time course of microvillar elongation, cells and bacteria were centrifuged for 3 min at 250 x *g*, then incubated for 15 min. Filters were fixed and processed for SEM as described above, and imaged using and FEI Quanta 250 ESEM. Coverslips were fixed and stained for immunofluorescence as described above, with goat polyclonal anti-Lipid A used to label EPEC (1:200), followed by Alexa Flour 488 donkey-anti-goat secondary antibody and Alexa Flour 568 phalloidin. Images were acquired using a Leica SP5 LSCM, and cropped and contrast adjusted using ImageJ version 1.47h.

Live cell imaging

Caco-2_{BBE} cells were seeded on glass-bottom dishes (MatTek) and simultaneously transfected (Effectene) with mCherry-Utr (Burkel *et al.*, 2007) or mCherry-espin (Loomis *et al.*, 2003) and/or PCDH24-GFP, PCDH24ΔEC1-GFP, or GFP-βactin, then grown for two days. EPEC were grown and activated as described above. Before imaging, DMEM cell culture media was replaced with CO_2-independent

media (Gibco). In order increase the chances of imaging productive binding events, high numbers of bacteria (~1x10^8 CFU) were added to the dishes. Cells were imaged using an Applied Precision DeltaVision deconvolution microscope with environmental chamber heated to 37° C, with z-stacks through the apical domain and time intervals of 20 sec or 1 min. Image files were exported and processed using ImageJ version 1.47h.

Drug treatment assays

Caco-2_{BBE} and HeLa cells were grown on glass coverslips, the former for 14 d post-confluency in order to reach late differentiation. Prior to the experiment, cells were treated with either DMSO (1:1000) or CK-666 reconstituted in DMSO (50 µg/ml, or 1:1000) for 2 hr. Following pretreatment, the cell culture media was replaced by serum-free DMEM containing recovered EPEC (2x10^5 CFU/ml) and fresh DMSO or CK-666. Samples were incubated 3 hr, fixed, and processed for immunofluorescence as above (anti-Lipid A and phalloidin). Coverslips were imaged by LSCM, and processed using ImageJ version 1.47h. For quantification, z-stacks were first converted to max intensity projections. The EPEC channel was thresholded and converted to a binary mask and measured, providing a quantification of total area covered by bacteria. The binary mask was multiplied with the actin channel to create a 32-bit float image. In this way, only the area under the mask (i.e. actin in pedestals, and not the surrounding brush border or cell cortex) was included in intensity measurements. The resulting image was converted to 8-bit, and actin signal measured to quantify both pedestal area and intensity.

CHAPTER III

ENTEROCYTE MICROVILLUS-DERIVED VESICLES DETOXIFY BACTERIAL PRODUCTS AND REGULATE EPITHELIAL-MICROBIAL INTERACTIONS

Originally published as:

Shifrin, D.A., Jr., McConnell, R.E., Nambiar, R., Higginbotham, J.N., Coffey, R.J., and Tyska, M.J. (2012). *Enterocyte microvillus-derived vesicles detoxify bacterial products and regulate epithelial-microbial interactions*. Current Biology *22*, 627-631.

And

Shifrin, D.A., Jr., and Tyska, M.J. (2012). Ready...aim...fire into the lumen: a new role for enterocyte microvilli in gut host defense. Gut Microbes *3*, 460-462.

CHAPTER III-A

Summary

The continuous monolayer of intestinal epithelial cells (IECs) lining the gut lumen functions as the site of nutrient absorption and as a physical barrier to prevent the translocation of microbes and associated toxic compounds into the peripheral vasculature (Louvard *et al.*, 1992). IECs also express host defense proteins such as intestinal alkaline phosphatase (IAP), which detoxify bacterial products and prevent intestinal inflammation (Koyama *et al.*, 2002; Bates *et al.*, 2007; Goldberg *et al.*, 2008; Ramasamy *et al.*, 2010). Our laboratory recently showed that IAP is enriched on vesicles that are released from the tips of IEC microvilli and accumulate in the intestinal lumen (McConnell and Tyska, 2007; McConnell *et al.*, 2009). Here, we show that these native ‘‘lumenal vesicles’’ (LVs) (1) contain catalytically active IAP that can dephosphorylate lipopolysaccharide (LPS), (2) cluster on the surface of native lumenal bacteria, (3) prevent the adherence of enteropathogenic E. coli (EPEC) to epithelial monolayers, and (4) limit bacterial population growth. We also find that IECs upregulate LV production in response to EPEC and other Gram-negative pathogens. Together, these results suggest that microvillar vesicle shedding represents a novel mechanism for distributing host defense machinery into the intestinal lumen and that microvillus-derived LVs modulate epithelial-microbial interactions.

Results and discussion

A defining feature of the intestinal epithelial cell (IEC) apical domain is the array of microvilli known as the brush border, which extends into the intestinal lumen (Louvard *et al.*, 1992). Within the microvillus, the apical membrane and underlying core actin bundle are linked by myo1a, a membrane-binding actin-based motor (Mooseker and Tilney, 1975; Collins and Borysenko, 1984). Our previous studies suggest that myo1a applies force to the apical membrane, leading to the accumulation of membrane at microvillar tips and ‘‘shedding’’ of vesicles into the lumen (McConnell and Tyska, 2007; McConnell *et al.*, 2009). In mice lacking myo1a, lumenal vesicles (LVs) are reduced in number and exhibit perturbations in morphology and composition (McConnell *et al.*, 2009). Proteomic studies revealed that native LVs are enriched in intestinal alkaline phosphatase (IAP) (McConnell *et al.*, 2009), a host defense factor that reduces the toxicity of lipopolysaccharide (LPS) and other bacterial compounds, limits TLR-4 signaling, and prevents mucosal inflammation (Koyama *et al.*, 2002; Bates *et al.*, 2007; Goldberg *et al.*, 2008; Park *et al.*, 2009; Ramasamy *et al.*, 2010). The absence of IAP also leads to alterations in gut microbiota (Malo *et al.*, 2010). Thus, IAP plays a critical role in preventing mucosal inflammation and maintaining gut homeostasis.

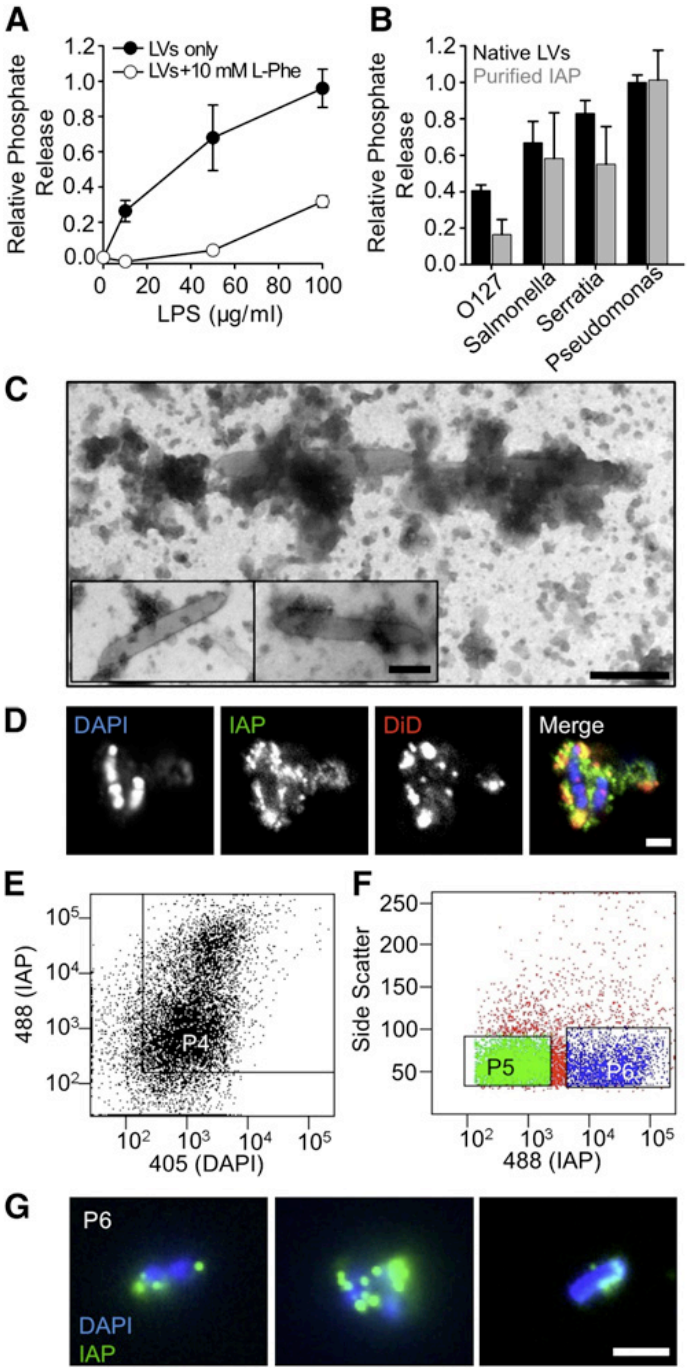

Figure 3-1: LVs dephosphorylate LPS and interact with native lumenal bacteria

(A) LVs release phosphate from *E. coli* O55:B5 LPS in a concentration-dependent manner; phosphate release is reduced by the IAP competitive inhibitor L-phenylalanine (L-Phe). (B) LVs (200 µg LVs/ml) and purified IAP (2 U/ml) differentially dephosphorylate LPS derived from various Gram-negative bacterial species. Data represent mean ± SEM. (C) TEM imaging reveals vesicle-like particles in close association with native lumenal bacteria from rat LV preparations. Scale bar represents 200 nm. (D) CM imaging reveals IAP enrichment (green) on membranes (red) associated with DAPI-stained bacteria (blue). Scale bars represent 2 µm. (E) Presort input material was analyzed for staining with both anti-IAP (LVs) and DAPI (bacteria) using the P4 gate. (F) P4 material was sorted using gates for IAP (P5, low IAP enrichment) and dual stained material (P6, high IAP enrichment). (G) CM images of sorted P6 material show native LV/microbe complexes (green = IAP, blue = DAPI). Scale bar represents 2 µm.

LV-associated IAP dephosphorylates LPS

Given the evidence implicating IAP in gut host defense and homeostasis (Koyama *et al.*, 2002; Bates *et al.*, 2007; Goldberg *et al.*, 2008; Park *et al.*, 2009; Malo *et al.*, 2010; Ramasamy *et al.*, 2010), we hypothesized that IAP-enriched LVs produced by microvilli regulate epithelial-microbial interactions. To test this proposal, we first sought to determine whether LVs could dephosphorylate the proinflammatory bacterial product, LPS. Dephosphorylation of LPS reduces the ability of this compound to activate TLR-4 on host cell membranes (Koyama *et al.*, 2002; Park *et al.*, 2009). Our laboratory previously developed methods for isolating native microvillus-derived LVs from rodent small intestine (McConnell *et al.*, 2009). Native vesicles isolated with these methods are able to dephosphorylate LPS from Escherichia coli serotype O55:B5 in a concentration-dependent manner, which was sensitive to the IAP inhibitor, L-phenylalanine (L-phe) (Figure 3-1A) (Fishman *et al.*, 1963). This activity was not specific to *E. coli* O55:B5 LPS because assays with other LPS variants also gave rise to robust phosphate release (Figure 1B, black bars). Purified IAP added at equivalent units of activity (0.1 U IAP = 10 mg LV, data not shown) demonstrated a comparable response (Figure 3-1B, gray bars). Kinetic analysis of phosphate release from *P. aeruginosa* and *E. coli* LPS (substrates that supported the highest and lowest activities, respectively) revealed that *P. aeruginosa* LPS gives rise to higher rates of phosphate release at lower substrate concentrations (i.e., exhibits a lower K_M; Figure 3-2). Thus, LV associated IAP is catalytically active and can dephosphorylate LPS from a variety of Gram-negative species.

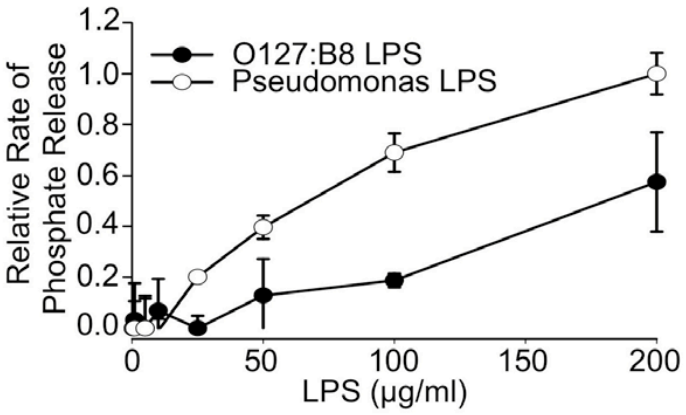

Figure 3-2: LVs exhibit differential affinity for LPS from different sources

Kinetic analysis of phosphate release using LPS from *E. coli* O127:B8 and *P. aeruginosa* indicates that LVs likely exhibit a differential affinity for different LPS isoforms. Data represent mean ± SEM

LVs physically interact with lumenal microbes

Because LVs are able to chemically modify bacterial compounds (Figures 3-1A and 3-1B; Figure 3-2), we next sought to determine whether these vesicles could interact directly with lumenal microbes. To address this question, we examined resuspended pellets produced during native LV preparations from rat intestinal lumen wash using negative stain transmission electron microscopy (TEM). The resulting images revealed rod-shaped bacteria coated or in contact with clusters of material that resembled small vesicles (Figure 3-1C). We labeled the same fraction with an anti-IAP antibody, a membrane dye (DiD), and DAPI (to label bacteria) and imaged samples using laser scanning confocal microscopy (LSCM). Consistent with the presence of microvillus-derived LVs, we found that microbe-associated material was highly enriched in IAP and DiD (Figure 3-1D).

To analyze minimally processed lumen wash material for the presence of LV/ microbe complexes, we also employed a modified form of fluorescence-activated vesicle sorting (FAVS) (Cao *et al.*, 2008; McConnell *et al.*, 2009). Raw lumen wash from

rat small intestine was allowed to settle at 1 x *g* and then passed through a 40 μm filter to remove large particulate matter. Samples were then labeled as in Figure 3-1D and applied to the flow cytometer. FAVS analysis revealed that 99% of all DAPI-labeled particles are associated with some level of IAP signal (P4, Figure 3-1E). Double-positive particles were further analyzed to select for populations with low (P5, Figure 3-1F) and high (P6, Figure 3- 1F) levels of IAP enrichment. Imaging of postsort ‘‘P6’’ material revealed numerous examples of rod-shaped bacteria surrounded by IAP-enriched puncta (Figure 3-1G). Thus, the LV/microbe complexes observed in conventional lumen wash preparations (Figures 3-1C and 3-1D) are most likely formed in the lumen and not as a result of centrifugation or other processing.

LVs prevent EPEC adherence to IECs

Because LVs bind directly to lumenal bacteria, microvillar vesicle shedding could serve as a host defense mechanism capable of preventing the adherence of pathogenic bacteria that target the IEC apical surface. To test this idea, we sought to determine whether LVs impacted the ability of enteropathogenic *E. coli* (EPEC, strain E2348/69) to infect human IECs (HT-29 and Caco-2_{BBE} cells) in culture. EPEC uses a type III secretion system to inject factors into host cells that lead to microvillar effacement, which in turn enables intimate adhesion to the apical surface, an event essential for EPEC pathogenesis (Vallance and Finlay, 2000). We incubated confluent monolayers of HT-29 cells with 1 x 10^5 colony-forming units (CFU) EPEC/ml media in the presence or absence of 200 μg LVs/ml media (See Chapter III, Materials and Methods). After a 3 hr incubation, monolayers were stained and then imaged using CM (Figures 3-3A and 3-3B) or SEM (Figures 3-3C and 3-3D). Consistent with a previous report (Dean *et al.*,

2006), we found that IAP was enriched on the surface of bacteria bound to the cell monolayer, independent of the presence of actin pedestals (arrowheads, Figures 3-3A and 3-3B). Confocal images were further analyzed by counting (1) the number of EPEC organisms bound per unit area, independent of stage of attachment (Figure 3-3E), and (2) the number of microcolonies per unit area (Figure 3-3F) (Scaletsky *et al.*, 1984). Both indices showed that LVs significantly reduced EPEC attachment to HT-29 monolayers (Figures 3-3E and 3-3F). Similar results were observed when experiments were carried out with Caco-2_{BBE} cells (data not shown). SEM on Caco-2_{BBE} cultures confirmed that EPEC actin pedestal formation was reduced in the presence of LVs (Figures 3-3C and 3-3D). Neither fixing LVs nor inhibiting LV-associated IAP activity with L-Phe impacted the ability of vesicles to limit EPEC attachment to HT-29 cells (Figures 3-3E and 3-3F). Finally, purified IAP had little impact on the number of bacteria bound to the monolayer surface (Figures 3-3E and 3-3F). Thus, LVs prevent EPEC from intimately attaching to IECs in culture via a mechanism that does not depend on IAP catalytic activity.

Bacteria and bacterial products activate proinflammatory NF-kB signaling (Wullaert *et al.*, 2011). Thus, we sought to determine whether LVs were capable of preventing activation of NF-kB signaling in response to EPEC. A hallmark of NF-kB pathway activation is translocation of the transcription factor RelA into the nucleus (Goldberg *et al.*, 2008). We transfected HT-29 cells with EGFP-tagged human RelA (Chen *et al.*, 2001), incubated cells in serum free media for 3 hr, and then scored the fraction of transfected cells with nuclear RelA. Under these conditions, 14% of cells expressing the construct demonstrated RelA in the nucleus (Figure 3-3G). In cells

treated with EPEC, nuclear localization of RelA is observed in 31% of expressing cells, compared with 21% in EPEC-exposed cells treated simultaneously with 200 µg LVs/ml (Figure 3-3G). The attenuated response observed here is likely due to the fact that IECs limit expression of cell-surface receptors such as TLR-4, to prevent constitutive proinflammatory signaling (Abreu *et al.*, 2001). Together these data indicate that LVs inhibit interactions between adherent pathogenic bacteria and IECs and limit the downstream NF-kB signaling that would otherwise be triggered by these interactions.

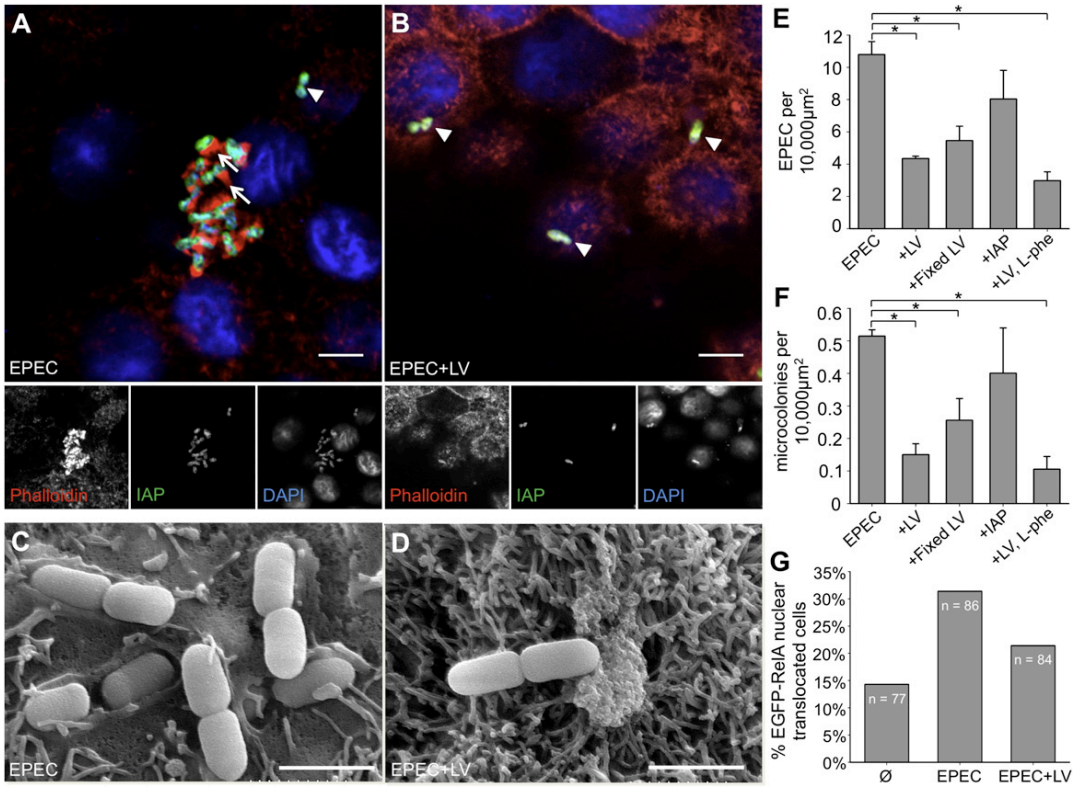

Figure 3-3: LVs prevent EPEC attac hment to IECs

(A and B) CM images of HT-29 monolayers treated with EPEC 6 LVs stained for IAP (green), F-actin (phalloidin, red), and bacteria (DAPI, blue), show striking enrichment of IAP surrounding attached bacteria. Most EPEC in non-LV treated samples (A) form microcolonies and are associated with actin pedestals (arrows), indicating intimate attachment, whereas this rarely occurs in the presence of LVs (B). Arrowheads in (A) and (B) denote examples of EPEC superficially attached to the monolayer, indicated by the absence of pedestal formation. Scale bars represent 5 mm. (C and D) Representative SEM images of CACO-2$_{BBE}$ cells demonstrate EPEC intimately associated with the cell surface in the absence (C), but not the presence of LVs (D). Scale bars represent 1.67 mm. (E) The number of EPEC attached to HT-29 cells is significantly reduced in the presence of LVs, LVs fixed in paraformaldehyde, and LVs with IAP activity inhibited by L-Phe, but not in the presence of purified IAP (*$p < 0.05$). Error bars represent SEM. (F) LVs also reduce the number of microcolonies formed. Error bars represent SEM. (G) Nuclear translocation of EGFP-RelA is increased in HT-29 cells incubated with EPEC, an effect that is partially ameliorated by treatment with LVs.

LVs limit bacterial population growth

Direct association with microbes might also enable LVs to impact bacterial viability. To investigate this possibility, we treated liquid cultures with ~2.5 x 10^4 CFU EPEC/ml with either 0 or 50 µg LVs/ml and incubated overnight; OD_{600} was measured at 10 min intervals. Although addition of LVs did not prevent initiation of log growth in EPEC (t = 4-8 hr), the maximum OD_{600} achieved in the presence of LVs was significantly reduced (Figure 3-4A, black lines). We carried out similar growth assays with bacterial isolates derived from native lumenal material using MacConkey selection (Macconkey, 1905). As with EPEC, native isolates entered log phase approximately 4 hr into the assay, but inclusion of 50 µg LVs/ml reduced the maximum OD_{600} (Figure 3-4A, red and blue lines). 16S ribosomal subunit DNA sequence analysis showed that both commensals used in this assay were members of the genus *Escherichia*, most likely *E. coli* (data not shown). Further experimentation revealed that the impact of LVs on bacterial population growth is not mediated by IAP or its catalytic activity. Addition of purified IAP to cultures at levels that presented 1-10X the catalytic activity of 50 µg/ml of LVs, did not alter the start of log phase or the plateau in OD_{600} (Fig. 3-5A, green lines). To examine the possibility that other catalytic activities associated with LVs (McConnell *et al.*, 2009) impact bacterial growth in these cultures, LVs were fixed with paraformaldehyde and then used in growth assays. Fixation of LVs did not impair their ability to reduce the maximum OD_{600} achieved by EPEC in this assay (Fig. 3-5B, light blue lines). Pre-treating growth media with LVs had no impact on the subsequent population growth of EPEC in the same media, indicating that LVs were not reducing the concentration of nutrients available to growing bacteria or otherwise conditioning the

culture environment (Fig. 3-5B, purple lines). Adding LVs to stationary phase EPEC cultures also led to a striking decline in OD_{600} over a similar 16 hr time course (Figure 3-4B, orange lines). Comparable results were obtained with stationary EPEC cultures that were first replenished with fresh growth media (Figure 3-4B, dark red lines). The reduced OD_{600} values observed in bacterial population growth assays (Figs. 3-4, 3-5) could be the result of LVs inhibiting bacterial growth, LVs accelerating bacterial death, or LVs inducing aggregation of bacteria. The first possibility is unlikely given that LVs are able to reduce the OD_{600} of stationary cultures, where growth is already significantly diminished. To distinguish between the latter two possibilities, we sonicated bacteria cultured in the presence or absence of LVs, to break up any aggregates following the 16 hr growth assays. We then plated dilutions of sonicated material on LB agar plates. The addition of LVs to both stationary cultures and those starting at ~$2.5x10^4$ CFU EPEC/ml led to a reduction in the number of colonies counted per plate (23% and 34%, respectively; Fig. 3-4C). Furthermore, imaging of non-sonicated material did not reveal significant aggregation in the presence of LVs. Thus, LVs most likely reduce OD_{600} values by accelerating bacterial death. Together, these results indicate that LVs limit the population density of commensal and pathogenic *E. coli* in a manner independent of the catalytic activity of IAP or other enzymes.

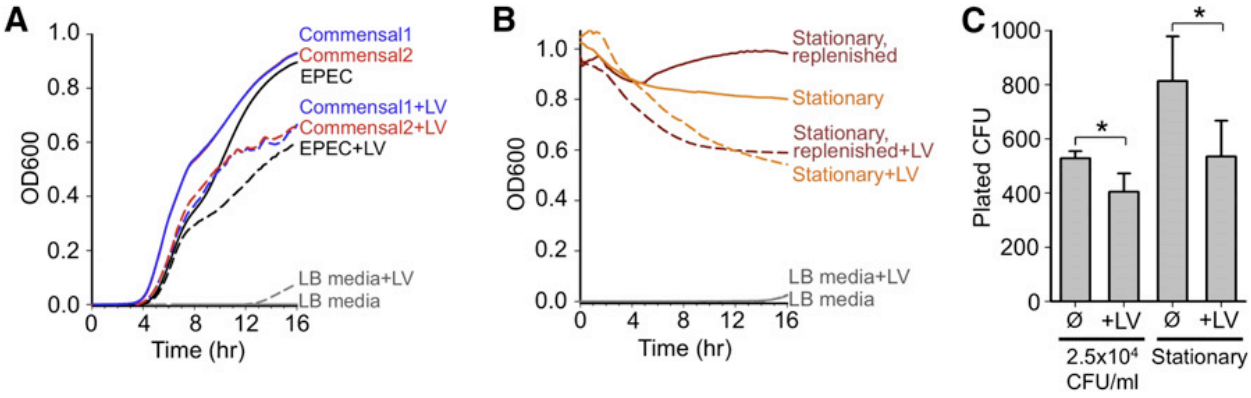

Figure 3-4: LVs inhibit bacterial population growth

(A) Incubating both EPEC and native intestinal bacterial cultures with 50 μg LVs/ml reduces OD_{600} achieved at stationary phase (t = 8–16 hr) following log growth (t = 4–8 hr). Black lines represent EPEC, blue and red lines represent native *E. coli.* (B) Stationary phase EPEC cultures incubated with LVs show a reduction in OD_{600} compared to untreated samples over the course of 16 hr, both in cultures with nutrient-depleted media (orange lines) or fresh media (dark red lines). Traces represent averaged recordings from multiple experiments (n = 3–8). (C) LVs reduce the number of viable bacteria (CFU), as sampled at the end of cultures started with 2.5 x 10^4 CFU/ml and incubated for 16 hr or stationary cultures incubated for 16 hr. *p < 0.05 versus untreated. Error bars represent SEM.

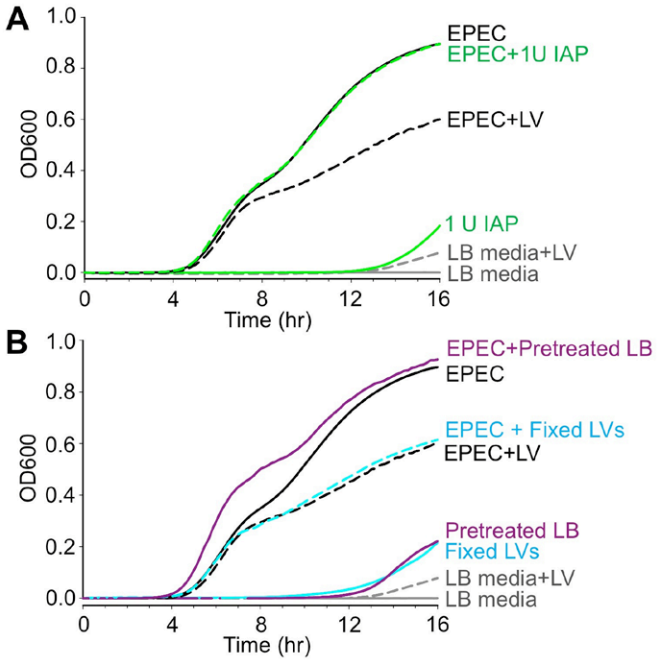

Figure 3-5: Inhibition of bacterial growth is not dependent on IAP activity

(A) Inhibition of growth is not a result of IAP activity, as treatment with 5U IAP/ml, equivalent. (B) Fixing LVs to prevent catalytic activity (light blue lines) does not impair the ability of LVs to inhibit EPEC population growth, while pre-treating growth media with LVs (purple lines) does not alter EPEC population growth. Traces represent averaged recordings from multiple (n = 3-8) experiments.

EPEC stimulates LV production

All of our assays with native LVs isolated from rodent small intestine (Figures 3-1 through 3-5) indicate that LVs likely function as a host defense platform. Because many host defense pathways and processes are regulated by bacterial toxins or intact bacteria (Garrett *et al.*, 2010; Sharma *et al.*, 2010), we sought to determine whether LV production was controlled in a similar manner. For these experiments, we developed a culture model of microvillar vesicle shedding using Caco-2_{BBE} cells (Peterson and Mooseker, 1992; Peterson *et al.*, 1993; Peterson and Mooseker, 1993). Caco-2_{BBE} cells polarize, form a well-ordered brush border, and demonstrate robust microvillar vesicle shedding similar to native IECs, as indicated by the accumulation of small vesicles (Figure 3-6A) containing LV markers, IAP and annexin A13b (McConnell *et al.*, 2009), in culture media (Figure 3-7A). When Caco-2_{BBE} cells were exposed to ~1 x 10^6 CFU EPEC/ml for 6 hr, total cellular levels of IAP increased dramatically (Figure 3-7B), consistent with previous work in zebrafish (Bates *et al.*, 2006). EPEC exposure also significantly increased the amount of IAP-enriched LVs released into culture media (Figure 3-7C). Accumulation of IAP in the 100,000 x *g* pellet likely represents bona fide vesicle shedding, rather than microvillar fragmentation, because no actin is observed in these fractions (Figure 3-7C). Additionally, Caco-2_{BBE} cells expressing the myo1a-TH1 domain (TH1 DN), which acts as a dominant negative inhibiting the function of endogenous myo1a (Tyska and Mooseker, 2004), do not release IAP-enriched vesicles into culture media (Figure 3-7C). We also found that vesicle shedding was stimulated, albeit to a lesser extent, by *Shigella*, another Gram-negative enteric pathogen (Figure 3-6B) (Schroeder and Hilbi, 2008). However, vesicle shedding was not stimulated by

EPEC-conditioned media (Kuehn and Kesty, 2005), heat-killed EPEC, or 10 µg/ml *E. coli* O55:B5 LPS (Figure 3-7C). These findings indicate that microvillar vesicle shedding is upregulated in response to EPEC exposure, and that this response requires live, intact bacteria.

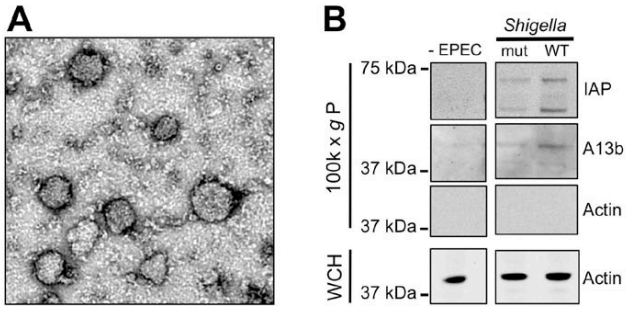

Figure 3-6. Live bacteria stimulate LV release from IECs

(A) Negative stain TEM of the 100,000 x *g* pellet reveals vesicle-like particles that exhibit the characteristic size (50-100 nm diam.) of native LVs. Bar, 100 nm. (B) Like EPEC, both WT *Shigella* and a strain lacking the virulence plasmid stimulate increased shedding of LVs from CACO-2_{BBE} cells, seen by the presence of IAP in the LV containing 100,000 x *g* pellet fraction.

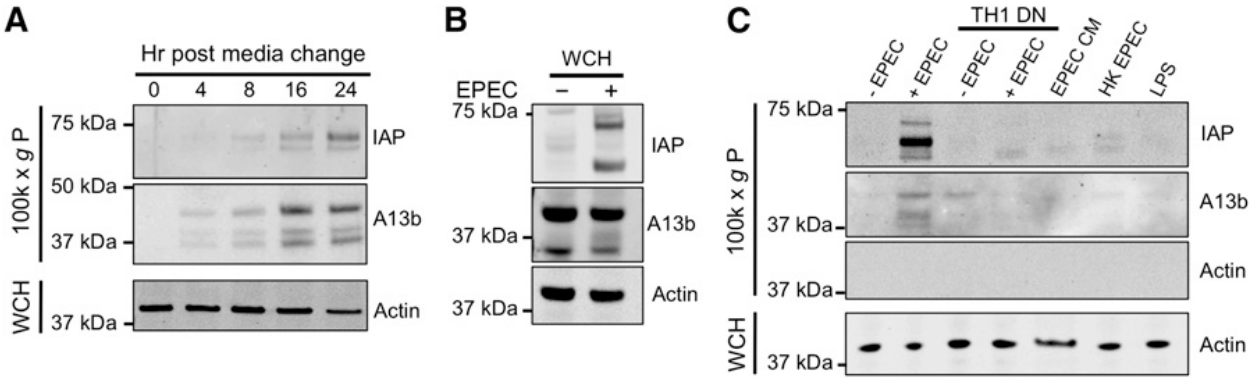

Figure 3-7: EPEC stimulates LV release from IECs

(A) LVs accumulate in Caco-2_{BBE} cell culture media over time. Media was subject to ultraspeed centrifugation and 100,000 x *g* pellets were processed for western blotting with probes for IAP and annexin A13b; whole cell homogenates (WCH) from each time point were processed in parallel and probed for actin. (B) Whole-cell IAP expression levels increase upon exposure to EPEC. (C) EPEC stimulates increased LV production from CACO-2_{BBE} cells, indicated by the presence of IAP in the LV-containing 100,000 x *g* pellet fraction. EPEC-stimulated LV production is attenuated by expression of a myo1a dominant-negative construct (TH1 DN). Shedding requires intact, live bacteria, because EPEC-conditioned media, heat-killed EPEC, and purified LPS fail to stimulate LV production.

Conclusions

Previous work investigating the physiological function of IAP has focused on the activity of this enzyme as a soluble or cell-associated host defense factor in the gut lumen (Koyama *et al.*, 2002; Bates *et al.*, 2007; Goldberg *et al.*, 2008; Chen *et al.*, 2010a; Ramasamy *et al.*, 2010). The findings reported here suggest that microvillar vesicle shedding is a mechanism for distributing IAP activity into the mucous layer or gut lumen. Deploying IAP in this manner would enable chemical modification of bacterial toxins (i.e., dephosphorylation of LPS; Figures 3-1A and 3-1B; Figure 3-2) at sites distal to the apical surface of IECs. However, LVs also limit the attachment of pathogenic bacteria to IECs and inhibit bacterial population growth (Figures 3-3, 3-4 and 3-5). Moreover, IAP expression and LV production are upregulated by pathogenic Gram-negative bacteria (Figure 3-6 and 3-7). Based on these data and the fact that trillions of microvilli extend from the surface of IECs, we propose that microvillar vesicle shedding represents a powerful mechanism for limiting the potentially harmful impact of microbes and associated proinflammatory compounds that accumulate in the intestinal lumen. Future studies must focus on defining mechanisms that regulate LV production in response to microbial signals, mechanisms responsible for the impact of LVs on bacterial viability, and the role of LV production in animal models of gut disease.

CHAPTER III-B

The intestinal lumen is home to an astoundingly large population of microbes, many of which contribute to normal physiological function (Backhed *et al.*, 2005). To prevent these and other, potentially pathogenic bacteria from stimulating inflammation in host tissues, the lumen is enclosed by a tightly regulated barrier formed from a monolayer of intestinal epithelial cells, also referred to as 'enterocytes'. Enterocytes carry out both absorption and barrier functions in part via an apical array of actin-based microvilli collectively known as the brush border. While a significant percentage of brush border proteins are involved in nutrient processing, nutrient absorption, and the maintenance of microvillar structure, others play roles in host defense (McConnell *et al.*, 2011). Among the most abundant of these is IAP, a GPI-anchored enzyme responsible for cleaving phosphate groups from bacterial compounds, including the potent pro-inflammatory toxin, LPS (Poelstra *et al.*, 1997). Dephosphorylation of these molecules renders them less effective at activating host cell TLRs (Rietschel *et al.*, 1994; Park *et al.*, 2009). Studies in the last decade have demonstrated that IAP expression is stimulated by intestinal microbes (Bates *et al.*, 2006) and that the resulting higher levels of IAP protect against microbe-induced inflammation (Bates *et al.*, 2007; Ramasamy *et al.*, 2010). Moreover, treatment with exogenous IAP can limit inflammation upon toxigenic insult *in vivo* (Beumer *et al.*, 2003; van Veen *et al.*, 2005). Thus, IAP is a critical component of innate intestinal immunity.

Work in our laboratory previously demonstrated that specialized membrane vesicles (lumenal vesicles, LVs) are released from the distal tips of enterocyte microvilli (McConnell and Tyska, 2007; McConnell *et al.*, 2009). Biochemical analysis of LVs

revealed that IAP (McConnell *et al.*, 2009) is concentrated on the lumenal surface of these membranes (McConnell *et al.*, 2009); such topology would allow the enzyme access to lumenal toxins and further suggested a physiological function for LVs in host defense. Our more recent studies showed that LVs are in fact able to interact with and limit the pro-inflammatory potential of both bacteria and bacterial products (Shifrin *et al.*, 2012). Based on these recently published findings, we propose a multi-faceted model for LV function in gut host defense (Figure 3-8). First, IAP-enriched LVs are released into the intestinal lumen where they likely function in detoxifying pro-inflammatory bacterial toxins such as LPS, which accumulate during the bacterial life cycle. Second, LVs also bind directly to bacteria, which may serve to aggregate microbes and facilitate their clearance from the intestine, or prevent the adherence of virulent species to the enterocyte apical surface, thereby reducing the probability of infection. Finally, because LVs also exhibit bactericidal properties, they might regulate the gut microbiota by preventing harmful overgrowth.

One important question is whether LVs are produced in large enough numbers to exert a significant effect on gut homeostasis. From a purely theoretical standpoint, the vast numbers of microvilli that extend into the lumen suggest an enormous potential for LV production to impact mucosal physiology. For example, the rodent small bowel contains approximately ~10^{12} microvilli and an estimated ~10^{8} microbes. Thus, LV-producing organelles outnumber bacterial organisms by at least four orders of magnitude. It is also worth noting that our recently described studies of LV function (Shifrin *et al.*, 2012) were carried out using at most a concentration of 200 μg/ml (total LV protein). This level is equivalent to the physiological concentration of LVs captured

from lumen wash preparations and was sufficient to produce robust effects in assays of bacterial attachment and growth (Shifrin *et al.*, 2012). Finally, although LVs can be collected from lumen wash samples (McConnell *et al.*, 2009; Shifrin *et al.*, 2012), our preliminary ultrastructural and immunofluorescence analyses suggest that a large fraction of LVs are trapped in the mucus layer that protects enterocytes. Such trapping is likely to further increase the effective lifetime and thus, the steady-state level of LVs present in the gut lumen.

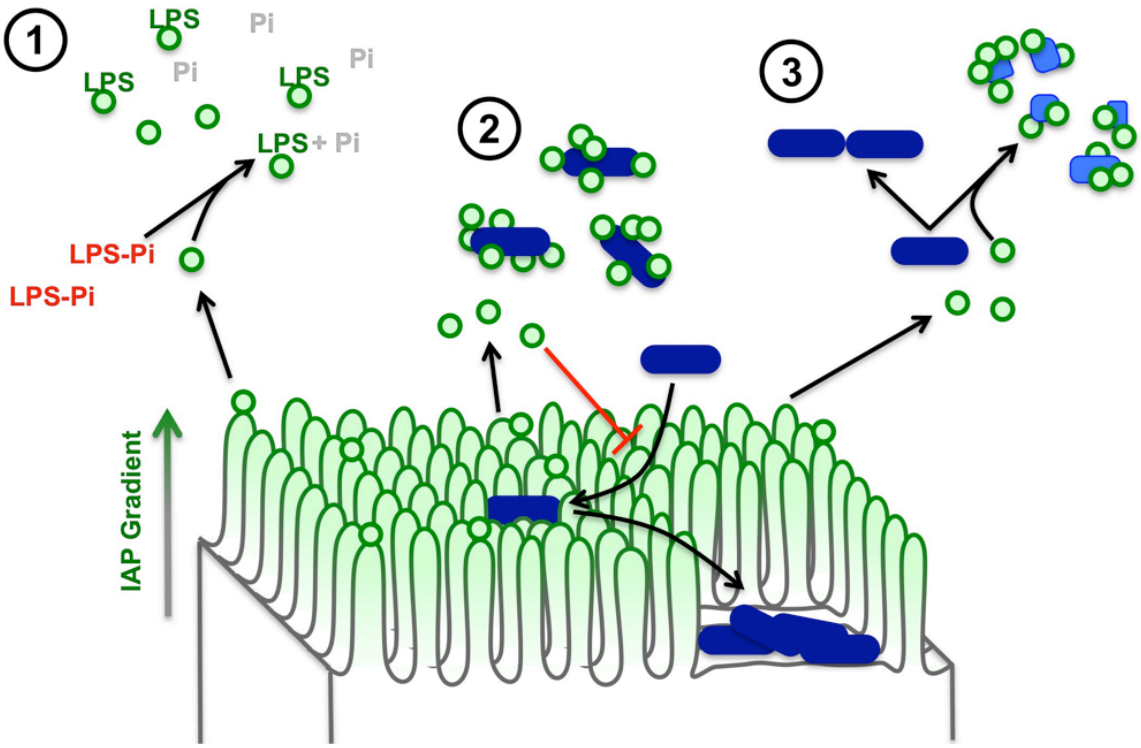

Figure 3-8: A multi-faceted role for LVs in gut homeostasis

The enterocyte brush border produces IAP-enriched LVs, which are found both in the gut lumen and trapped in the mucus layer. As a result, LVs are well positioned to: (1) detoxify soluble bacterial LPS using IAP catalytic activity, (2) bind lumenal bacteria to facilitate clearance and to prevent potential pathogens from adhering to the epithelial surface, and (3) help regulate microbial populations by exerting a bactericidal effect.

If LV production does play a role in limiting host-microbe interactions in the gut, defective vesicle production would be expected to produce significant perturbations in gut homeostasis such as inflammation and a dysregulated microbiota. Mice that lack the shedding motor, myosin-1a (myo1a), produce fewer LVs and those that are formed lack the characteristic enrichment of IAP (McConnell *et al.*, 2009). These animal do shows signs of chronic low level inflammation, including a greater number of goblet cells per villus, increases in the cytokines IL-1α and IL-6, and shifts in the small intestine microbiota at the family level (unpublished observations). Despite these differences, however, myo1a KO mice show no overt phenotype (Tyska *et al.*, 2005), most likely as a result of compensatory mechanisms such as the expression of the closely related motor, myosin-1d (Benesh *et al.*, 2010). In this light, additional animal models that demonstrate more complete loss of LV production must be developed before we can fully appreciate the full range of LV functions *in vivo*.

Several important questions regarding the mechanism of LV production remain unanswered. How is the GPI-anchored protein IAP targeted to microvillar tips, and why is this enrichment lost in the myo1a KO brush border (McConnell *et al.*, 2009)? Our unpublished observations show that microvillar tips are enriched in cholesterol, which provides the backbone for lipid raft formation (Karnovsky *et al.*, 1982). Moreover, microvilli and LVs both contain raft-associated annexin 2 as well as A13b (Massey-Harroche *et al.*, 1998; McConnell *et al.*, 2011), proteins that have been implicated in membrane organization and deformation (Gerke *et al.*, 2005). Thus, one possibility is that a distinct lipid raft-like environment, which favors high membrane curvature, exists at the distal tips of microvilli and helps to attract machinery that might drive LV budding.

High levels of cholesterol would also favor the enrichment of IAP, which is anchored to the external leaflet via a GPI-anchor (Paulick and Bertozzi, 2008). An alternative possibility is that ESCRT complex components mediate vesicle formation. ESCRT complexes are involved in membrane abscission, and as such play a role in viral budding, cytokinesis, and multi-vesicular body formation (Henne *et al.*, 2011). Given that these events are topologically similar to LV release from microvillar tips, ESCRT proteins are also good candidates for driving this process. Beyond these speculative points, a detailed investigation of protein and lipid composition at microvillar tips has yet to be described, but will be needed before we fully understand the molecular mechanism of this novel facet of gut host defense.

CHAPTER IV

THE ABSENCE OF MYO1A LEADS TO INTESTINAL PERTURBATION

Summary

Data from biochemical, cell culture, and bacterial culture assays demonstrate that LVs are enzymatically active organelles that also have a possible physical role in inhibiting bacterial attachment to host cells (Shifrin *et al.*, 2012). The intestinal lumen contains vast numbers of bacteria, many of which are Gram-negative and carry toxins that are IAP substrates (Chen *et al.*, 2010b). Our model of LV function suggests that these organelles are released by enterocyte microvilli, following which some are released into the lumen and others likely become incorporated into the mucus layer lining enterocytes (Fig. 5-1). LVs then interact with lumenal contents, binding to bacteria and inhibiting pathogenic attachment to the epithelia, while LV-bound IAP dephosphorylates LPS and other toxins released during the bacterial life cycle. In the absence of vesicle shedding, therefore, we would hypothesize that pro-inflammatory signaling increases, leading to loss of intestinal homeostasis.

Results

IAP enrichment at microvillar tips is reduced in the absence of myo1a

Previous work from our lab established that the absence of myo1a gives rise to perturbations in LV production; mice lacking myo1a produce fewer LVs, which contain lower levels of IAP and are significantly larger than LVs produced by WT animals (McConnell *et al.*, 2009). Consistent with this, immunofluorescence staining revealed that IAP distribution is altered in the brush borders of myo1a KO small intestine. IAP

signal is evident along the length of KO microvilli, with a heavy concentration observed in a band just above the terminal web at the base of microvilli (Fig. 4-1A). Concomitantly, few tip-enriched IAP puncta, which represent LV precursors, are observed in KO tissue (Fig. 4-1B). This distribution is inverted relative to WT animals; some microvillar localization is seen, with a slight accumulation at the base of microvilli and a gradient along the length of the actin (Fig. 4-1A). However, the majority of IAP signal in WT tissue is past the distal tips of the microvilli in LV precursors (Fig. 4-1B). It is possible that the absence of myo1a perturbs microvillar lipid composition, altering the distribution of cholesterol enriched lipid rafts and thereby preventing normal segregation of raft-associated proteins. A population of myo1a is important for retaining SI in the microvillus, and SI is depleted in LVs relative to microvillar membrane (Tyska and Mooseker, 2004; McConnell *et al.*, 2009). Thus, myo1a may be important for partitioning microvillar membrane by linking a sub-population of membrane lipids to the underlying core actin bundle. IAP-containing rafts, unconstrained by a cross-linker and with a possible preference for high-curvature, could diffuse out to the distal tips and for LV precursors. A specific mechanism for IAP enrichment and LV scission from microvillar tips should be the focus of future studies.

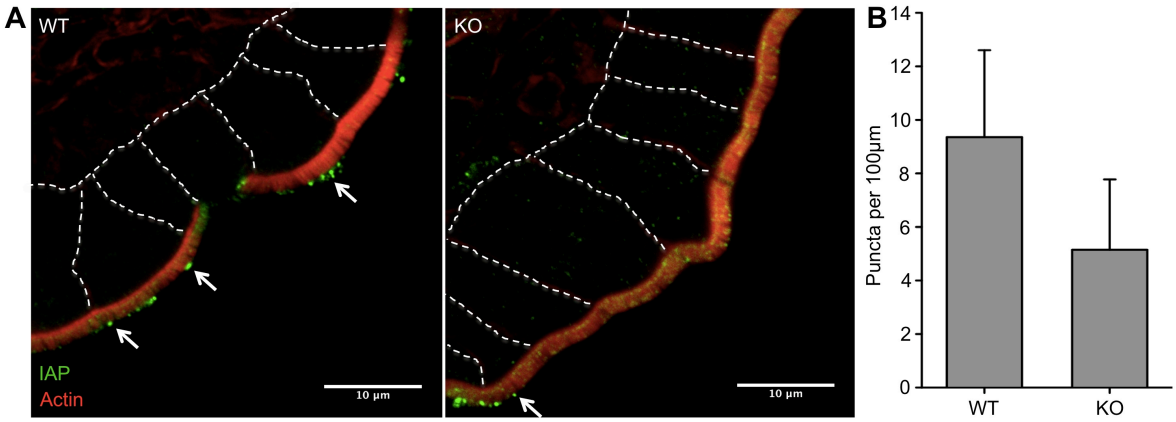

Figure 4-1: IAP distribution is altered in the absence of myo1a

(A) LSCM images of frozen sections from WT and myo1a-KO mouse small intestine show that characteristic WT IAP enrichment at the distal tips of microvilli is reduced in the absence of myo1a. IAP signal in KO microvilli is observed less frequently at microvillar tips, and instead is seen more evenly distributed along the microvillar axis. Tissue processing and staining is described in (McConnell and Tyska, 2007). (B) Quantification of IAP puncta at the tips of microvilli in WT and myo1a KO small intestine. n = 4 WT and 3 KO small intestines.

Defects in LV production are linked to alterations in the lumenal microbiota in vivo

Given that microvillus-derived LVs interact directly with native lumenal bacteria, prevent adherence of pathogenic bacteria to epithelial cells, and impact the growth of the *E. coli* strains *in vitro*, we examined the possibility that LVs might function in regulating the growth and diversity of bacterial species that reside in the gut lumen. To determine if defective LV production observed in myo1a KO mice is associated with perturbations in the gut microbiota, we isolated DNA from WT and myo1a KO distal gut contents and amplified bacterial DNA encoding the 16S ribosomal subunit using the conserved 8F/1492R primer set (Eden *et al.*, 1991; Schmidt and Relman, 1994). We then sequenced amplified PCR products with the conserved primer 907R (Wen *et al.*, 2008), and used the Ribosomal Database Project (Wang *et al.*, 2007) to identify bacteria from which the DNA was derived, discarding sequences with < 80% confidence at the

genus level (n of sequences ≥ 80% confidence = 458 for WT and 433 for myo1a KO). Although we did not observe significant changes at the phylum level when comparing WT and myo1a KO samples, two striking shifts occur within the phylum *Bacteroidetes* (blue segments, Fig. 4-2), one of the two dominant phyla that comprise the distal gut microbiota (Ley *et al.*, 2008). As proportions of total sequences, family *Bacteroidaceae* is increased in KO animals by 43.0% and family *Porphyromonadaceae* is reduced by 21.3% (Fig. 4-2 and Table 4-1). Other notable changes include a 10.7% increase in the abundance of *Prevotellaceae* and 13.9% increase in *Rikenellaceae*.

Although the percent change varies from previously published studies, the bacterial families affected in our analysis are consistent with other work demonstrating shifts in the microbiota following antibiotic treatment (Wlodarska *et al.*, 2011), infection by the murine pathogen *Citrobacter rodentium* (Lupp *et al.*, 2007), and genetic manipulation of the TLR-4/NF-κB pathway in a mouse model of diabetes (Wen *et al.*, 2008). Little is known about the function of *Porphyromonadaceae* in the intestine, or the consequences of alterations in relative abundance. *Prevotellaceae*, however, are commensals observed to be opportunistic pathogens in humans (2009). Similarly, the genera *Bacteroides* of the family *Bacteroidaceae*, contains both critical commensal species, as well as opportunistic pathogens such as *B. fragilis* (Wexler, 2007). These results show that the absence of myo1a and associated defects in LV production are linked to alterations in the gut microbiota and suggest a role for microvillar vesicle shedding in maintaining gut homeostasis.

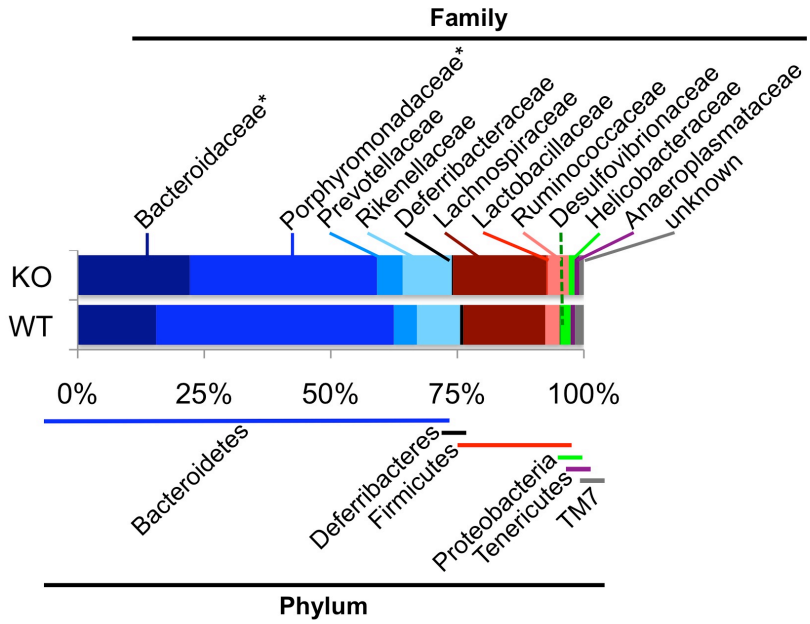

Figure 4-2: Deficiencies in LV shedding are associated with an altered gut microbiome

Analysis of bacterial 16s rDNA sequences isolated from the WT and myo1a KO mice reveals shifts in the distal gut microbiota, especially in families of the Gram-negative phylum *Bacteroidetes* (blue segments), which is the predominant gut phylum and includes species of commensals and opportunistic pathogens. Notable shifts include increased numbers of the family *Bacteroidaceae* and decreases in *Porphyromonadaceae*, which consist primarily of benign commensal species but also include opportunistic pathogens.

Phylum	Family	WT (n = 458)	KO n = (433)
Bacteroidetes	*Bacteroidaceae**	15.50% (71)	22.17% (96)
	*Porphyromonadaceae**	46.94% (215)	36.95% (160)
	Prevotellaceae	4.59% (21)	5.08% (22)
	Rikenellaceae	8.52% (39)	9.70% (42)
Deferribacteres	*Deferribacteraceae*	0.66% (3)	0.23% (1)
Firmicutes	*Lachnospiraceae*	16.16% (74)	18.48% (80)
	Lactobacillaceae	0.00% (0)	0.23% (1)
	Ruminococcaceae	2.84% (13)	4.16% (18)
Proteobacteria	*Desulfovibrionaceae*	0.22% (1)	0.00% (0)
	Helicobacteraceae	1.97% (9)	1.15% (5)
Tenericutes	*Anaeroplasmataceae*	0.87% (4)	0.92% (4)
TM7	*unknown*	1.75% (8)	0.92% (4)

TABLE 4-1. Changes in the distal gut microbiome of LV-deficient myo1a KO mice

*Analysis of over 400 bacterial 16S sequences isolated from the distal intestines of seven WT and seven myo1a KO FVB mice (identity at ≥ 80% confidence) reveals striking increases in the *Bacteroidaceae* population and concomitant decreases in the *Porphyromonadaceae*, both of the Gram-negative phylum *Bacteroidetes*.

Myo1a KO mice exhibit signs of chronic, low-level intestinal inflammation

Alterations in the gut microbiota are frequently associated with an inflammatory state; shifts in bacterial populations can both cause intestinal perturbation and be the result thereof (Peterson *et al.*, 2008; Packey and Sartor, 2009). In light of our data showing family level shifts in the microbiota of myo1a KO mice, we next sought to determine if these animals exhibit an inflammatory phenotype. Original characterization of the myo1a KO mouse found significant ultrastructural changes relative to WT (Tyska *et al.*, 2005). These include variable microvillar length and loss of tight hexagonal packing, substantial membrane herniations at the tips of microvilli, changes to villar morphology, and a loss or reduction in the localization of several brush border proteins (Tyska *et al.*, 2005). However, these animals were of comparable size to WT and had normal behavioral habits. Clearly, although the absence of the microvillar motor myo1a caused alterations to the KO enterocyte, the defects were not strong enough to significantly perturb overall animal health. For this analysis, then, we focused specifically on inflammatory markers, which had not been investigated in the original work.

Goblet cells secrete mucins, which form a two-layer coating across the intestinal epithelia to prevent bacterial contact with the host cells and subsequent infection (McGuckin *et al.*, 2011). We stained small intestine Swiss rolls with Periodic acid-Schiff (PAS)/Alcian blue to label the glycoproteins, glycolipids, and mucopolysaccharides produced by goblet cells. Quantification revealed a ~25% increase in the number of goblet cells per villus in the small intestine . Along the length of the tissue, the number of goblet cells per villus decreased slightly from proximal to distal in the WT intestine, from

~8.5 to ~7.25 (Fig. 4-3A, B). This decrease is likely due in part to the steady decline in villus length that occurs from the duodenum to the ileum. Interestingly, no decrease was observed along the myo1a KO intestine, with the average number of goblet cells per villus remaining steady at 10 (data not shown). The microbiota is important for cell fate decisions in intestinal epithelia; germ-free mice have lower numbers of goblet cells than their normally colonized counterparts (Kandori *et al.*, 1996; Fukushima *et al.*, 1999). Goblet cell differentiation is defective in mouse models of ulcerative colitis, leading to a defficient mucus layer due to reduction in mucus and defensin secretion (Gersemann *et al.*, 2011; Gersemann *et al.*, 2012). Infection and subsequent inflammation increases significantly in mice lacking MUC1, a mucin produced by goblet cells (McGuckin *et al.*, 2011). Furthermore, mutations in this same gene have been implicated in inflammatory bowel disease in humans (McGuckin *et al.*, 2011). Goblet cell metaplasia is also observed in mouse models of airway inflammation, a response which can be attenuated by the introduction of non-pathogenic *E. coli* (Pang *et al.*, 2013). It may be, then, that shifts in the microbiota cause perturbations to intestinal homeostasis, inducing a slight increase in goblet cell differentiation to help protect the epithelium.

We also observed regions of excessive eosinophil infiltration in myo1a KO colon tissue (Fig. 4-3C). As with the increase in goblet cell numbers, eosinophils are likely part of a low-level inflammatory response. Although specific roles for these cells in the intestine remain unclear, eosinophils have been implicated in antimicrobial processes in response to the presence of Gram-negative lipopolysaccharide, as well as promoting increased mucus production (Woodruff *et al.*, 2011).

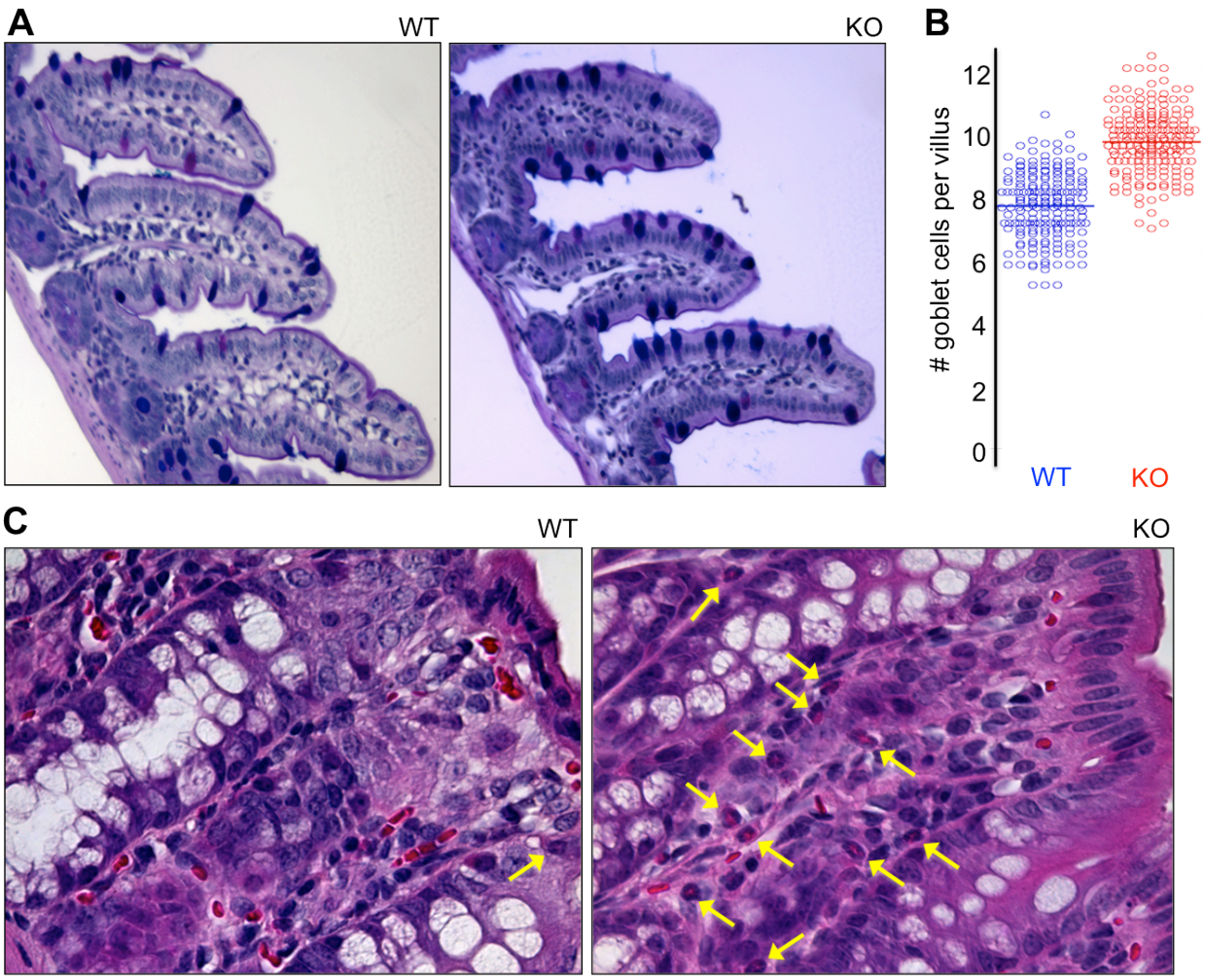

Figure 4-3: Myo1a KO intestines show histological signs of inflammation

(A) PAS/Alcian blue staining of paraffin-embedded small intestine to label mucus-producing goblet cells shows that a greater number of these cells occur in myo1a KO villi when compared with WT. Increased numbers of goblet cells is associated with inflammation. (B) Quantification of tissue shown in 'A.' Each data point represents one villus. (C) Hematoxylin & Eosin staining of mouse colon shows regions of eosinophil infiltration into the lamina propria layer of myo1a KO tissue.

A hallmark and key regulator of inflammatory signaling is the increased expression of various cytokines. Interleukin-1α (IL-1α) and IL-6 are two of these proinflammatory cytokines, responsible for activating an array of immune responses (Bankers-Fulbright *et al.*, 1996; Jin *et al.*, 2010). We flushed WT and myo1a KO small intestines, removed and homogenized the mucosal layer, and subjected the resulting material to ELISA analysis for IL-1α and IL-6. Both cytokines were slightly elevated in KO tissue, with IL-1α levels increased by ~25% and IL-6 expression up by ~70% (Fig. 4-4).

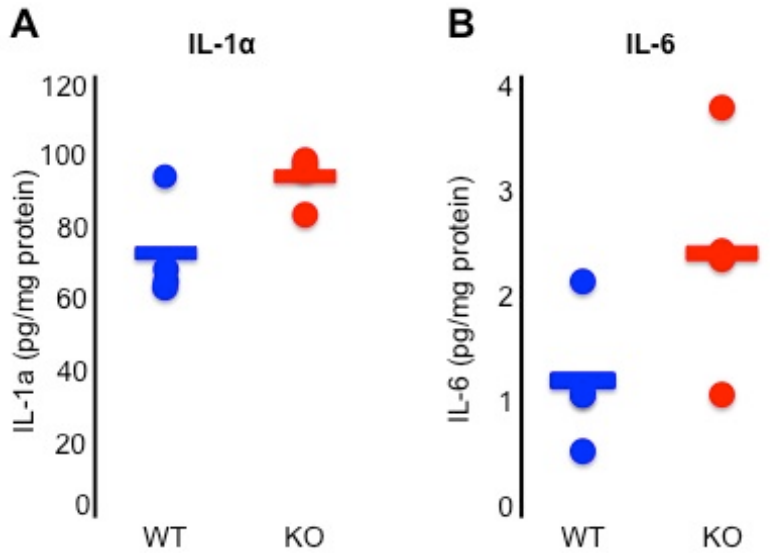

Figure 4-4: Increased cytokine production in myo1a KO intestinal tissue

ELISA of homogenized small intestinal mucosa for two proinflammatory cytokines, (A) IL-1α and (B) IL-6, show slight, but notable increases in the absence of myo1a. These molecules are key regulators of inflammatory signaling, elevation indicates perturbation of intestinal homeostasis.

Discussion

Together, these histological and biochemical findings suggest chronic, though low-level inflammation in the myo1a KO intestine. Despite the observed changes in the microbial population markers of inflammation, these animals are healthy under typical laboratory housing conditions. Clearly, the loss of normal LV shedding is enough to perturb intestinal physiology, but not enough to cause a significant deficit in host defense. This is likely due to multiple factors, centered around the idea that because the mamallian intestine is critical for survival in the context of both nutrient absorption and host defense, intestinal architechure is highly redundant to minimize significant problems. Importantly, IAP still reaches the lumen in the myo1a KO intestine. LVs are no longer shed in a regulated manner from myo1a KO microvilli; however, membrane is still released as a result of microvillar herniations (Tyska *et al.*, 2005; McConnell and Tyska, 2007; McConnell *et al.*, 2009). Similarly, IAP is still present in these membrane fractions, though not specifically enriched (McConnell *et al.*, 2009). A soluble form of IAP is found in serum after feeding, likely released from membrane by the action of PI-PLC or PI-PLD and secreted from the basolateral compartment (Harris, 1990); it is possible that there may also be a limited amount of IAP released from the apical domain.

The constant pressure of inflammatory signals could also lead to a downregulation of TLRs in myo1a KO epithelia. TLR-4 levels are relatively low in enterocytes as a means to prevent excessive response to the permanent presence of bacterial signaling molecules in the intestinal lumen (Abreu *et al.*, 2001). Similarly, IAP deficient mice are less responsive to treatment with LPS due to downregulation of its receptor, TLR-4 (Chen *et al.*, 2010a). Thus, a reduction in IAP-enriched LVs in the

intestinal lumen would leave higher concentrations of phosphorylated (i.e. toxic) bacterial molecules, forcing the host epithelia to downregulate receptors in order to limit an inflammatory signaling cascade.

A final possible component to the limited phenotype observed in myo1a KO animals is the presence of a compensatory motor protein, myosin-1d (myo1d). Work from our lab has shown that in the absence of myo1a, myo1d localization in the microvillus increases by > 2-fold over WT and distributes along the length of microvilli. This shift in localization from characteristic bands at the base and tip of microvilli may allow myo1d to partially rescue membrane tension by serving as a compensatory cross-linker with microvillar actin (Benesh *et al.*, 2010).

These studies further support the growing body of literature demonstrating the importance of IAP in maintenance of intestinal homeostasis, and strongly implicate LVs as mediators of IAP delivery to the intestinal lumen. Without the ability to completely ablate LV/membrane release, it will be difficult to fully elucidate the extent to which IAP-enriched LVs function in host defense. Future studies should also focus on the response of myo1a KO mice to pathogenic challenge. It is possible that the limited inflammatory phenotype observed during normal conditions could be exacerbated in the presence of an enteric pathogen such as *Citrobacter rodentium*, the murine equivalent of EPEC.

CHAPTER V

EXTRACELLULAR VESICLES: COMMUNICATION, COERCION, AND CONDITIONING

Originally published as:

Shifrin, D.A., Jr., Beckler, M.D., Coffey, R.J., and Tyska, M.J. (2013). *Extracellular vesicles: communication, coercion, and conditioning.* Molecular Biology of the Cell *24*, 1253-1259.

Introduction

Cells play an active role in shaping their local environment by releasing factors that impact neighboring cells or manipulate the biochemical properties of the extracellular milieu. Although soluble protein ligands have received the most experimental attention in this regard, a rapidly growing field of investigation suggests that these events are also mediated by small extracellular vesicles (ECVs). Indeed, ECVs are now known to affect events ranging from immune signaling to angiogenesis to detoxification of bacterial products (Thery *et al.*, 2009; Mause and Weber, 2010; Shifrin *et al.*, 2012). In these cases and many others, ECVs facilitate the distribution of specific cargoes that mediate communication with or coercion of other cells, or the conditioning of the extracellular environment.

ECVs range in size from ~50-500 nm and are typically enriched in specific proteins and lipids, which differentiates their composition from the plasma membrane (Mause and Weber, 2010). One challenge for investigators new to this field is the variable and confusing nomenclature that exists in the ECV literature; this is primarily a result of the many cellular sources, isolation procedures, and apparently distinct mechanisms of formation. For the purposes of this discussion, we group ECVs into two broad categories that are distinguished by their mechanism of formation: exosomes and ectosomes. Exosomes (40-100 nm) are likely produced through an exocytic pathway via the formation of multi-vesicular bodies (MVBs) and their subsequent fusion with the plasma membrane (Mathivanan *et al.*, 2010). In contrast, ectosomes range from 100-500 nm in diameter and are released through outward budding of the plasma membrane. Other names for ectosomes one might encounter in the literature are

'microvesicles', 'membrane particles', 'microparticles,' or 'nanoparticles' (Bastida *et al.*, 1984; Thery *et al.*, 2001; Cocucci *et al.*, 2009; Mathivanan *et al.*, 2010; van der Pol *et al.*, 2012). Both exosomes and ectosomes are formed such that the original plasma membrane topology is maintained, i.e. vesicles are released into the extracellular space with membranes 'right-side out' (van der Pol *et al.*, 2012). Exosomes and ectosomes are produced by a vast array of cell types in a variety of physiological contexts, suggesting that they may contribute to many essential aspects of cell and tissue function, some of which will be discussed in more detail below.

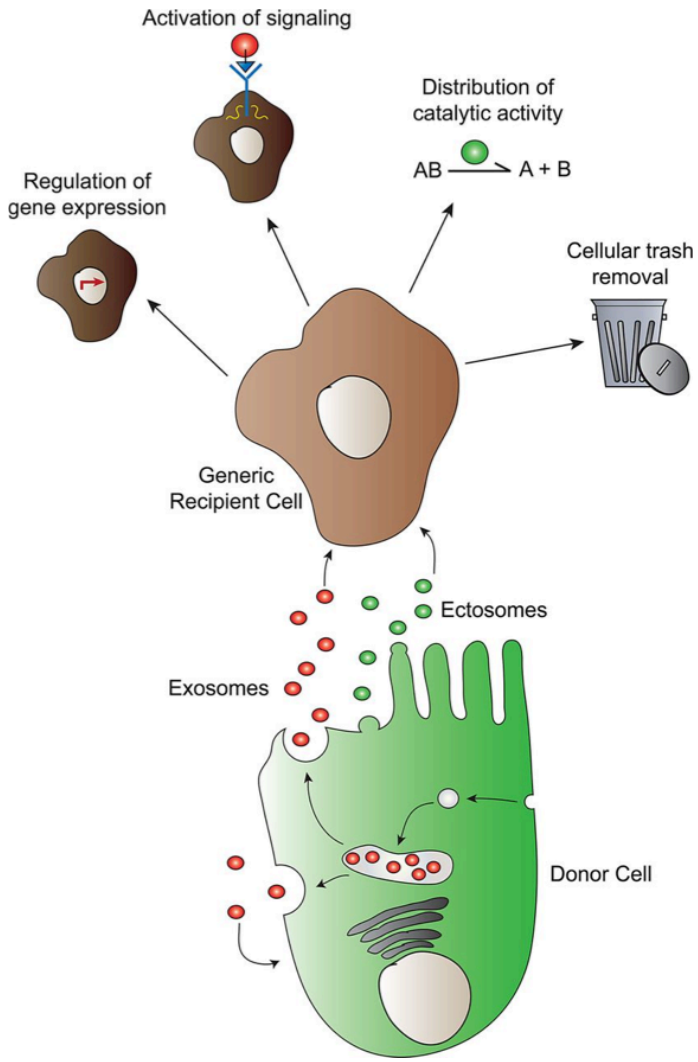

Figure 5-1: Extracellular vesicle biogenesis and function.

Extracellular vesicles are formed via two known biogenesis pathways: exosomes via an endomembrane MVB intermediate, and ectosomes via direct budding from the plasma membrane. Once released into the extracellular environment, ECVs perform one of four general functions: 1) regulation of gene expression, 2) activation of cell signaling, 3) distribution of catalytic activity, and 4) cellular trash removal.

Mechanisms of ECV formation

Exosome biogenesis

Although the molecular details underlying exosome production remained unclear for many years, recent models have converged on a late-endosomal, MVB-dependent pathway (de Gassart *et al.*, 2004; Hurley and Odorizzi, 2012). How specific cargoes destined for exosomes sort into these membranes and how differentiated vesicles bud into the lumen of the MVB is still a matter of debate. An initial lipid-centric model suggested that ceramide enrichment in endosomal membranes was a major driving force (Trajkovic *et al.*, 2008). Because of the small size of its head group, ceramide may directly influence the shape of the membrane to promote bending and downstream budding of vesicles. This model also invokes ceramide in the formation of raft-like domains that presumably function to sort specific cargo molecules into exosomal membranes, although this point has not been tested directly. A second model that has gained support more recently suggests that exosome formation follows a mechanism that parallels the endolysomal degradation pathway, which relies on the function of ESCRT (**e**ndosomal **s**orting **c**omplex **r**equired for **t**ransport) complex machinery to generate MVBs (van Niel *et al.*, 2006). Indeed, RNAi silencing of key ESCRT components tumor susceptibility gene 101 (TSG101, ESCRT-I), vacuolar protein sorting (VPS)22 (ESCRT-II), charged multivesicular body protein (CHMP)2A, CHMP4A/B/C (ESCRT-III), VPS4A/B, or ALIX (an ESCRT-III interacting protein) significantly reduces exosome production in MCF-7 cells (Baietti *et al.*, 2012). Other studies reported decreased exosome secretion from dendritic cells after silencing of the ESCRT-0 protein hepatocyte growth factor-regulated tyrosine kinase substrate (Hrs) (Tamai *et al.*,

2010). Cargoes destined for endolysomal degradation are selectively recruited to the limiting membrane of the MVB through a process that involves their ubiquitylation and subsequent ubiquitin-dependent interactions with ESCRT-0, I, and II (Raiborg and Stenmark, 2009). However, ALIX can bind directly to exosomal cargo molecules, which might represent a ubiquitin-independent recruitment mechanism and also provide a point of distinction between sorting into exosomes versus endolysosomes (Baietti *et al.*, 2012; Hurley and Odorizzi, 2012). Although the extent of functional overlap between the ceramide-dependent and ESCRT-dependent pathways outlined here is currently unclear, the mechanistic details will likely become the focus of future studies.

Following MVB formation, a subset of these organelles fuse with the plasma membrane and release their constituent exosomes (Thery *et al.*, 2002). Although little is known about the direct regulation of MVB fusion with the plasma membrane, it appears that several Rab GTPases, including Rab5, Rab27, and Rab35 are involved in exosome secretion (Vanlandingham and Ceresa, 2009; Hsu *et al.*, 2010; Ostrowski *et al.*, 2010; Baietti *et al.*, 2012). Further investigation will be needed to clarify the role of various Rab proteins in MVB fusion with the plasma membrane and exosome release.

Ectosome biogenesis

Although comparatively little is known about the details of ectosome formation, current evidence suggests that ectosomes are produced not from an endomembrane system as for exosomes, but by direct budding from the plasma membrane (Thery *et al.*, 2009). Despite this seemingly significant mechanistic distinction, proposed models of ectosome formation include elements that are common to the production of exosomes. For example, the topology of outward budding from the plasma membrane is

equivalent to budding into the MVB lumen. Thus, one might expect the ESCRT system to be involved in ectosome formation. Indeed, recent studies revealed that arrestin-domain containing-1 (ARRDC1) interacts with the ESCRT component TSG101, during ectosome shedding directly from the plasma membrane (Nabhan *et al.*, 2012). Another parallel with exosome production is related to the significance of specific lipids in vesicle budding from the plasma membrane. ECVs of both types are enriched in cholesterol, ceramide, and other lipids implicated in raft formation. In glial cells, for example, production of ceramide is thought to promote membrane curvature during ectosome formation (Bianco *et al.*, 2009).

An alternative pathway for ectosome formation might involve actin-based motors. In the context of the enterocyte brush border, the membrane-binding motor, myo1a, distributes along the length of the microvillus where it exerts plus-end (tip-ward) directed force on the apical membrane (McConnell and Tyska, 2007). This activity leads to the accumulation of membrane at microvillar tips, which in turn drives the formation and release of ectosomes into the gut lumen (80-100 nm in diameter). Mice lacking myo1a produce fewer ectosomes and those that are released lack characteristic enrichment of cargo molecules, such as the host defense factor intestinal alkaline phosphatase (McConnell *et al.*, 2009). Although the involvement of myo1a in this system is likely an adaptation linked to the unique morphology of the microvillus, these studies suggest that manipulation of plasma membrane mechanics is of central importance to the mechanism of ectosome formation.

TABLE 5-1: Physiological roles of ECVs

Category	Location/Source	Function	Cargo	Refs (*Review)
Immunity	Enterocyte	Anti-inflammatory, anti-bacterial	Intestinal alkaline phosphatase	(Shifrin *et al.*, 2012)
	Macrophage, Mast cell, B Cell, Dendritic cell	Immune cell activation, antigen presentation, MHC transfer	IL-1β, TNF- α, HMGB1	(Thery *et al.*, 2009; Cicero, 2013)*
	T-Cell, PMN	Immune modulation	FasL	(van der Pol *et al.*, 2012)*
	Microglial cell	Immunostimulation, increased neruotransmission	IL-1β	(Turola *et al.*, 2012)*
	Mono/lymphocyte	Promote T. cruzi infection	TGF-β	(Cestari *et al.*, 2012)
	Syncytiotrophoblast	Immunosupression	CD63, PLAP, TGF- β, FasL, ULBP, mRNAs, miRNAs	(Mincheva-Nilsson and Baranov, 2010)*
	Dendritic cell	T_H1 response-activation, natural killer activation, anti-inflammatory	MHC proteins, antigens, T-cell stimulatory molecules	(Zitvogel *et al.*, 1998; Thery *et al.*, 2001; van der Pol *et al.*, 2012)*
Development	Stem cell	Tissue repair, plasticity, reprogramming	mRNA, miRNA	(Camussi *et al.*, 2011; Tetta *et al.*, 2011)*
	Cardiomyocyte in culture	Gene transfer, gene expression changes	mRNA, chromosomal DNA	(Waldenstrom *et al.*, 2012)
	Endothelial progenitor cell	Angiogenesis	mRNA	(Mause and Weber, 2010)*
	Lung tissue	Fate determination, marrow cell phenotype	mRNA	(Aliotta *et al.*, 2007; Aliotta *et al.*, 2010; Aliotta *et al.*, 2012)*
	Experimentally induced in HEK-293	Confer permissiveness for iPSC generation	mCAT-1	(Mangeot *et al.*, 2011)
Neurological	Microglial cell	Immunostimulation, increased neruotransmission	IL-1β	(Turola *et al.*, 2012)*
	Primary neuron, esp. somatodendritic compartment	"synaptic transmission and plasticity," Neurodegeneration	GluR2	(Schneider and Simons, 2012)
Bone	Epiphysis	Cartilage calcification	TNAP	(Golub, 2009, 2011)*
Blood/ Cardiovascular	Platelets	Thrombus formation, Immune cell activation, angiongenesis/neovascularization	Tissue factor, Chemokines, IL-1β, signaling lipids	(Hundelshausen and Weber, 2007; Mause and Weber, 2010; Owens and Mackman, 2011; Rautou *et al.*, 2011; Zwicker *et al.*, 2011)*
	Endothelial Cell	May promote athlerosclerosis		(Rautou *et al.*, 2011)*
	Smooth Muscle cells (Aorta)	May promote athlerosclerosis		(Bobryshev *et al.*, 2012)
Cancer	MDA- MB-231	Increase tumor cell invasion	Amphiregulin	(Higginbotham *et al.*, 2011)
	Most cancer cell tyeps (Medullablastoma, melanoma, glioblastoma, colon, gastric, etc.)	Increased invasiveness, Anti-tumor Immunosuppression, possibly T-cell priming	Oncogenic sequences, ssDNA, retrotransposons, tumor antigens, cytokines	(D'Souza-Schorey and Clancy, 2012)* (Iero *et al.*, 2008)*
	Glioma cell	Transfer of EGFRvIII	EGFRvIII	(Al-Nedawi *et al.*, 2008)

Physiological roles of ECVs

ECVs are released from a variety of 'donor' cell types and contribute to an array of physiological processes. In the following section, our discussion of ECV function is organized according to physiological context; key examples and relevant references are highlighted in Table 5-1.

Development

While relatively little is known about ECVs during vertebrate development, several reports provide clues as to how these vesicles might contribute to normal morphogenesis. ECVs are detected in the peripheral circulation of pregnant women and ECV cargo vary based on the phase of gestation (Abrahams *et al.*, 2004; Frangsmyr *et al.*, 2005; Atay *et al.*, 2011; Clifton *et al.*, 2012). Although it is unknown how ECVs act during gestation, studies have shown that proteins with established functions in development are found in ECVs. For example, β-catenin, Wnt, and the Wnt cargo receptor Evi are components of exosomes purified from cultured human (HEK293, Caco-2) and Drosophila (S2,Kc167) cells (Chairoungdua *et al.*, 2010; Gross *et al.*, 2012). The function of β-catenin- and Wnt-containing exosomes is not clear at present, but given the central role these proteins play in tissue and organ development (Petersen and Reddien, 2009), it is tempting to speculate that their function may be facilitated by distribution in ECVs. Additionally, sonic hedgehog (SHH) is contained in ECVs from activating T lymphocytes**,** and these vesicles appear to function in promoting neovascularization (Soleti and Martinez, 2012). SHH has critical functions during embryogenesis, including patterning of the nervous system (Fuccillo *et al.*, 2006) and development of the GI system and other endoderm-derived organs (van den Brink,

2007). Thus, with high concentrations of the morphogen, it seems likely that SHH-containing ECVs could exert similar effects on developing organs and tissues. Combined, these studies are suggestive of developmental roles for ECVs, but future studies are warranted to clarify functional roles and molecular mechanisms.

Immunity

ECVs are shed from immune cells, with upregulated production occurring upon stimulation by inflammatory signaling (van der Pol *et al.*, 2012; Cicero, 2013). Conversely, infected cells can also release ECVs, which target immune cells and activate innate responses (Dreux *et al.*, 2012). For example, hepatitis C-infected cells release viral RNA packaged inside exosomes (genetic material is a common ECV cargo), which are then taken up by plasmacytoid dendritic cells (Dreux *et al.*, 2012). Moreover, ectosomes shed from intestinal epithelial cells are highly enriched in intestinal alkaline phosphatase, and serve to both detoxify soluble bacterial LPS and inhibit bacterial colonization of the intestinal epithelial surface (Shifrin *et al.*, 2012). Lumenal ECVs are shed constitutively as they can be isolated from the small intestine of uninfected rodents and sterile cell culture models. However, ectosome production increases dramatically in the presence of bacterial pathogens (Shifrin *et al.*, 2012). Similarly, ECV shedding from macrophages and microglial cells is dependent upon activation of the ATP receptor and ligand-gated ion channel $P2X_7$, which can be induced by exogenous ATP (e.g. as a result of cellular injury) or through normal ATP release into the extracellular environment of astrocyte-microglia co-cultures ((Bianco *et al.*, 2005; Thomas and Salter, 2010). $P2X_7$ can also be activated during sterile inflammation (Thomas and Salter, 2010). ATP released from astrocytes in culture is sufficient to

stimulate ECV release from microglia (Bianco *et al.*, 2005); these vesicles carry pro-inflammatory cytokines, including IL1-β, and are capable of activating other macrophages and perhaps dendritic cells (Thomas and Salter, 2010). Activation of macrophages by ECVs suggests the initiation of a large-scale inflammatory response. However, it is possible that in some instances the targeted, local activation of ECV shedding through TLR-4 signaling or other inflammatory mechanisms could actually prevent such a system-wide process. By releasing lumenal ECVs to combat bacterial attachment, for example, enterocytes could mitigate the spread of the infection, thereby abrogating the need for mounting a systemic anti-inflammatory response (Shifrin *et al.*, 2012). In the case of virally infected cells, host cells use ECVs to communicate with neighboring uninfected cells, which serves to initiate an immune response (Dreux *et al.*, 2012). This allows an appropriate local scale response without hyper-activating the immune system or further spreading the pathogen.

Bone formation

Matrix ECVs found in the epiphysis of long bones bear a strong resemblance to ECVs shed from enterocyte microvilli. Matrix ECVs are ectosomes, released during the calcification process and are highly enriched in tissue non-specific alkaline phosphatase (Golub, 2009, 2011). This enzyme decreases the concentration of inorganic pyrophosphate, increases that of inorganic phosphate, and as a result promotes hydroxyapatite formation and bone mineralization (Golub, 2011). Although isolated from entirely different contexts, microvillus-derived ECVs and matrix ECVs share a common function in biochemically conditioning their local microenvironment. In the former case, dephosphorylation of LPS by alkaline phosphatase significantly reduces LPS toxicity

(Poelstra *et al.*, 1997); in the latter, production of inorganic phosphate is critical for proper assembly of normal bone. In both systems, however, the ability to produce ECVs with specific, enriched catalytic activity is needed for maintaining homeostasis.

Distribution of catalytic activity is not the only function of EVCs in bone, however, as Aliotta *et al* discovered that marrow cell phenotype is altered by lung-derived ECVs through transfer of mRNA, aiding in recovery of lung tissue after injury (Aliotta *et al.*, 2007; Aliotta *et al.*, 2010). This suggests that ECVs may be involved in regulating stem cell fate decisions during tissue repair by regulating gene expression.

Cardiovascular function

In the cardiovascular system, circulating ECVs are released from virtually every cell type, including platelets, immune cells (van der Pol *et al.*, 2012; Cicero, 2013), endothelial and vascular smooth muscle cells. In some cases, these vesicles have been shown to participate in the coagulation process (Cocucci *et al.*, 2009), while other work revealed that cardiovascular ECVs can distribute HSP60 (Gupta and Knowlton, 2007). Waldenstrom et al “transfected” fibroblasts with nucleic acid-containing ECVs isolated from adult mouse cardiomyocytes and demonstrated that genetic material from ECVs is transferred into target cells where it induces changes in gene expression (Waldenstrom *et al.*, 2012). Similarly, ECVs isolated from endothelial progenitor cells were able to stimulate vessel formation in culture and in a SCID mouse model, a process dependent upon mRNA contained in the ECVs (Deregibus *et al.*, 2007). In disease states, cardiovascular ECV production is upregulated, such as increased vesicle shedding observed in pre-atherosclerotic areas of the aorta (Bobryshev *et al.*, 2012), and in cases of pro-thrombotic anemias (Zwicker *et al.*, 2011). Bastida *et al* described ECVs from

isolated human glioblastoma cells that contain factors capable of activating clotting and platelet aggregation *in vitro* (Bastida *et al.*, 1984); this work is consistent with earlier findings of ECVs isolated from human breast cancer and guinea pig hepatocarcinoma cells (Dvorak *et al.*, 1983). A notable feature of glioblastoma ECVs is their potent activity, showing up to 10-fold greater procoagulant activity compared to cellular membrane fractions. Similar to other systems, this finding demonstrates the utility of ECVs as distributors of a highly concentrated biological activity, allowing source cells to propagate the relevant signal in a targeted, efficient manner.

Nervous system function

In neural tissue, exosomes are released from many cell types (Turola *et al.*, 2012), while ectosomes are shed by microglial cells (discussed above), neurons (Schiera *et al.*, 2007), astrocytes (Bianco *et al.*, 2005), and possibly oligodendrocytes (Turola *et al.*, 2012; Verderio *et al.*, 2012). Neuronal ECVs are enriched in FGF2 and VEGF, and could function in regulating angiogenesis (Schiera *et al.*, 2007). Astrocytic ECVs carry IL-1β, implicating the organelles in mediating immune responses, while an examination of oligodendrocyte-derived ECVs from patients with multiple sclerosis also suggests a role in pro-inflammatory signaling (Verderio *et al.*, 2012). In 2006, Faure *et al* demonstrated the release of exosomes from neurons and astrocytes, which contained the GluR2 subunit of the glutamate receptor and other proteins (Faure *et al.*, 2006). Though further work investigating the function of neuronal ECVs is needed, this and a subsequent study (Lachenal *et al.*, 2011) suggest that neuronal-derived ECV play a regulatory role in the CNS for neuronal plasticity, perhaps by recycling or disposing of various receptors or by transferring cargo proteins to receiving cells. ECVs were long

thought to be a general cellular “trash disposal,” an idea that was mostly discarded as investigators discovered specific ECV functions. In the nervous system, however, removing cellular detritus is still considered a primary function of ECVs, and one that may play a significant role in maintaining homeostasis by regulating receptors on the cell surface and removing pathology-inducing proteins targeted for degradation (Von Bartheld and Altick, 2011).

ECV function in disease

Based on the broad contributions to normal physiology it is perhaps not surprising that ECVs play roles in numerous diseases (athlerosclerosis, coagulopathies, inflammation, infection and autoimmune disease (Thomas and Salter, 2010; Zwicker *et al.*, 2011; Bobryshev *et al.*, 2012; Dreux *et al.*, 2012; Verderio *et al.*, 2012)). However, here we focus on their role in cancer.

A key finding that first implicated ECVs in cancer was the discovery that membrane vesicles shed from metastatic cells could induce lung metastasis (Poste and Nicolson, 1980). Early research on exosomes in the immune system (Chaput *et al.*, 2004) led to their eventual identification as vesicles secreted both from mouse and human tumor cells and biofluids (Wolfers *et al.*, 2001; Andre *et al.*, 2002). Although we still do not fully understand the differences between ECV released from normal and cancer cells, recent work suggests that ECVs facilitate horizontal transfer of cargo and harness the activity of these cargoes to stimulate intracellular signaling pathways, promoting tumor progression (Muralidharan-Chari *et al.*, 2010; Lee *et al.*, 2011; Demory Beckler *et al.*, 2012). Although we focus on protein cargo of ECVs in our discussion below, it is becoming increasingly apparent that these vesicles contain DNA and RNA,

which may also confer important pro-neoplastic effects (Valadi *et al.*, 2007; Skog *et al.*, 2008; Hong *et al.*, 2009; Pisetsky *et al.*, 2011).

Oncogenes represent an important class of active ECV cargoes that modulate recipient cells. Tissue transglutaminase (tTG)-containing ECVs purified from cancer cells induced NIH-3T3 cell survival and anchorage-independent growth, effects that were linked to transfer of tTG via ECVs. Moreover, exosomes purified from colon cancer cells transfer mutant G13D KRAS and induce anchorage-independent growth and colony formation in 3D collagen matrix, further suggesting oncogene-containing exosomes promote cancer-related phenotypes (Demory Beckler *et al.*, 2012). Additionally, treatment of mildly aggressive glioma cells with EGFRvIII-containing ECVs increased observed levels of EGFRvIII in these cells, which may be partly responsible for the observed increases in VEGF production and anchorage-independent growth of recipient cells (Al-Nedawi *et al.*, 2008). Not surprising, given the variety of cargo and roles in intercellular communication, it seems that in addition to promoting cancer phenotypes, ECVs also carry tumor suppressors. A recent study showed functional PTEN in exosomes purified from fibroblast cells and treatment of cells with these exosomes reduced cellular proliferation (Putz *et al.*, 2012). Combined, these data provide strong support for ECVs as vehicles for protein cargo transfer to recipient cells, allowing for promotion and suppression of tumor-related phenotypes.

In addition to inducing features of tumor initiation, data also indicate a role for ECVs in promoting angiogenesis, invasion, and metastasis. ECVs contain a wide variety of pro-metastatic cargo, including insulin-degrading enzyme, matrix metalloproteinases, tetraspanins, heat shock proteins, plasminogen, integrin family

members, and growth factors, (VEGF and FGF) (Graner, 2011; D'Souza-Schorey and Clancy, 2012). Pro-angiogenic effects of ECVs include enhanced endothelial cell tubule formation and vascularization of *in vivo* Matrigel plugs (Hood *et al.*, 2009; Mineo *et al.*, 2012). Cathepsin B-containing ECVs and EGFR ligand-containing exosomes are two examples of ECVs that elicit recipient cell invasion *in vitro* (Giusti *et al.*, 2008; Higginbotham *et al.*, 2011). Luga *et al.* recently reported that exosomes secreted from fibroblasts enhance breast cancer cell motility and metastasis, a mechanism that was suggested to require exsosome association with Wnt11 and activation of recipient breast cancer planar cell polarity proteins (Luga *et al.*, 2012). This study provides additional support for the cross-talk of stroma and tumor and implicates stromal fibroblast ECVs with cancer progression. The identity of cargoes packaged in ECVs and their ability to induce invasion both support a role for these vesicles in promoting metastatic phenotypes.

Several key *in vivo* studies have demonstrated the ability of ECVs to prime metastatic niches. Melanoma exosomes selectively home to and prime sentinel lymph nodes for melanoma cell metastasis (Hood *et al.*, 2011). Similarly, pretreatment of mice with melanoma exosomes results in accelerated lung metastasis (Liu *et al.*, 2010). Finally, it was recently reported that melanoma exosomes reprogram bone marrow-derived cells to a more pro-vasculogenic phenotype that supports enhanced tumor growth and metastasis (Peinado *et al.*, 2012). Together, these reports strongly indicate that ECVs act to enhance metastatic properties of recipient cells. Future studies are needed, however, to identify the mechanisms by which ECVs exert these actions.

Common themes and conclusions

Despite the diverse physiological contexts highlighted above, ECV functions generally partition into one of four categories: regulation of gene expression, induction of signaling, distribution of catalytic activity, and disposal of cellular 'trash' (Fig. 5-1). Even more broadly, ECVs serve to protect, concentrate, or remove cargo. Genetic material must be protected from degradation as it is transported from source to target cell. Ligands or receptors may need to be concentrated in order to efficiently activate a signaling cascade, while catalytic activity may be enhanced by concentrating an enzyme on the surface of an ECV. Thus, ECVs are highly adaptable cargo-carrying platforms.

As discoveries from the past decade have demonstrated the near-ubiquity of ECVs, several new areas of investigation will be important for developing a full understanding of these organelles. More detailed studies of exosome and ectosome formation will provide much needed clarity into the distinctions between these two pathways. Moreover, very little is known about how ECVs are captured by recipient/ target cells. Initial studies implicate specific lipids (e.g. phosphatidylserine) and integrins in this process but the details are only beginning to come into focus (Deregibus *et al.*, 2007; Iglesias *et al.*, 2012). Once precise mechanisms of ECV tethering, fusion and/or internalization with target cells have been established, understanding the transfer of enriched cargo molecules and downstream effects can be clarified.

Translational applications of ECV biology are in their infancy, but include their use as therapeutic delivery vehicles and disease biomarkers. Recent studies showed that stem cell ECVs are able to reprogram diseased cells (Iglesias *et al.*, 2012), while

“custom” ECVs are capable of delivering experimental cargos (Mangeot *et al.*, 2011). Other potential ECV-based therapies such as tissue repair and revascularization are being investigated (Lee *et al.*, 2012). ECVs also serve as attractive biomarkers of disease progression. In addition to blood and serum, ECVs can be purified from other biofluids such as urine (Dear *et al.*, 2012) and their cargo composition and rate of production is altered during various pathologies. However, a better understanding of ECV formation, uptake and function is needed to expand current studies of ECVs as therapeutic delivery systems (Mangeot *et al.*, 2011; Lee *et al.*, 2012), to tailor synthetic ECVs for treatment of disease, or to use these organelles as biomarkers.

CHAPTER VI

THE ENTEROCYTE BRUSH BORDER ACTS AS A BARRIER TO EPEC ATTACHMENT

Introduction

For pathogens that penetrate the inner mucus layer covering enterocytes *in vivo*, the brush border is the first cellular structure encountered (McGuckin *et al.*, 2011). Ultrastructural analysis of EPEC attachment and effacement have found this process to be comprised of two primary steps. Following initial contact with enterocytes, EPEC first sink into the brush border by ~30 minutes, then form A/E lesions and develop pedestals (Dean *et al.*, 2006). The first step is mediated by Tir and intimin, the second, by Map and EspF (Dean *et al.*, 2006). Attachment and effacement invariably follows from infection by WT EPEC. Mechanisms underlying EPEC virulence are highly adapted to hijack host cell machinery, and ultimately enterocytes are unable to prevent intimate bacterial attachment. However, based on the two-step process of attachment described above, as well as the highly ordered and tightly packed nature of the brush border, we speculated that the brush border could function as a physical barrier to EPEC attachment by slowing, though not entirely preventing the A/E process. We hypothesized that disheveled or immature brush borders (i.e. those without normal microvillar packing and density) would be more susceptible to EPEC infection, as bacteria would be able to bypass initial interactions with microvilli and more readily make direct contact with the enterocyte apical surface.

Results

Bacterial attachment increases in the absence of PCDH24

A key regulator of brush border formation and maintenance of microvillar length and packing is the adhesion molecule protocadherin-24 (PCDH24). Ongoing work in our lab has shown that microvilli are connected near their distal tips by a web of inter-microvillar links comprised of PCDH24/Mucin-like protocadherin (MLPCDH) heterodimers (Crawley *et al.*, submitted). Microvillar packing is defective in the absence of PCDH24, and the precise microvillar length regulation seen in WT enterocytes is also lost. Thus, we chose to utilize shRNA mediated knockdown of PCDH24 in Caco-2_{BBE} cells as a model for investigating the consequences of defective brush border structure on EPEC attachment.

We grew cells on coverslips for 14 d post-confluency, a time point at which scramble shRNA control cells have formed a well-developed, though not fully packed brush border. At this same time point, the brush borders of PCDH24 KD cells lag significantly behind their control counterparts. Two weeks post-confluence represents a developmental stage where inherent differences between the two cells lines will be maximized. PCDH24 KD brush borders are disheveled and irregular, with fewer microvilli than in control cells (Crawley *et al.*, submitted). At 14 d, we added EPEC to the coverslips, and incubated the cells with bacteria for 1 and 3 hrs. Cells were fixed and stained with phalloidin to label the actin cytoskeleton and an α-Lipid A antibody to label EPEC. We subsequently imaged the coverslips and counted the number of bacteria adhered per unit area. Following a 3 hr incubation, the number of EPEC, the number of microcolonies, and the average microcolony area increased on PCDH24 KD cells (Fig.

6-1A-C). At one hour, the number of EPEC counted on Caco-2_{BBE} monolayers increased by an average of 25% in the absence of PCDH24 (Fig. 6-1D). In samples fixed three hours following infection, the absence of PCDH24 caused a ~20% increase in the number of attached bacteria (Fig. 6-1D).

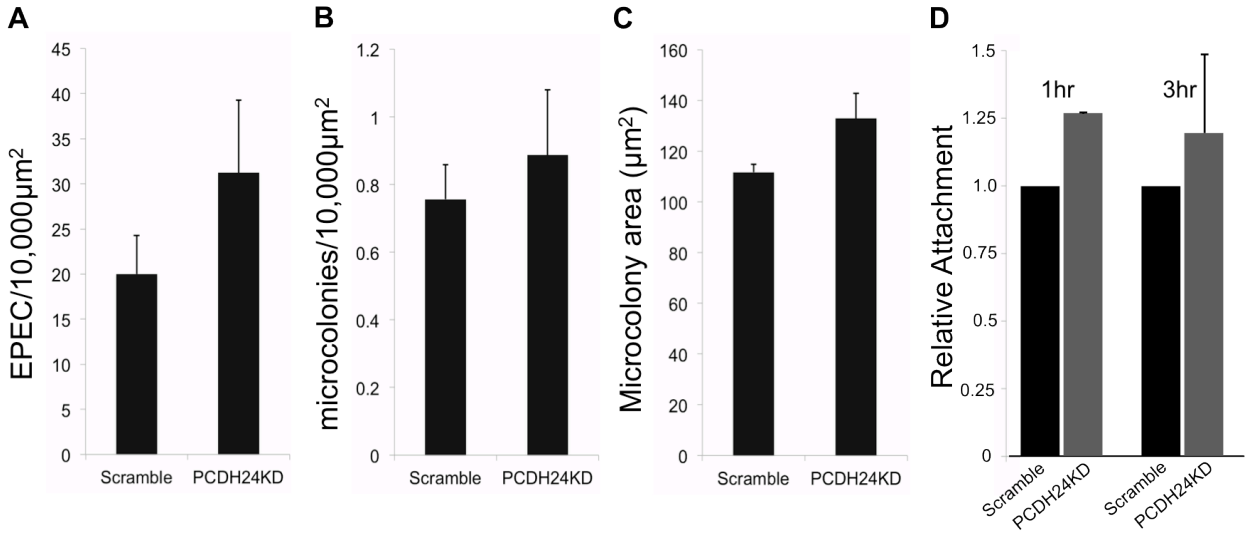

Figure 6-1: Absence of PCDH24 increases bacterial attachment to enterocytes

(A) Total number of EPEC attached per unit area in control and PCDH24KD Caco-2_{BBE} cells following 3 hr incubation. (B) Total number of bacterial microcolonies per unit area after 3 hr. (C) Average area of EPEC microcolonies on control and PCDH24KD cells after 3 hr. Larger microcolonies indicates the bacteria reached intimate attachment earlier, allowing for growth and division. (A-C) example of representative experiment. (D) Relative number of EPEC attached to confluent monolayers of scramble and PCDH24 cells at 1 and 3 hr; average of three separate experiments. $p > 0.05$

EPEC attachment is inversely proportional to brush border maturity

A disordered brush border caused by the absence of PCDH24 leads to increased bacterial attachment. We hypothesized that the brush border of an undifferentiated or partially differentiated enterocyte, with clusters of microvilli of variable length and gaps between clusters, would be similarly susceptible to infection. To further investigate the relationship between brush border maturity and bacterial attachment, we grew Caco-2_{BBE} cells on glass coverslips and infected them with EPEC at 3 d intervals over

the course of differentiation. Following one hour incubation with bacteria, the cells were fixed and stained as before, imaged, and EPEC quantified. Consistent with our hypothesis, the number of bacteria per unit area decreased as differentiation progressed and microvilli packed together to form a well-ordered brush border (Fig. 6-2A-C). At one day post-confluency, when microvilli are short, dispersed, and few in number, an average of ~0.85 bacterial cells per 10,000 μm^2 attached to monolayers (Fig. 6-2D). By two weeks post-confluency, the number of bacteria adhered decreased by 2-fold and remained ~0.3 bacteria per 10,000 μm^2 during the final week. As discussed above, polarization of Caco-2_{BBE} cells on glass coverslips occurs over approximately three weeks. Expression of PCDH24 increases with, and helps to regulate formation of the brush border (Fig. 6-2D). By the end of the second week of polarization, gaps between clusters of microvilli have begun to close and microvillar length becomes consistent across the surface of the cell. The decline in bacterial attachment during the first two weeks and subsequent minima maintained through the remaining time, could represent an optimal microvillar density for inhibiting bacterial contact with the apical cell surface by forming a “chain-link fence” to impair bacterial contact.

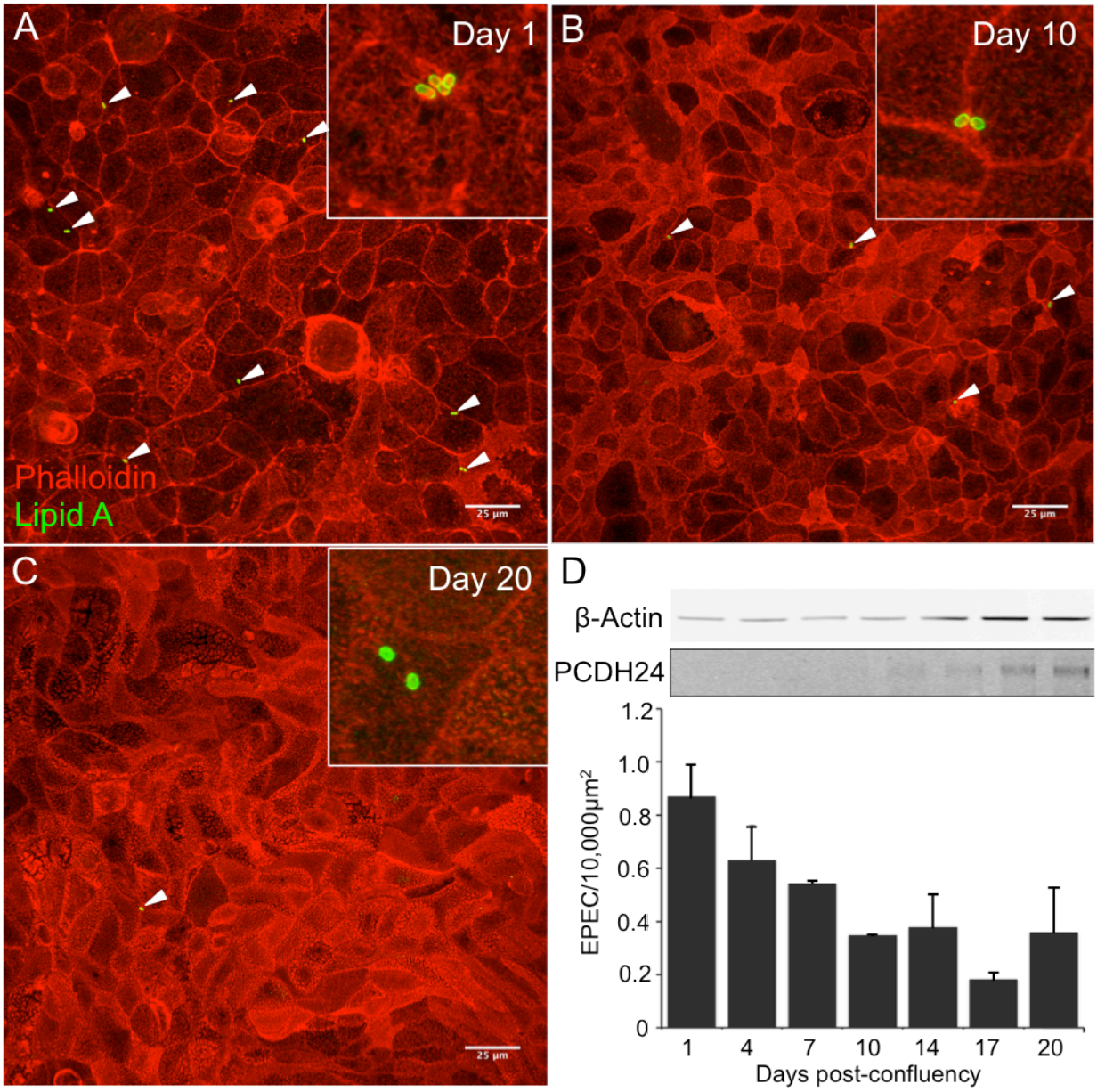

Figure 6-2: Bacterial attachment decreases with brush border development

(A-C) Representative images of Caco-2_{BBE} cells at increasing stages of differentiation on glass coverslips; (A) 1, (B) 10 and (C) 20 days post-confluency. As differentiation progresses, early EPEC attachment decreases, seen in the reduction of lipid A-labeled bacteria (arrowheads). Insets show progression of brush border maturation at higher magnification. (D) PCDH24 expression increases with brush border development, inversely proportional to the number of EPEC attached following 1 hr incubation.

Conclusions

These results demonstrate the importance of a well-ordered brush border for maintaing the integrity of the intestinal epithelial barrier. By simply breaking the normal packing of enterocyte microvilli, we have shown that alterations to brush border morphology leave enterocytes more susceptible to EPEC infection. Tight junctions are critical for barrier function, preventing direct translocation of toxins and microbes to the underlying tissue through what would otherwise be gaps between cells. During infection, EPEC disrupt tight junctions, leading to breakdown of the epithelial barrier and subsequent fluid efflux (Weflen *et al.*, 2009). Data shown above demonstrates that the brush border also serves as a physical impediment to bacterial attachment. This finding places the brush border and tight junctions in a similar category as mechanical/ physical mechanisms of innate immunity, with the brush border likely working upstream of tight junctions. As the first contact point for pathogens, the brush border may function as a fence to slow attachment and limit activation of intracellular pathways leading to disruption of tight junctions. PCDH24, as a regulator of microvillar length and packing density, is central to this feature. Increased variability between microvilli due to the absence or reduction of the adhesion molecule is associated with increased infection, including both early attachment and microcolony formation. Thus, brush border morphology is not only optimized for proper nutrient absorption, but also for maintaining gut homeostasis.

CHAPTER VII

MICROVILLAR DYNAMICS DURING EPEC ATTACHMENT

Introduction

It is clear that EPEC is highly adapted to infect enterocytes regardless of brush border maturity. Although the chain-link fence model of brush border function may allow enterocytes to reduce the rate of attachment and perhaps provide time for other defense mechanisms to be activated, it is not sufficient to ultimately prevent infection. EPEC pathogenicity is dependent upon the bacterium's ability to rearrange the apical domain of enterocytes through disruption of tight junctions, hijacking of cytoskeletal machinery, and effacement of the brush border (Dean and Kenny, 2009). Thus, another question that arises from studying interactions between pathogen and brush border is how the morphology of this domain is disrupted during attachment, and whether or not microvilli contribute in some way to the attachment process. The enterocyte brush border is a highly ordered array of actin-based protrusions, the microvilli, which exhibit tight hexagonal packing. Over the course of the A/E process, which occurs on the order of hours, EPEC ablate the brush border and reduce the enterocyte apical membrane to a smooth surface save for pedestals. Although the events surrounding later stages of intimate EPEC attachment and pedestal formation are well characterized, initial contact between a bacterial cell and the brush border have not been well studied. Additionally, limited temporal data for EPEC attachment and the A/E process exists. SEM imaging has provided important insight into the ultrastructure of the early A/E process, but these studies lacked a true kinetic component as the samples were taken every 20 min (Phillips *et al.*, 2000; Dean *et al.*, 2006). More recently, confocal microscopy was used

to track the accumulation of actin at sites of attachment. However, this study only included a quantification of actin signal to analyze the ability of EPEC BFP mutants to form pedestals, and did not investigate the structural changes occurring on the host cell surface (Zahavi *et al.*, 2011). Live cell imaging could therefore be utilized to reveal brush border and microvillar dynamics, such as elongation and effacement, during early EPEC attachment.

The signaling cascade from Tir to Arp2/3 activation has been well characterized; however, to our knowledge a direct investigation as to the source of actin that is incorporated into pedestals has not been undertaken. The assumption that free G-actin monomers, most likely released from profilin-mediated sequestration in the cytosol, are polymerized into nascent filaments by the activity of N-WASP and Arp2/3. However, this model may be incomplete, as Arp2/3 binds to the sides of existing F-actin and nucleates new daughter filaments at a 70° angle (Pollard *et al.*, 2000). Therefore, proper formation of a branched actin network such as a bacterial pedestal requires the presence F-actin "templates." In a polarized enterocyte, the brush border contains a huge population of such F-actin filaments in the form of bundled microvillar actin. It is intriguing to consider the idea that microvilli could in fact provide a source of pedestal actin. Disassembly of microvillar actin during effacement could increase the local concentration of free G-actin monomers available for re-polymerization into pedestals, while remaining fragments of microvillar actin filaments could serve as the necessary templates for Arp2/3.

Despite the significant insight into the function of bacterial effector proteins − including EspF and intimin − in pedestal formation, and the importance of these molecules for microvillar elongation (Phillips *et al.*, 2000; Shaw *et al.*, 2005), no work

has yet elucidated a specific host cell mechanism by which elongation occurs. Additionally, seemingly peripheral parts of the A/E process, including microvillar elongation and effacement, have been noted as hallmarks of EPEC infection, but not studied in the context of their potential contributions to pedestal formation. In order to address these gaps, and to investigate the idea that microvilli could contribute to pedestal actin, we utilized time-lapse deconvolution microscopy to visualize bacterial attachment and associated ultrastructural changes, complemented by SEM imaging.

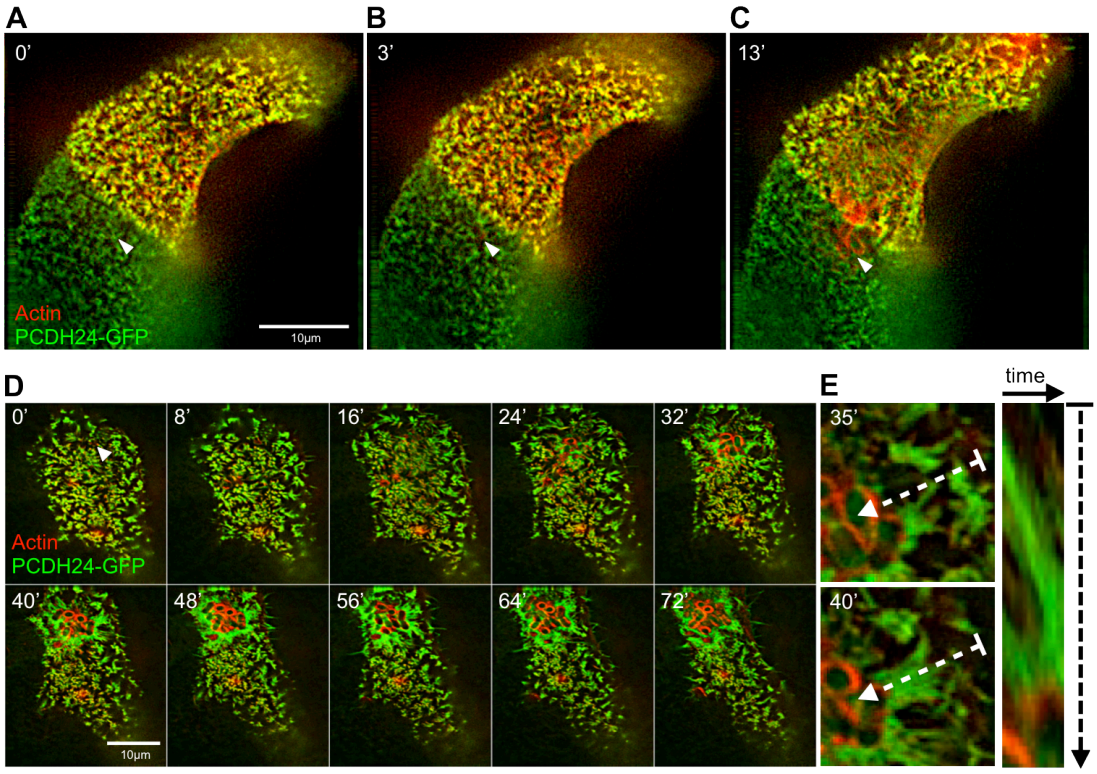

Figure 7-1: Dynamics of pedestal formation and brush border flow during EPEC attachment

(A) Caco-2_{BBE} cell at t_0, the point of first EPEC contact. Site of attachment shown by arrowhead. (B) Pedestal formation begins within 3 min of initial bacterial contact; (C) mature pedestals develp in 10 min (13 min after initial contact). (D) The enterocyte brush border flows towards sites of EPEC attachment (arrowhead), and microvilli coalesce around the periphery of developing microcolonies as actin accumulates in pedestals. (E) Example of microvillar cluster folding into the edge of the microcolony; dashed arrow represents linescan taken for kymograph in right panel.

Results

Dynamics of the enterocyte brush border during early attachment

To visualize EPEC attachment to IECs, we transiently transfected Caco-2_{BBE} cells with a fluorescent protein-tagged version of the utrophin calponin homology domain (mCherry-Utr), which binds to F-actin without disrupting actin dynamics (Burkel *et al.*, 2007). Additionally, we transfected the cells with GFP-PCDH24 both to label membrane and to promote brush border integrity. Activated EPEC were added to Caco-2_{BBE} cells on glass bottom dishes and imaged at 10-20 sec intervals using deconvolution microscopy. By ~3 min following initial contact between EPEC and host cell, actin begins to accumulate underneath the bacterium, and ~10 min later a fully formed pedestal is seen (Fig. 7-1A-C). EPEC attachment involves a series of steps in which the BFP helps mediate initial contact and then retracts, drawing the bacterium closer to the host cell surface (Zahavi *et al.*, 2011). Injection of TIR, binding of its ligand intimin, and activation of N-WASP and Arp2/3 mediated actin polymerization follow (Wong *et al.*, 2011). Ultrastructual analysis demonstrated that EPEC begin to sink into the brush border within 5 min of attachment (Dean *et al.*, 2006). Our live cell imaging data show that actin polymerization occurs on a similar time scale, although there may be a delay *in vivo* due to tighter microvillar packing than in cells used here.

Remarkably, in addition to localized pedestal formation we also observed significant brush border dynamics across the surface of enterocytes within 5-10 min of initial attachment. In cells with relatively tightly packed brush borders, microvilli clustered together, turned and folded towards the bacterium (Fig. 7-1D, E). Over the course of an hour, as the A/E lesion expanded due to attachment and division of

additional bacteria, this directed flow occurred across the surface of the cell. Microvilli distal to the bacteria were drawn across the cell into the microcolony and subsequently effaced. As a result, the periphery of the lesion was surrounded by an expanding ring of microvillar membrane overlaying the disassembling actin bundles, while the center of the lesion was devoid of PCDH24 and actin was found exclusively in the pedestals (Fig. 7-1D). From these time-lapse sequences, we conclude that EPEC attachment and brush border effacement is not simply a matter of localized destruction of microvilli in the immediate vicinity of bacterial adhesion, but rather a dynamic process in which the entire brush border is rearranged, coalescing at sites of attachment and then disassembling to allow for pedestal formation. This finding is consistent with the hypothesis that microvillar actin is used by EPEC to form pedestals. By initiating brush border flow, bacterial cells could recruit a large pool of microvillar F-actin to sites of attachment, stockpiling the cytoskeletal protein for use in pedestal formation.

PCDH24 regulates brush border flow

In addition to bulk flow of the brush border during attachment, we also observed events where individual microvilli elongate towards bacteria. These extensions likely represent the formation of previously described microvillar-like processes (MLP) (Bernet-Camard *et al.*, 1996; Phillips *et al.*, 2000; Cleary *et al.*, 2004; Shaw *et al.*, 2005; Dean *et al.*, 2013). However, imaging the dynamics of individual microvilli was difficult due to the high microvillar density in our cells. Because inter-microvillar adhesion is mediated by PCDH24 (Crawley *et al.*, submitted), and we observed striking accumulation of PCDH24-GFP signal as microvilli coalesce around adhering EPEC, it is possible that the adhesion molecule was tying microvilli together to produce bulk flow. In

order to better investigate the dynamics of individual microvilli, we overexpressed a dominant-negative PCDH24-GFP construct (PCDH24-ΔEC1) in which deletion of the first extracellular domain prevents formation of the PCDH24-MLPCDH heteromeric complex (Crawley, unpublished data). Similar to PCDH24 knockdown, expression of this construct reduced normal microvillar packing. PCDH24-ΔEC1 provided an excellent tool both to dissociate microvilli from each other and to increase the space between microvilli for better analysis of individual protrusions. Additionally, PCDH24-ΔEC1 limited brush border flow, seen in images where frames at 0 and 30 min attachment were overlaid (Fig. 7-2). Cells expressing PCDH24-GFP with high-density brush borders contracted over time, and the microvilli lost their distinct punctate appearance by condensing around sites of attachment (Fig. 7-2A, dashed regions). By contrast, while sites of attachment could be seen on PCDH24-ΔEC1-GFP expressing cells, the rest of the cell surface remained relatively unperturbed (Fig. 7-2B, dashed regions). Without brush border flow, the dynamics of individual microvilli on PCDH24-ΔEC1-GFP expressing cells became much more amenable to analysis.

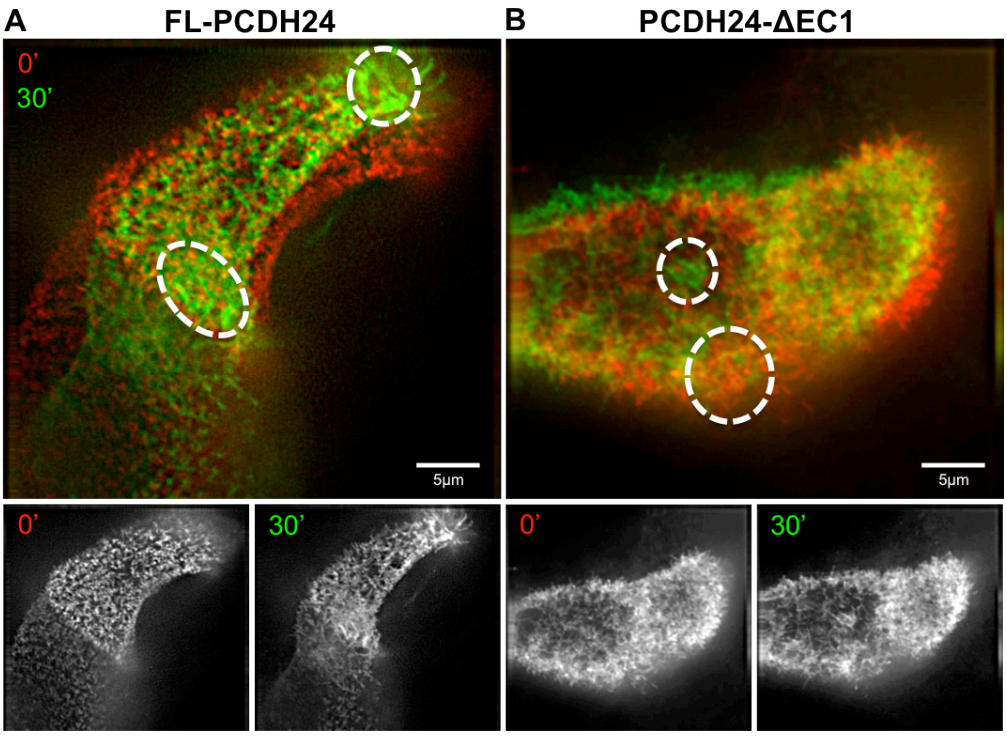

Figure 7-2: PCDH24 regulates brush border flow

(A) Representative Caco-2_{BBE} cell expressing full-length PCDH24 shows signs of microvilli moving across the surface into sites of EPEC attachment (dashed regions), as well as significant contraction of the cell circumference. (B) Both brush border flow and changes in apical cellular morphology are reduced in cell expressing dominant negative construct, PCDH24-ΔEC1. Note the lack of significant microvillar accumulation 30 min after attachment. Red = t_0, green = t_{30} after initial attachment.

Microvilli elongate during early EPEC attachment

Numerous examples of elongated microvilli contacting bacteria were observed using live cell microscopy on Caco-2_{BBE} cells expressing mCherry-Utr and PCDH24-ΔEC1-GFP (Fig. 7-3A, B). These features resembled clusters of elongated microvilli in SEM images of cells infected with EPEC for three hours (Fig. 7-3D), consistent with previous work describing MLP (Bernet-Camard *et al.*, 1996; Phillips *et al.*, 2000; Cleary *et al.*, 2004; Shaw *et al.*, 2005; Dean *et al.*, 2013). Contrary to observations made by Phillips *et al.* (2000), however, we regularly observed microvillar elongation during the earliest stages of EPEC attachment, as well as at the later stages of microcolony formation (Fig. 7-3E, F). Furthermore, confocal microscopy of phalloidin-stained

samples revealed that the protrusions, including those formed within 15’ of initial bacterial attachment are indeed actin-filled (Fig. 7-3E, F). This finding suggests that the formation of elongated microvilli is due to rapid actin polymerization stimulated by the presence of EPEC, rather than simply membrane tubules that might occur if a lightly attached bacterium moved away from the site of initial adhesion and drew microvillar membrane out in a tether. We found that microvilli elongate at ~50nm/s (data not shown), a rate consistent with previous studies of actin polymerization both in solution and in cellular protrusions (Pollard and Mooseker, 1981; Argiro *et al.*, 1985).

Imaging of attachment events indicates that microvillar elongation is a directed phenomenon with the distal tips of microvilli extending towards bacteria. In cells infected with EPEC, rare examples of random microvillar elongation can be found; that is, microvilli will extend in the absence of a nearby bacterium. However, this is likely due in some way to the presence of bacteria, possibly the result of released bacterial products such as outer membrane vesicles (Kuehn and Kesty, 2005), as uninfected cells showed very little evidence of microvillar elongation (data not shown). Additionally, elongation did not occur on cells incubated with 2 μm silica or polystyrene beads, demonstrating that this phenomenon is the result of a biochemical, rather than mechanical stimulus (data not shown). Microvilli within ~5 μm of an attachment event rotated and oriented their distal tips towards the pathogen. Rapid elongation immediately followed until the tip of the microvillus contacted the bacterial cell or surrounding membrane. In some instances microvilli retracted, returning to original length almost instantaneously (Fig. 7-3C, dashed lines). Retraction may be the result of an inability of the protrusion to bind the bacterium, although the mechanisms involved are unknown and should be the focus

of future studies. Over time, productive microvillar binding events accumulated, leading to formation of a web of protrusions radiating between the bacterium host cell surface (Fig. 7-3A, right panel, Fig. 7-3D). Remarkably, we also noted instances of microvillar elongation occurring towards bacteria attached to a neighboring cell (Fig. 7-3B). Thus, EPEC does not have to be attached to stimulate elongation, further suggesting that it is a factor released from bacteria, rather than the bacteria themselves, stimulating this response.

Where brush border flow might be used by bacteria to recruit actin to sites of attachment, stimulated - and directed - microvillar elongation could allow EPEC to tether individual host cell protrusions, pulling them into place for repurposing of the underlying F-actin. Intriguingly, preliminary data from our lab, along with previously published work, indicates that a functional BFP is required for microvillar elongation. In confocal images, BFP filaments were seen linking EPEC with microvilli, and retraction of BFP is known to draw the bacterium into close contact with the host cell surface (Cleary *et al.*, 2004; Zahavi *et al.*, 2011). It is interesting to speculate that attachment of BFP to a microvillus and subsequent retraction could exert enough force on the protrusion to stimulate elongation, and future studies should focus on the interaction between EPEC adhesion molecules such as BFP and microvilli.

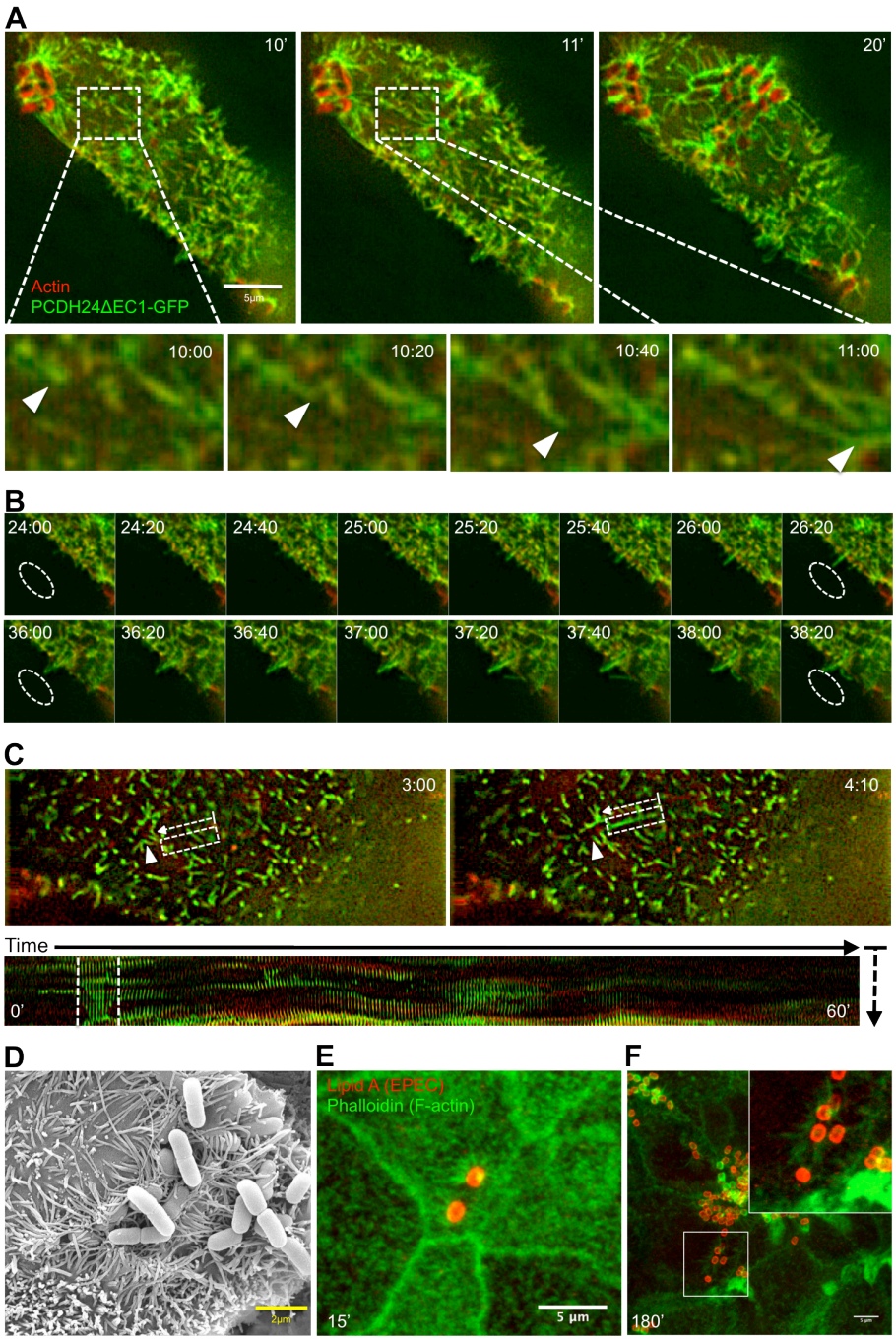

Figure 7-3: Rapid microvillar elongation occurs during all stages of EPEC attachment

(A) Microvilli elongate towards adhering EPEC. Elongation occurs at a rate of ~50nm/s, and terminates when the microvillar tip (arrowheads) contacts the bacteria or the surrounding pedestal. (B) Protrusion from cell shown in (A) extends towards bacterium attached to neighboring cell, demonstrating direct contact between EPEC and host cell is not required to stimulate elongation. Dashed oval indicates location of EPEC. (C) Example of two microvilli elongating simultaneously towards bacteria, then retracting. Boxed region in upper panels indicates region used for time lapse montage in bottom panel. Dashed lines in montage indicate the microvillar elongation. (D) SEM image of microvillar elongation in Caco-2_{BBE} cells following 3 hr incubation with EPEC. (E, F) Confocal image of microvillar elongation in Caco-2_{BBE} cells following 15 min (E) and 3 hr (F) incubations with EPEC, showing elongated processes are actin-based and therefore likely true microvilli. Time stamps in (A, B, C) indicate time elapsed from first bacterial contact.

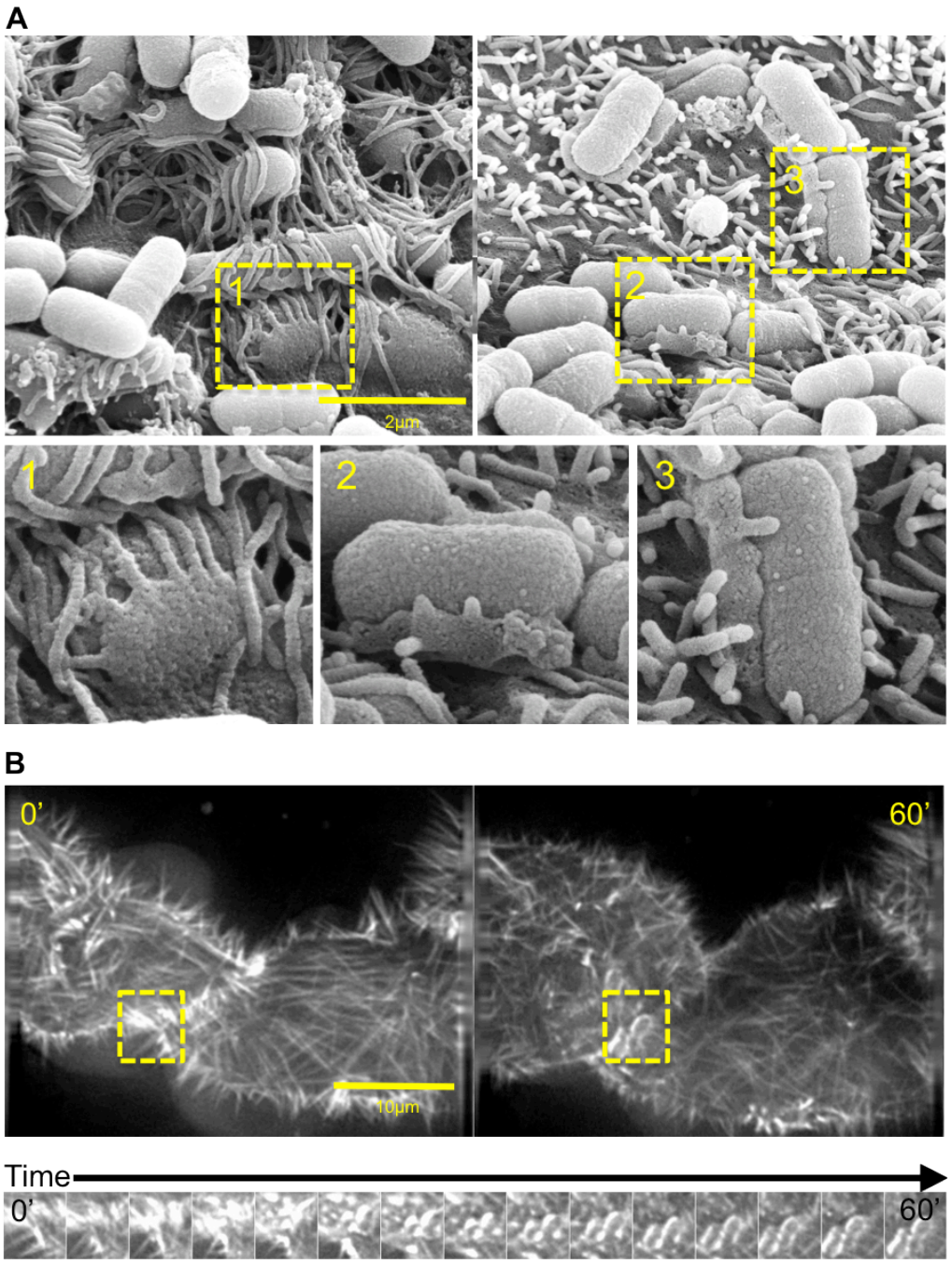

Figure 7-4: Microvilli coalesce and incorporate into developing pedestals

(A) As pedestals form, microvilli coalesce around bacteria in a “hand-of-doom” structure. Three examples at varying stages in boxes 1-3. (B) In Caco-2_{BBE} cells expressing mCherry-espin, microvillar coalescence is seen in real time. As pedestal formation progresses, espin signal accumulates, indicating that parallel actin from merging microvilli is incorporated into these nascent structures. Boxed region in upper panels indicates region used for montage. Images in montage at 1 min intervals.

Microvillar actin is incorporated into pedestals

As discussed above, the major steps in the A/E process have been described using SEM and genetic manipulation of EPEC virulence factors and host cytoskeletal machinery. Our work points to a novel component of intimate EPEC attachment, wherein microvilli could be used by bacteria as a source of actin. To further elucidate potential contributions of brush border actin to pedestal formation, we again utilized a combination of SEM and live cell deconvolution microscopy to investigate physical interactions between EPEC and microvilli.

If microvilli are incorporated into nascent pedestals, microvillar coalescence should be evident in micrographs of pedestal formation. Pedestals on Caco-2_{BBE} cells have a characteristic bun-like morphology, cupping a bacterial cell on both sides along its long axis (Fig. 7-4A). This structure is comprised of an actin network encased in spectrin and overlaid by cellular membrane (Ruetz *et al.*, 2012). Our data showed that pedestals began to form soon after initial contact between bacterium and host cell, as we observed enrichment of actin surrounding EPEC by 3 min (Fig. 7-1A, B). By 2-4 hr, bacteria that adhered early on formed robust pedestals and went through several rounds of division, leading to establishment of microcolonies ((Dean *et al.*, 2006), Fig. 7-4A). In SEM images of monolayers incubated with EPEC for 3 hrs, we observed numerous examples of individual pedestals encasing the bacteria within a microcolony. While the overall morphology of these structures is consistent, we noted the presence of protrusions of varying length extending from the apical edge of many pedestals (Fig. 7-4A, boxes 1-3). The diameter of these protrusions are consistent with that of microvilli. Some protrusions are only tens of nanometers long and appear to have coalesced into

the underlying pedestal (Fig. 7-4A, boxes 2, 3) while others are at least hundreds of nanometers (Fig. 7-4A, box 1) and are only partially engulfed. Although the analysis is limited by the static nature of the samples, these images suggest that microvilli surrounding bacteria do merge and coalesce into the pedestal wall. This is consistent with data described above, where brush border flow and microvillar elongation provide a mechanism for subsequent incorporation of microvillar actin into pedestals.

We next repeated the live cell attachment assays, imaging Caco-2_{BBE} cells expressing mCherry-tagged espin. An actin bundling protein, espin, stabilizes parallel actin bundles and allows microvilli to reach > 5 μm (Loomis *et al.*, 2003). By using this construct, we hypothesized that the additional stability of the actin and the longer microvilli would allow us to more readily visualize microvillar interactions with bacteria, as well as determine how microvilli associate with each other during the attachment process. Consistent with data shown in (Fig. 7-1), we observed examples of microvilli folding and contacting each other around bacteria. Even more striking, however, was the rapid accumulation of mCherry-espin signal in the characteristic oval shape of pedestals (Fig. 7-4B). This finding is noteworthy because espin bundles parallel actin, whereas pedestals are thought to be comprised of branched actin networks polymerized *de novo* (Bartles, 2000; Campellone, 2010). That is, the presence of espin in pedestals can be viewed as a proxy for the presence of bundled, parallel actin filaments, indicating that bacteria lesions are not comprised exclusively of a branched network. Espin does not bind G-actin monomers; therefore, the presence of this molecule suggests that either microvillar actin is incorporated into pedestals directly or newly polymerized actin filaments within a pedestal are immediately bundled by espin. Although this latter

possibility has not been tested directly, it is likely to be far less energetically favorable than the former. Direct incorporation eliminates the need to depolymerize microvillar actin, then utilize significant amounts of ATP to re-polymerize and bundle it into filaments within the pedestal. Furthermore, the transition microvilli make from independent protrusions to clusters to oval pedestals supports our hypothesis developed from SEM images that microvilli coalesce into these structures. To our knowledge, the finding that parallel actin bundles from microvilli are incorporated into nascent pedestals has not been described. Our data lead to an intriguing model where a second pathway of pedestal formation, based on the presence of a vast pool of pre-formed actin filaments in the form of the brush border, functions in polarized epithelial cells in parallel to the canonical Arp2/3 mediated pathway.

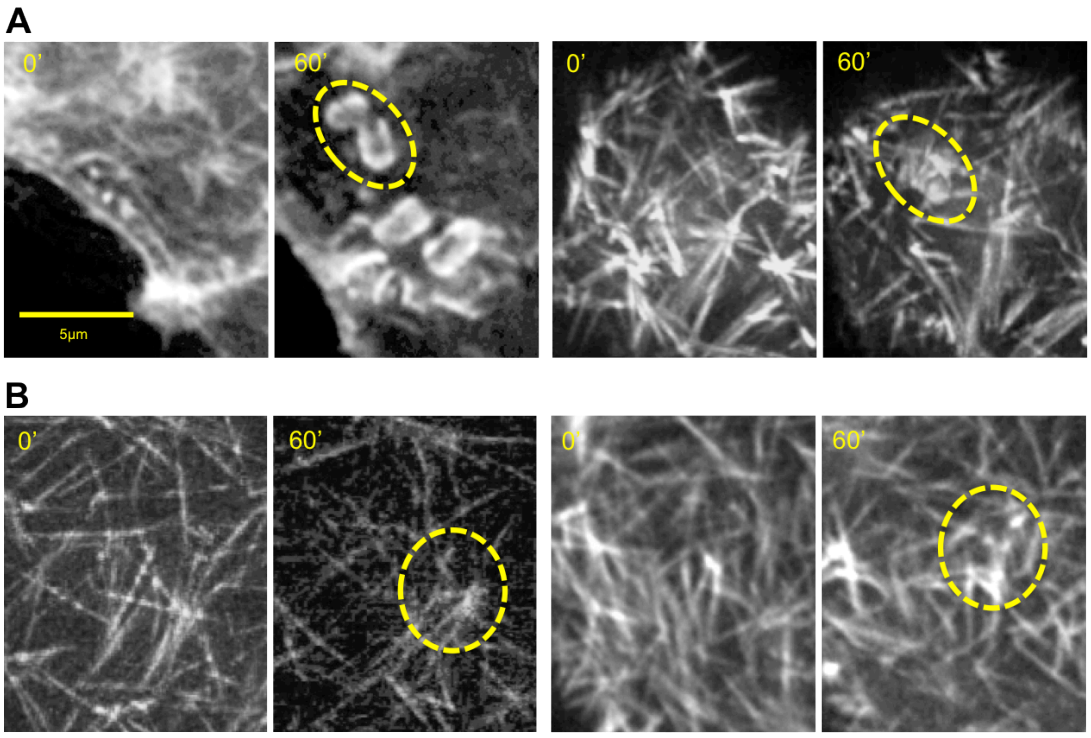

Figure 7-5: Espin overexpression alters the dynamics of pedestal formation

Highly cross-linked microvillar actin bundles in Caco-2_{BBE} cells expressing mCherry-espin are correlated with altered rates of pedestal formation. (A) Cells forming pedestals following EPEC attachment. Left panel, example of fully formed pedestals after 1 hr; right panel, immature, though visible pedestal following 1 hr incubation. (B) Not all infected cells form pedestals, seen in the lattice-like pattern of microvilli without the characteristic oval pedestal shape. Yellow dashed regions indicate attachment sites.

Actin bundling inhibits pedestal formation

Further imaging of mCherry-espin-expressing Caco-2_{BBE} cells revealed that not all cells with EPEC contacting the brush border ultimately formed robust pedestals. In several instances, bacteria settled onto the elongated microvilli of espin-expressing cells and went through normal division over the course of a 1 hr assay. Despite the typical behavior of the bacteria, microvilli responded to a much lesser extent when compared to those expressing mCherry-Utr. Almost no elongation occurred, and though not entirely eliminated the reorientation of microvilli with their distal tips pointed towards bacteria was noticeably reduced. After 1 hr of incubation with EPEC, only half of cell analyzed (3/6) showed any signs of pedestal formation, of these two had reached normal stages of development (Fig. 7-4B, Fig. 7-5A, left panels). Additionally, the rate at which pedestals appeared varied widely, from 3 min (comparable to non-espin-expressing cells; Fig. 7-4B) to > 15 min (Fig. 7-5A, right panels). One possibility is that this variability is due to differences between cells in espin expression levels. However, plotting the onset of pedestal formation with the intensity of mCherry-espin in several of these cells revealed no obvious correlation (data not shown). In the remaining cells microvilli appeared to fold into a lattice-like structure, but no subsequent remodeling occurred and pedestal formation did not progress (Fig. 7-5B). We also co-transfected cells with mCherry-espin and GFP-βActin to confirm that this result was not simply a matter of espin being excluded from some pedestals. Indeed, to the extent they formed at all, pedestals were always visible in both channels; none contained GFP-βActin only (data not shown).

These results are unexpected based on the canonical model of pedestal formation. Brush border effacement has traditionally been described as a hallmark of the A/E process, but very few studies have made a direct connection between disassembly of the actin-based microvillus and emergence of the actin-based pedestal. Because the latter is thought to arise from *de novo* assembly of a branched actin network, the idea that existing filaments found in the microvillus could be repurposed for use in pedestals, thus providing an explanation for brush border effacement, has not been considered. Our data suggest that a pathway exists in parallel with Arp2/3-mediated polymerization, where microvilli are recruited to sites of EPEC attachment, coalesce around the bacterium, and the underlying cytoskeleton is remodeled into the dense network of pedestal actin. As this process proceeds, the overlying plasma membrane would be expected to remodel as the morphology of its cytoskeletal support changes. Indeed, the unusual “hand of doom” phenomenon seen in (Fig. 7-4A) appears to represent such an intermediate structure.

Pedestal formation is not dependent upon Arp2/3

If our model of microvillar contributions to pedestal formation is correct, we would expect that inhibition of the Arp2/3 pathway should not completely inhibit pedestal formation. Conversely, if *de novo* formation of a branched actin network occurs exclusively via Arp2/3-mediated polymerization, inhibition should prevent pedestal formation. To further investigate the possibility that microvilli may contribute to the EPEC attachment process independent of canonical pedestal formation, we took advantage of a recently developed small molecule inhibitor of the ArpC2 subunit of Arp2/3, called CK-666 (Nolen *et al.*, 2009). Caco-2_{BBE} monolayers grown for two weeks post-

confluency were incubated 2 hr with DMSO control or CK-666. EPEC was then added in the presence of DMSO or the drug, and incubated for 3 hr. The cells were fixed and stained with phalloidin to mark actin and α-LipidA to label EPEC. Intriguingly, the presence of CK-666 did not inhibit pedestal formation (Fig. 7-6A, B), nor was there a significant change in the number of bacteria adhered to the monolayer (Fig. 7-6C). We repeated the experiment using HeLa cells, which lack a brush border and instead form sparse dorsal filopodia. As with Caco-2_{BBE} cells, pedestals still formed in the presence of CK-666 (data not shown). The number of bacteria (quantified here as the percentage of total area covered by bacteria) was reduced in drug-treated HeLa cells when compared to DMSO-treated controls (Fig. 7-6C). A second Arp2/3 inhibitor, CK-869, also did not prevent pedestal formation, although it caused significant morphological changes in HeLa cells (Nolen *et al.*, 2009) (data not shown). In these cells, impaired pedestal formation due to a lack of Arp2/3 activity could be limiting intimate attachment, resulting in fewer bacteria counted after 3 hr. At the same time, pedestal formation is clearly not eliminated, which strongly indicates a secondary, though less efficient pathway exists that makes use of existing actin filaments. In other cell culture models, we have observed complete inhibition of lamellar dynamics upon treatment with CK-666, indicating the drug is highly effective. It is still possible, however, that CK-666 is not fully penetrant in HeLa cells, allowing some Arp2/3 activity and pedestal formation. In Caco-2_{BBE} cells, multi-drug resistance transporters could pump out CK-666, limiting its effectiveness and confounding the assays described above (Hirohashi *et al.*, 2000). Therefore, further work using knockdown of Arp complex components is needed to

confirm these results, and drug treatments such as cytochalasin B should be tested to determine the effect altered actin dynamics have on pedestal formation.

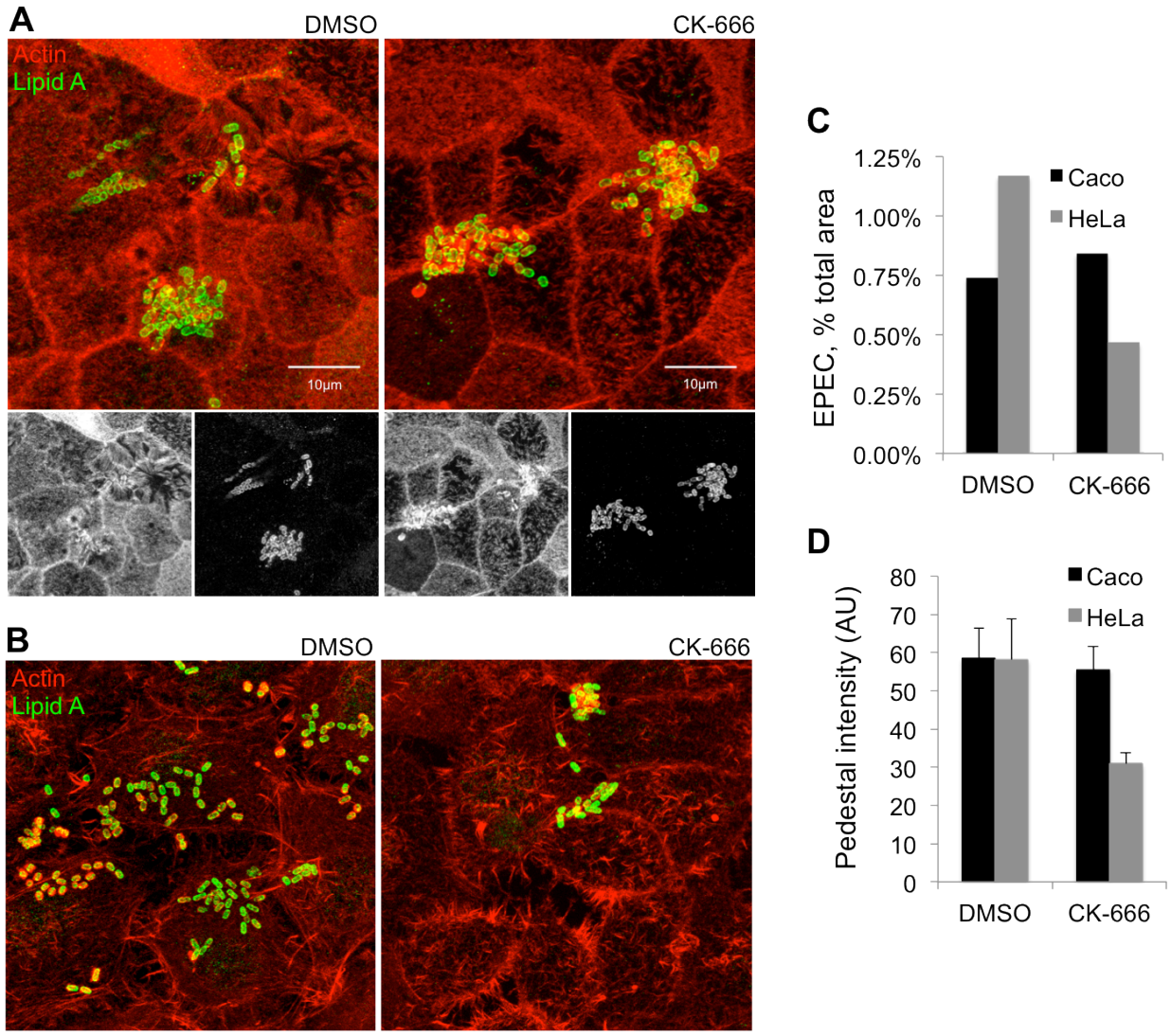

Figure 7-6: Arp2/3 inhibition does not prevent pedestal formation

(A) CK-666-treated Caco-2_{BBE} cells infected with EPEC for 3 hr show normal pedestal formation compared to DMSO controls, indicating that Arp2/3 is not required for this process. (B) Fewer EPEC attach to HeLa cells treated with CK-666 than those treated with DMSO, and although some pedestals still form, they have lower actin levels than in controls. (C) Percent of total area covered by EPEC in Caco-2_{BBE} and HeLa cells reveals the reduction in EPEC attachment in CK-666 treated HeLa cells, and the lack of response in Caco-2_{BBE}. (D) Actin intensity in pedestals is reduced in HeLa cells, but not in Caco-2_{BBE}, indicating inhibited pedestal formation in the former. Bars represent standard deviation

Conclusions

Our work demonstrates the tug-of-war nature of the relationship between enterocyte and pathogen. Host cells appear to utilize the highly ordered brush border, regulated by inter-microvillar links comprised of PCDH24 and MLPCDH, to maintain a barrier against pathogens making intimate contact with the apical surface (Figs. 6-1, 6-2). Conversely, the interconnected nature of brush border microvilli may provide a means for EPEC to collect F-actin in order to improve pedestal formation (Figs. 7-1, 7-5). Enteric pathogens are well adapted to the environment of the intestinal mucosa, and therefore even an intact brush border will eventually be compromised by the bacterium. Despite this problem, slowing the adherent/invasive process to any extent is likely beneficial to the host, providing time for activation of other defensive pathways.

From the standpoint of bacterial hijacking of enterocyte cellular machinery, we have also developed a new model of EPEC attachment that begins to connect microvillar effacement with pedestal formation. In this model, bacteria stimulate the flow of the brush border towards sites of attachment and cause elongation of microvilli, where the protrusions coalesce and may be partially disassembled or severed before microvillar actin bundles are recycled into a nascent pedestal. Having such a mechanism in place could be energetically favorable, potentially avoiding the need for much of the ATP expenditure required to build a *de novo* actin network, as well as possibly increasing the overall efficiency of the process by reusing existing cytoskeletal building blocks. Further work is needed to elucidate 1) the mechanism by which brush border flow occurs, 2) actin binding and severing proteins involved in microvillar

elongation and recycling, and 3) the bacterial components responsible for stimulating these processes.

There are significant challenges associated with these outstanding questions. It is difficult to dissect attachment, as there is known redundancy and cooperatively among EPEC virulence factors, and thus many host cell pathways are perturbed simultaneously (Dean and Kenny, 2009). Furthermore, the difference between a defensive host cell response and the pathogenic activity of bacteria may be difficult to distinguish. For example, microvillar elongation may help stabilize bacteria on the surface during early attachment, but the absence of this phenomenon does not eliminate pedestal formation in cells without microvilli such as HeLa. Conversely, it is possible that elongation is a defensive mechanism to prevent attachment or “sample” the pathogen in a manner similar to dendritic cells extending protrusions. Our observations that microvillar elongation can target EPEC attached to neighboring cells suggests this as a possibility. Like other host cell processes, elongation could be a normal cellular response that has been hijacked by a well-adapted pathogen to improve attachment. Historically, investigators have used EPEC mutants lacking various virulence factors to elucidate pathways involved in infection. Similar studies are needed, along with genetic manipulation of enterocyte brush border proteins, in order to begin building a complete understanding of both the process of microvillar elongation and its purpose during EPEC attachment.

It is interesting to note the paucity of information regarding microvillar effacement during infection, and the lack of a connection between this process and pedestal formation. Many of the early studies investigating actin polymerization during pedestal

formation relied upon *Xenopus* egg extracts or non polarized cells, primarily HeLa but also including MEFs, COS1, and HEp-2 [for example (Campellone *et al.*, 2002; Campellone and Leong, 2005)]. These cell lines are attractive due to their amenability to genetic manipulation and transfection. However, they lack a brush border, building instead a sparse network of microvilli or “dorsal filopodia” (Bohil *et al.*, 2006). additionally, as part of the differentiation process, epithelial cells utilized polarized trafficking pathways to segregate and maintain the apical and basolateral compartments (Cao *et al.*, 2012). Although the Caco-2_{BBE} cells used for live cell microscopy in the work described here were transiently transfected and thus not left in culture long enough to reach a fully polarized state, they do begin to assemble microvilli within hours of plating and thus rapidly acquire a significant apical network of parallel actin bundles. It is possible that the lack of true microvilli on the dorsal surface of non-polarized cells alters their interaction with A/E pathogens. In the absence of actin bundles, HeLa cells might be forced to rely on *de novo* actin polymerization through Arp2/3. Studies in these cells would therefore focus entirely on the Arp2/3 pathway, and subsequent work in intestinal epithelial cells would understandably target the same mechanism of pedestal formation. In the work described here, we focused on investigating microvillar dynamics during EPEC attachment, rather than directly targeting known signaling pathways. In this way, we have discovered that microvillar actin may play a role in the A/E process, and our data point to the possibility of an intriguing complementary pathway for pedestal formation. Future experiments will be needed to elucidate if and how these two pathways intersect, and their relative contributions to pedestal formation under physiological conditions.

CHAPTER VIII

CONCLUSIONS AND FUTURE DIRECTIONS

The work described here has revealed several novel aspects of enterocyte brush border function and dynamics during interactions with intestinal pathogens. We demonstrated that microvilli of the intestinal brush border shed IAP-enriched vesicles into the intestinal lumen as a means to condition the gut environment and maintain homeostasis (Shifrin *et al.*, 2012; Shifrin and Tyska, 2012). Importantly, through these studies we have found a mechanism to package and deliver IAP into the intestinal lumen. Concentrating the enzyme on vesicles, rather than releasing soluble IAP, may provide enterocytes a mechanism to increase its efficacy in conditioning the lumenal environment. LV-bound IAP detoxifies LPS from several bacterial species through dephosphorylation, thereby reducing the pro-inflammatory potential of this molecule (Fig. 3-1A, B; Fig. 3-3G). LVs also limit attachment of bacteria to the enterocyte (Fig. 3-3). Because LVs coat the surface of lumenal microbes (Fig. 3-1C, D), we hypothesize that LVs act as a physical buffer, blocking direct contact between a bacterium and enterocyte, thus preventing injection of virulence factors. However, this model remains untested, and should be the focus of future studies. Additionally, the precise nature of LV-microbe interactions remain unclear. It is possible that pathogens “infect” LVs via structures such as the BFP and the T3SS, with the vesicles serving as decoys for microvillar membrane. It is also possible that proteins on the surface of LVs, many of which are glycosylated, could simply stick to bacterial cell wall components through charged interactions. These ideas, which are by no means mutually exclusive, should be tested through a combination of biochemistry (e.g. stripping the surface of LVs of

sugar moieties and/or proteins) and genetic manipulation of bacterial molecules. LVs also inhibit bacterial population growth in an IAP-independent manner, reducing the plateau phase of bacterial cultures and actually reducing the number of viable microbes (Figs. 3-4, 3-5). We have carried out preliminary mass spectrometry on LVs isolated from WT and myo1a KO mice. No obvious bactericidal proteins were found in this analysis, but a more detailed investigation into the mechanism of LV-mediated bacterial death should be undertaken. Finally, although LV shedding is a constitutive process (Fig. 3-6), it is upregulated in the presence of pathogenic bacteria (Fig. 3-7). Interestingly, we found that EPEC conditioned media was not sufficient to stimulate shedding. EPEC culture media contains cellular fragments and bacterial outer membrane vesicles (OMV), which carry virulence factors, promote bacterial infection, and stimulate host immune responses (Kuehn and Kesty, 2005). In light of the potency of OMVs, it is somewhat surprising that EPEC conditioned media did not increase LV shedding. One explanation is that a single treatment with this media is simply not enough to cause a detectable increase in LV production. That is, without constant release of new OMVs from live EPEC to replenish the existing pool, the stimulatory effect never reaches a threshold level in our cell culture model. Future studies could investigate this idea by adding fresh conditioned media at regular intervals, or by using a filter to separate intestinal epithelial cells from bacteria, thereby allowing only the OMVs through.

In the absence of normal LV shedding in myo1a KO mice [Fig. 4-1 and (McConnell *et al.*, 2009)], we found signs of chronic inflammation. These included increased cytokine production, increased numbers of goblet cells along the length of the

small intestine, and pockets of eosinophil infiltration (Figs. 4-3, 4-4). Furthermore, these animals had altered gut bacterial populations, with shifts at the family level that, though subtle, were consistent with those seen in previous studies of intestinal perturbation (Fig. 4-2, Table 4-1). Together, these results demonstrate that LVs have a multi-faceted role in host defense and homeostasis, distributing catalytic activity into the lumen, inhibiting attachment of pathogens to the epithelial surface, and maintaining a normal intestinal microbiome.

Both the work described here and the original characterization of the myo1a KO mouse found only subtle deficiencies in the intestine, but none were severe enough to cause gross abnormalities in the animal under normal laboratory housing conditions (Tyska *et al.*, 2005). It is possible that the limited differences between WT and myo1a KO animals would be accentuated under conditions of intestinal distress. Therefore, future studies should induce perturbations to intestinal homeostasis using the murine pathogen *Citrobacter rodentium*, toxic bacterial compounds such as LPS, or DSS.

We also attempted to directly assay inflammatory signaling through activation of the NF-kB signaling pathway by using the NF-kB-GFP-Luciferase (NGL) mouse developed at Vanderbilt (Everhart *et al.*, 2006). Upon crossing these animals with our myo1a KO line, we hoped to use GFP and/or luciferase signal to compare levels of inflammation to WT. Preliminary results were promising but not reproducible, and we also found significant variability in the apparent expression levels of the GFP and luciferase reporters during homeostasis. In light of these confounding factors, we discontinued our studies using the NGL mouse model.

In the second part of this work, we focused on direct interactions between an A/E pathogen and the brush border, and dynamics associated with microvillar effacement during infection. We found that not only does the the brush border play an active role in host defense through the shedding of LVs, but it also serves as a physical barrier to limit bacterial attachment. Cells with normal microvillar packing density are less susceptible to bacterial attachment during the first few hours of infection (Figs. 6-1, 6-2). Throughout the literature on intestinal host-microbe interactions, barrier function of the mucosal layer has been a primary focus, in particular the regulation of epithelial permeability by tight junctions. Our data describe a subset of epithelial barrier function, in which the morphology of the apical domain of enterocytes plays a role in this process of limiting infection. As discussed in Chapter VI, even if enterocytes are unable to completely prevent infection when pathogens make contact, slowing the rate of infection may still be desirable. In the intestine, bacteria lacking intimate attachment are more likely to be eliminated by shear flow of lumenal contents and peristalsis. A lag in intimate attachment could also allow for activation of other immune responses, without causing a full inflammatory cascade.

We also provide evidence that PCDH24 is a molecular regulator of brush border barrier function, thus showing the adhesion molecule to be important not only in enterocyte morphogenesis (Fig. 6-1; Crawley *et al.*, submitted), but also in maintenance of the apical domain and, by extension, intestinal homeostasis. Interestingly, our results using a dominant negative PCDH24 construct showed that this molecule may also be used indirectly by bacteria to collect actin at sites of attachment (Fig. 7-2). Live cell imaging revealed that brush border flow is a hallmark of the attachment process, and

appears to increase with greater microvillar packing density (Figs. 7-1, 7-2). We hypothesize that by tying microvilli together, PCDH24 provides a mechanism for force transduction across the entire apical surface. As microvilli surrounding a bacterial cell elongate and coalesce, the inter-microvillar bonds could tug on neighboring protrusions, causing a domino effect towards the attachment site. By breaking inter-microvillar links formed by PCDH24, we were able to more carefully investigate the dynamics of microvillar elongation and coalescence, both events which we observed in SEM images.

An interesting component of host cell machinery that is compromised during EPEC infection, which we did not investigate here, is the motor protein myosin-2 (myo2). It is activated during EPEC infection, causing disruption of the tight junctions by pulling on junction-associated actin (Yuhan *et al.*, 1997). Contraction of the junctional actomyosin ring near the apical pole of enterocytes could be partly responsible for changes in cellular circumference we described (Fig. 7-2). Myo2 is also found in the terminal web (Bement and Mooseker, 1996). Activation of the motor during infection could cause contraction of actin in and around the terminal web, which in turn would be expected to pull on microvillar actin rootlets cross-linked to the terminal web cytoskeleton. Coupled with possible contributions of PCDH24 to force transduction between microvilli, this process could be an extremely effective mechanism for promoting bacterial-mediated apical remodeling of enterocytes by drawing the brush border towards sites of attachment. Live cell microscopy should be undertaken using the myo2 inhibitor blebbistatin, as well as inhibition or knockdown of myo2 regulators such as myosin light-chain kinase to test this hypothesis.

Using PCDH24-ΔEC1 transfected cells, we found that microvillar elongation is a directed phenomenon, in which actin polymerization is stimulated by the presence of bacteria (Fig. 7-3). Microvilli also coalesce as they cluster around bacteria, and actin and membrane from the protrusions is apparently remodeled into pedestals. SEM images show striking examples of bacteria cupped by a structure we have termed the "hand of doom," which appears to be a pedestal forming from the coalescence of microvilli (Fig. 7-4). Further support for a model of microvillar actin contributing to pedestals came from overexpression of the bundling protein espin (Loomis *et al.*, 2003). This molecule is observed in pedestals, but also slows their formation or abolishes it altogether (Figs. 7-4, 7-5). Thus, parallel actin is likely incorporated into pedestals, while the high degree of cross-linking in espin-stabilized microvilli inhibits this process. More broadly, our findings hint that actin binding proteins regulate the recycling process, an idea discussed further below. Finally, we tested this novel mechanism by inhibiting Arp2/3, the actin-nucleating complex thought to be critical for pedestal formation (Wong *et al.*, 2011). CK-666 inhibition of Arp2/3 did not prevent pedestal formation in Caco-2_{BBE} cells, and while the number of attached EPEC and pedestal actin intensity were reduced in HeLa cells, bacterial lesions were still observed (Fig. 7-6). This led us to conclude that a lack of parallel actin bundles on the dorsal surface forces HeLa cells to primarily utilize the Arp2/3 pathway; inhibition of Arp2/3 therefore limits pedestal formation.

Throughout this work, we have investigated the relationship between host cell and pathogen by inverting the approach used in many previous studies. Rather than beginning with molecular pathways involved in EPEC infection and using microscopy as

a readout for genetic or biochemical manipulations, we instead started by imaging the attachment process in real time. In this way, we were able to fill in some of the gaps in the field by providing kinetic data on dynamics of the enterocyte brush border and individual microvilli during the A/E process. For future studies, it will be important to use the live cell analysis carried out in this work as a foundation for biochemical and genetic studies in order to elucidate the molecular factors responsible for processes such as brush border flow, microvillar elongation, and microvillar coalescence.

These proposed studies are not trivial, as the host-pathogen interaction is extremely complex on a molecular level. The process of EPEC infection involves dozens of peptides and virulence factors supplied by the bacterium, which activate multiple host cell pathways. It is important to note that several of the steps, though part of the "canonical" EPEC signaling cascade, are not absolutely required for intimate attachment and pedestal formation under all circumstances. EspA-mediated adhesion can occur in the absence of BFP, although the rate of intimate attachment is reduced significantly (Cleary *et al.*, 2004). Work in a cell culture and tissue explant models of EPEC attachment found that effacement is a two-step process, and at least three virulence factors play somewhat overlapping roles in microvillar effacement (Dean *et al.*, 2006). Map, EspF, Tir, and intimin work in concert to promote elongation and effacement, with EspF in particular being necessary for elongation in biopsy samples (Shaw *et al.*, 2005; Dean *et al.*, 2006). Our preliminary SEM data indicates that BFP is required for microvillar elongation in Caco-2_{BBE} cells, while intimin is not, although onset of elongation is delayed and pedestals do not form. In another example, PIP_2-containing lipid rafts cluster at sites of attachment and recruit the actin-membrane adaptor protein

A2. However, this process appears to be independent of Tir, and may represent an alternative pathway to cytoskeletal manipulation (Zobiack *et al.*, 2002; Rescher *et al.*, 2004). Nck-deficient cells still form pedestals in a Tir-dependent manner, and several putative Tir-binding partners such as c-Src and tyrosine kinases have been described [reviewed in (Campellone, 2010)]. It is likely that these multiple parallel and/or compensatory pathways contribute to the heterogeneity of responses observed in cellular models of EPEC attachment. To date, though many pieces of the attachment process, and many putative interactions between host and bacterial proteins have been elucidated [reviewed by Wong *et al.* (2011)], a complete map of the interactions between bacterial effectors and host machinery does not exist. It would be interesting to utilize EPEC lacking some of the virulence factors just described in live cell assays to better understand how these molecules alter host cell machinery in real time. Super-resolution microscopy can also provide significant insight into the many aspects of infection, including recruitment of host cell molecules by virulence factors to attachment sites, reorganization of lipid rafts and associated proteins, and changes in structure or dynamics of pedestal formation in the absence of one or more bacterial proteins.

Focusing on the host cell, another important avenue will be to investigate the actin-associated proteins involved in microvillar elongation and effacement. Based on our findings with espin-overexpressing cells, as well as what is known about actin remodeling in other cellular protrusions, actin nucleating, binding and severing proteins are certainly involved in the process of microvillar elongation and recycling. The proteins espin, fimbrin, and villin localize to microvilli and are involved in regulation of the actin core (Bretscher and Weber, 1979, 1980; Bretscher, 1981; Bartles *et al.*, 1998). Villin and

fimbrin, along with another actin-binding protein ezrin, are recruited to sites of attachment and are thought to help regulate formation of pedestal actin (Goosney *et al.*, 2000). We have preliminary data showing that both fluorescent protein-tagged cofilin and fimbrin localize to pedestals, and in filopodia, the bundling protein fascin and the severing factor cofilin work synergistically to regulate actin bundles (Breitsprecher *et al.*, 2011). Microvillar length is regulated by a family of actin-binding proteins called Eps8. Regulated by interactions with ezrin, the founding member, Eps8, bundles actin filaments, while Eps8L1a caps them (Zwaenepoel *et al.*, 2012). Eps8L1a localizes to microvillar tips, where growth of filaments occurs, and loss of Eps8L1a leads to elongated microvilli (Zwaenepoel *et al.*, 2012). The authors of this work suggest that elongation is a result of uncontrolled actin polymerization in the absence of the Eps8L1a cap. This could very likely parallel the process by which microvilli elongate during EPEC attachment, and Eps8L1a localization and function should therefore be assessed in this context.

Additional clues to the role microvillar actin might play in pedestal formation, and the process by which recycling occurs, can be found in work on other cellular protrusions. At the leading edge of migrating and spreading cells, Arp2/3 activity produces the lamellipodium, a dense network of branched actin. Filopodia, consisting of parallel actin bundles nucleated by formins, extend distally from lamellipodium to sense the surrounding environment (Mattila and Lappalainen, 2008). Intriguingly, work investigating mechanisms of lamellipodia formation found they are nucleated from filopodia (Guillou *et al.*, 2008). Live cell imaging of spreading fibroblasts showed that lamellipodia emerge from established filopodia through a process the authors call

“filopodial swelling.” In the resulting model, parallel actin bundles of filopodia serve as “scaffold” for formation of the lamellipodial branched actin network, allowing the cell to feel out the surrounding environment then migrate forward. Microvilli and pedestals share many fundamental similarities, and microvillar coalescence and the “hand of doom” could mirror the process of filopodial swelling. That is, microvilli recruited to sites of EPEC attachment could serve as templates for formation of the pedestal, with Arp2/3 binding to the sides of the existing filaments and nucleating a branched network. In the absence of Arp2/3 activity, as with CK-666 treatment, the presence of parallel actin and its associated severing and bundling proteins may be sufficient to produce a rudimentary pedestal.

Significant work needs to be done in order to investigate this emerging model of EPEC attachment to enterocytes. In particular, using genetic tools to manipulate the many actin-associated proteins discussed above will help develop a detailed molecular mechanism for brush border remodeling during early attachment. Doing so, however, will be extremely informative and lead to significant advances in our understanding not only of host-microbe interactions, but also the formation and maintenance of the enterocyte brush border.

REFERENCES

(2009). Bacteroides and Prevotella Infections. Red Book *2009*, 230-231.

Abrahams, V.M., Straszewski-Chavez, S.L., Guller, S., and Mor, G. (2004). First trimester trophoblast cells secrete Fas ligand which induces immune cell apoptosis. Mol Hum Reprod *10*, 55-63.

Abreu, M.T., Vora, P., Faure, E., Thomas, L.S., Arnold, E.T., and Arditi, M. (2001). Decreased expression of Toll-like receptor-4 and MD-2 correlates with intestinal epithelial cell protection against dysregulated proinflammatory gene expression in response to bacterial lipopolysaccharide. J Immunol *167*, 1609-1616.

Akira, S., and Takeda, K. (2004). Toll-like receptor signalling. Nat Rev Immunol *4*, 499-511.

Al-Nedawi, K., Meehan, B., Micallef, J., Lhotak, V., May, L., Guha, A., and Rak, J. (2008). Intercellular transfer of the oncogenic receptor EGFRvIII by microvesicles derived from tumour cells. Nat Cell Biol *10*, 619-624.

Aliotta, J.M., Pereira, M., Johnson, K.W., de Paz, N., Dooner, M.S., Puente, N., Ayala, C., Brilliant, K., Berz, D., Lee, D., Ramratnam, B., McMillan, P.N., Hixson, D.C., Josic, D., and Quesenberry, P.J. (2010). Microvesicle entry into marrow cells mediates tissue-specific changes in mRNA by direct delivery of mRNA and induction of transcription. Exp Hematol *38*, 233-245.

Aliotta, J.M., Sanchez-Guijo, F.M., Dooner, G.J., Johnson, K.W., Dooner, M.S., Greer, K.A., Greer, D., Pimentel, J., Kolankiewicz, L.M., Puente, N., Faradyan, S., Ferland, P., Bearer, E.L., Passero, M.A., Adedi, M., Colvin, G.A., and Quesenberry, P.J. (2007). Alteration of marrow cell gene expression, protein production, and engraftment into lung by lung-derived microvesicles: a novel mechanism for phenotype modulation. Stem Cells *25*, 2245-2256.

Alto, N.M., Weflen, A.W., Rardin, M.J., Yarar, D., Lazar, C.S., Tonikian, R., Koller, A., Taylor, S.S., Boone, C., Sidhu, S.S., Schmid, S.L., Hecht, G.A., and Dixon, J.E. (2007). The type III effector EspF coordinates membrane trafficking by the spatiotemporal activation of two eukaryotic signaling pathways. J Cell Biol *178*, 1265-1278.

Andre, F., Schartz, N.E., Movassagh, M., Flament, C., Pautier, P., Morice, P., Pomel, C., Lhomme, C., Escudier, B., Le Chevalier, T., Tursz, T., Amigorena, S., Raposo, G., Angevin, E., and Zitvogel, L. (2002). Malignant effusions and immunogenic tumour-derived exosomes. Lancet *360*, 295-305.

Argiro, V., Bunge, M.B., and Johnson, M.I. (1985). A quantitative study of growth cone filopodial extension. J Neurosci Res *13*, 149-162.

Atay, S., Gercel-Taylor, C., Kesimer, M., and Taylor, D.D. (2011). Morphologic and proteomic characterization of exosomes released by cultured extravillous trophoblast cells. Exp Cell Res *317*, 1192-1202.

Backhed, F., Ding, H., Wang, T., Hooper, L.V., Koh, G.Y., Nagy, A., Semenkovich, C.F., and Gordon, J.I. (2004). The gut microbiota as an environmental factor that regulates fat storage. Proc Natl Acad Sci U S A *101*, 15718-15723.

Backhed, F., Ley, R.E., Sonnenburg, J.L., Peterson, D.A., and Gordon, J.I. (2005). Host-bacterial mutualism in the human intestine. Science *307*, 1915-1920.

Baietti, M.F., Zhang, Z., Mortier, E., Melchior, A., Degeest, G., Geeraerts, A., Ivarsson, Y., Depoortere, F., Coomans, C., Vermeiren, E., Zimmermann, P., and David, G. (2012). Syndecan-syntenin-ALIX regulates the biogenesis of exosomes. Nat Cell Biol *14*, 677-685.

Bankers-Fulbright, J.L., Kalli, K.R., and McKean, D.J. (1996). Interleukin-1 signal transduction. Life Sci *59*, 61-83.

Barker, N., van de Wetering, M., and Clevers, H. (2008). The intestinal stem cell. Genes Dev *22*, 1856-1864.

Bartles, J.R. (2000). Parallel actin bundles and their multiple actin-bundling proteins. Curr Opin Cell Biol *12*, 72-78.

Bartles, J.R., Zheng, L., Li, A., Wierda, A., and Chen, B. (1998). Small espin: a third actin-bundling protein and potential forked protein ortholog in brush border microvilli. J Cell Biol *143*, 107-119.

Bastida, E., Ordinas, A., Escolar, G., and Jamieson, G.A. (1984). Tissue factor in microvesicles shed from U87MG human glioblastoma cells induces coagulation, platelet aggregation, and thrombogenesis. Blood *64*, 177-184.

Bates, J.M., Akerlund, J., Mittge, E., and Guillemin, K. (2007). Intestinal alkaline phosphatase detoxifies lipopolysaccharide and prevents inflammation in zebrafish in response to the gut microbiota. Cell Host Microbe *2*, 371-382.

Bates, J.M., Mittge, E., Kuhlman, J., Baden, K.N., Cheesman, S.E., and Guillemin, K. (2006). Distinct signals from the microbiota promote different aspects of zebrafish gut differentiation. Dev Biol *297*, 374-386.

Bement, W.M., and Mooseker, M.S. (1996). The cytoskeleton of the intestinal epithelium: Components, assembly and dynamic rearrangements. In: The

cytoskeleton, vol. 3, ed. J.E.a.P. Hesketh, I. F., Greenwich, CT: Jai Press, 359-404.

Benesh, A.E., Nambiar, R., McConnell, R.E., Mao, S., Tabb, D.L., and Tyska, M.J. (2010). Differential localization and dynamics of class I myosins in the enterocyte microvillus. Mol Biol Cell *21*, 970-978.

Bernet-Camard, M.F., Coconnier, M.H., Hudault, S., and Servin, A.L. (1996). Pathogenicity of the diffusely adhering strain Escherichia coli C1845: F1845 adhesin-decay accelerating factor interaction, brush border microvillus injury, and actin disassembly in cultured human intestinal epithelial cells. Infect Immun *64*, 1918-1928.

Beumer, C., Wulferink, M., Raaben, W., Fiechter, D., Brands, R., and Seinen, W. (2003). Calf intestinal alkaline phosphatase, a novel therapeutic drug for lipopolysaccharide (LPS)-mediated diseases, attenuates LPS toxicity in mice and piglets. J Pharmacol Exp Ther *307*, 737-744.

Bianco, F., Perrotta, C., Novellino, L., Francolini, M., Riganti, L., Menna, E., Saglietti, L., Schuchman, E.H., Furlan, R., Clementi, E., Matteoli, M., and Verderio, C. (2009). Acid sphingomyelinase activity triggers microparticle release from glial cells. Embo J *28*, 1043-1054.

Bianco, F., Pravettoni, E., Colombo, A., Schenk, U., Moller, T., Matteoli, M., and Verderio, C. (2005). Astrocyte-derived ATP induces vesicle shedding and IL-1 beta release from microglia. J Immunol *174*, 7268-7277.

Bobryshev, Y.V., Killingsworth, M.C., and Orekhov, A.N. (2012). Increased shedding of microvesicles from intimal smooth muscle cells in athero-prone areas of the human aorta: implications for understanding of the predisease stage. Pathobiology *80*, 24-31.

Bohil, A.B., Robertson, B.W., and Cheney, R.E. (2006). Myosin-X is a molecular motor that functions in filopodia formation. Proc Natl Acad Sci U S A *103*, 12411-12416.

Breitsprecher, D., Koestler, S.A., Chizhov, I., Nemethova, M., Mueller, J., Goode, B.L., Small, J.V., Rottner, K., and Faix, J. (2011). Cofilin cooperates with fascin to disassemble filopodial actin filaments. J Cell Sci *124*, 3305-3318.

Bretscher, A. (1981). Fimbrin is a cytoskeletal protein that crosslinks F-actin in vitro. Proc Natl Acad Sci U S A *78*, 6849-6853.

Bretscher, A., and Weber, K. (1978). Localization of actin and microfilament-associated proteins in the microvilli and terminal web of the intestinal brush border by immunofluorescence microscopy. J Cell Biol *79*, 839-845.

Bretscher, A., and Weber, K. (1979). Villin: the major microfilament-associated protein of the intestinal microvillus. Proc Natl Acad Sci U S A *76*, 2321-2325.
Bretscher, A., and Weber, K. (1980). Fimbrin, a new microfilament-associated protein present in microvilli and other cell surface structures. J Cell Biol *86*, 335-340.

Burkel, B.M., von Dassow, G., and Bement, W.M. (2007). Versatile fluorescent probes for actin filaments based on the actin-binding domain of utrophin. Cell Motil Cytoskeleton *64*, 822-832.

Campellone, K.G. (2010). Cytoskeleton-modulating effectors of enteropathogenic and enterohaemorrhagic Escherichia coli: Tir, EspFU and actin pedestal assembly. FEBS J *277*, 2390-2402.

Campellone, K.G., Giese, A., Tipper, D.J., and Leong, J.M. (2002). A tyrosine-phosphorylated 12-amino-acid sequence of enteropathogenic Escherichia coli Tir binds the host adaptor protein Nck and is required for Nck localization to actin pedestals. Mol Microbiol *43*, 1227-1241.

Campellone, K.G., and Leong, J.M. (2005). Nck-independent actin assembly is mediated by two phosphorylated tyrosines within enteropathogenic Escherichia coli Tir. Mol Microbiol *56*, 416-432.

Cao, X., Surma, M.A., and Simons, K. (2012). Polarized sorting and trafficking in epithelial cells. Cell Res *22*, 793-805.

Cao, Z., Li, C., Higginbotham, J.N., Franklin, J.L., Tabb, D.L., Graves-Deal, R., Hill, S., Cheek, K., Jerome, W.G., Lapierre, L.A., Goldenring, J.R., Ham, A.J., and Coffey, R.J. (2008). Use of fluorescence-activated vesicle sorting for isolation of naked2-associated, basolaterally-targeted exocytic vesicles for proteomic analysis. Mol Cell Proteomics.

Chairoungdua, A., Smith, D.L., Pochard, P., Hull, M., and Caplan, M.J. (2010). Exosome release of beta-catenin: a novel mechanism that antagonizes Wnt signaling. J Cell Biol *190*, 1079-1091.

Chappelet-Tordo, D., Fosset, M., Iwatsubo, M., Gache, C., and Lazdunski, M. (1974). Intestinal alkaline phosphatase. Catalytic properties and half of the sites reactivity. Biochemistry *13*, 1788-1795.

Chaput, N., Taieb, J., Schartz, N.E., Andre, F., Angevin, E., and Zitvogel, L. (2004). Exosome-based immunotherapy. Cancer Immunol Immunother *53*, 234-239.

Chen, K.T., Malo, M.S., Beasley-Topliffe, L.K., Poelstra, K., Millan, J.L., Mostafa, G., Alam, S.N., Ramasamy, S., Warren, H.S., Hohmann, E.L., and Hodin, R.A. (2010a). A role for intestinal alkaline phosphatase in the maintenance of local gut immunity. Dig Dis Sci *56*, 1020-1027.

Chen, K.T., Malo, M.S., Moss, A.K., Zeller, S., Johnson, P., Ebrahimi, F., Mostafa, G., Alam, S.N., Ramasamy, S., Warren, H.S., Hohmann, E.L., and Hodin, R.A. (2010b). Identification of specific targets for the gut mucosal defense factor intestinal alkaline phosphatase. Am J Physiol Gastrointest Liver Physiol *299*, G467-475.

Chen, L., Fischle, W., Verdin, E., and Greene, W.C. (2001). Duration of nuclear NF-kappaB action regulated by reversible acetylation. Science *293*, 1653-1657.

Cheroutre, H. (2005). IELs: enforcing law and order in the court of the intestinal epithelium. Immunol Rev *206*, 114-131.

Cicero, A.L.R., Graça. (2013). Emerging Concepts of Tumor Exosome–Mediated Cell-Cell Communication. In: The Cell Biology of Exosomes: Historical and Perspectives, ed. H.-G. Zhang, New York: Springer.

Claesson, M.J., O'Sullivan, O., Wang, Q., Nikkila, J., Marchesi, J.R., Smidt, H., de Vos, W.M., Ross, R.P., and O'Toole, P.W. (2009). Comparative analysis of pyrosequencing and a phylogenetic microarray for exploring microbial community structures in the human distal intestine. PLoS One *4*, e6669.

Cleary, J., Lai, L.C., Shaw, R.K., Straatman-Iwanowska, A., Donnenberg, M.S., Frankel, G., and Knutton, S. (2004). Enteropathogenic Escherichia coli (EPEC) adhesion to intestinal epithelial cells: role of bundle-forming pili (BFP), EspA filaments and intimin. Microbiology *150*, 527-538.

Clifton, V.L., Stark, M.J., Osei-Kumah, A., and Hodyl, N.A. (2012). Review: The feto-placental unit, pregnancy pathology and impact on long term maternal health. Placenta *33 Suppl*, S37-41.

Cocucci, E., Racchetti, G., and Meldolesi, J. (2009). Shedding microvesicles: artefacts no more. Trends Cell Biol *19*, 43-51.

Collins, J.H., and Borysenko, C.W. (1984). The 110,000-dalton actin- and calmodulin-binding protein from intestinal brush border is a myosin-like ATPase. J Biol Chem *259*, 14128-14135.

Consortium, T.H.M.P. (2012). Structure, function and diversity of the healthy human microbiome. Nature *486*, 207-214.

D'Souza-Schorey, C., and Clancy, J.W. (2012). Tumor-derived microvesicles: shedding light on novel microenvironment modulators and prospective cancer biomarkers. Genes Dev *26*, 1287-1299.

Danielsen, E.M., and Hansen, G.H. (2003). Lipid rafts in epithelial brush borders: atypical membrane microdomains with specialized functions. Biochim Biophys Acta *1617*, 1-9.

de Gassart, A., Geminard, C., Hoekstra, D., and Vidal, M. (2004). Exosome secretion: the art of reutilizing nonrecycled proteins? Traffic *5*, 896-903.

De La Cruz, E.M., and Ostap, E.M. (2004). Relating biochemistry and function in the myosin superfamily. Curr Opin Cell Biol *16*, 61-67.

Dean, P., and Kenny, B. (2009). The effector repertoire of enteropathogenic E. coli: ganging up on the host cell. Curr Opin Microbiol *12*, 101-109.

Dean, P., Maresca, M., Schuller, S., Phillips, A.D., and Kenny, B. (2006). Potent diarrheagenic mechanism mediated by the cooperative action of three enteropathogenic Escherichia coli-injected effector proteins. Proc Natl Acad Sci U S A *103*, 1876-1881.

Dean, P., Young, L., Quitard, S., and Kenny, B. (2013). Insights into the pathogenesis of enteropathogenic E. coli using an improved intestinal enterocyte model. PLoS One *8*, e55284.

Dear, J.W., Street, J.M., and Bailey, M.A. (2012). Urinary exosomes: A reservoir for biomarker discovery and potential mediators of intra-renal signaling. Proteomics.

Deibel, C., Kramer, S., Chakraborty, T., and Ebel, F. (1998). EspE, a novel secreted protein of attaching and effacing bacteria, is directly translocated into infected host cells, where it appears as a tyrosine-phosphorylated 90 kDa protein. Mol Microbiol *28*, 463-474.

Demory Beckler, M., Higginbotham, J.N., Franklin, J.L., Ham, A.J., Halvey, P.J., Imasuen, I.E., Whitwell, C., Li, M., Liebler, D.C., and Coffey, R.J. (2012). Proteomic analysis of exosomes from mutant KRAS colon cancer cells identifies intercellular transfer of mutant KRAS. Mol Cell Proteomics.

Deregibus, M.C., Cantaluppi, V., Calogero, R., Lo Iacono, M., Tetta, C., Biancone, L., Bruno, S., Bussolati, B., and Camussi, G. (2007). Endothelial progenitor cell derived microvesicles activate an angiogenic program in endothelial cells by a horizontal transfer of mRNA. Blood *110*, 2440-2448.

Donnenberg, M.S., Tzipori, S., McKee, M.L., O'Brien, A.D., Alroy, J., and Kaper, J.B. (1993). The role of the eae gene of enterohemorrhagic Escherichia coli in intimate attachment in vitro and in a porcine model. J Clin Invest *92*, 1418-1424.

Dreux, M., Garaigorta, U., Boyd, B., Decembre, E., Chung, J., Whitten-Bauer, C., Wieland, S., and Chisari, F.V. (2012). Short-range exosomal transfer of viral RNA

from infected cells to plasmacytoid dendritic cells triggers innate immunity. Cell Host Microbe *12*, 558-570.

Dvorak, H.F., Van DeWater, L., Bitzer, A.M., Dvorak, A.M., Anderson, D., Harvey, V.S., Bach, R., Davis, G.L., DeWolf, W., and Carvalho, A.C. (1983). Procoagulant activity associated with plasma membrane vesicles shed by cultured tumor cells. Cancer Res *43*, 4434-4442.

Eckburg, P.B., Bik, E.M., Bernstein, C.N., Purdom, E., Dethlefsen, L., Sargent, M., Gill, S.R., Nelson, K.E., and Relman, D.A. (2005). Diversity of the human intestinal microbial flora. Science *308*, 1635-1638.

Eden, P.A., Schmidt, T.M., Blakemore, R.P., and Pace, N.R. (1991). Phylogenetic analysis of Aquaspirillum magnetotacticum using polymerase chain reaction-amplified 16S rRNA-specific DNA. Int J Syst Bacteriol *41*, 324-325.

Evans, D.J., and Evans, D.G. (1996). Escherichia Coli in Diarrheal Disease. In: Medical Microbiology, ed. S. Baron, Galveston (TX).

Everhart, M.B., Han, W., Sherrill, T.P., Arutiunov, M., Polosukhin, V.V., Burke, J.R., Sadikot, R.T., Christman, J.W., Yull, F.E., and Blackwell, T.S. (2006). Duration and intensity of NF-kappaB activity determine the severity of endotoxin-induced acute lung injury. J Immunol *176*, 4995-5005.

Falk, P.G., Hooper, L.V., Midtvedt, T., and Gordon, J.I. (1998). Creating and maintaining the gastrointestinal ecosystem: what we know and need to know from gnotobiology. Microbiol Mol Biol Rev *62*, 1157-1170.

Fallingborg, J. (1999). Intraluminal pH of the human gastrointestinal tract. Dan Med Bull *46*, 183-196.

Faure, J., Lachenal, G., Court, M., Hirrlinger, J., Chatellard-Causse, C., Blot, B., Grange, J., Schoehn, G., Goldberg, Y., Boyer, V., Kirchhoff, F., Raposo, G., Garin, J., and Sadoul, R. (2006). Exosomes are released by cultured cortical neurones. Mol Cell Neurosci *31*, 642-648.

Ferrary, E., Cohen-Tannoudji, M., Pehau-Arnaudet, G., Lapillonne, A., Athman, R., Ruiz, T., Boulouha, L., El Marjou, F., Doye, A., Fontaine, J.J., Antony, C., Babinet, C., Louvard, D., Jaisser, F., and Robine, S. (1999). In vivo, villin is required for Ca(2+)-dependent F-actin disruption in intestinal brush borders. J Cell Biol *146*, 819-830.

Fishman, W.H., Green, S., and Inglis, N.I. (1963). L-phenylalanine: an organ specific, stereospecific inhibitor of human intestinal alkaline phosphatase. Nature *198*, 685-686.

Frangsmyr, L., Baranov, V., Nagaeva, O., Stendahl, U., Kjellberg, L., and Mincheva-Nilsson, L. (2005). Cytoplasmic microvesicular form of Fas ligand in human early placenta: switching the tissue immune privilege hypothesis from cellular to vesicular level. Mol Hum Reprod *11*, 35-41.

Frank, D.N., St Amand, A.L., Feldman, R.A., Boedeker, E.C., Harpaz, N., and Pace, N.R. (2007). Molecular-phylogenetic characterization of microbial community imbalances in human inflammatory bowel diseases. Proc Natl Acad Sci U S A *104*, 13780-13785.

Frankel, G., Philips, A.D., Novakova, M., Batchelor, M., Hicks, S., and Dougan, G. (1998). Generation of Escherichia coli intimin derivatives with differing biological activities using site-directed mutagenesis of the intimin C- terminus domain. Mol Microbiol *29*, 559-570.

Fuccillo, M., Joyner, A.L., and Fishell, G. (2006). Morphogen to mitogen: the multiple roles of hedgehog signalling in vertebrate neural development. Nat Rev Neurosci *7*, 772-783.

Fukushima, K., Sasaki, I., Ogawa, H., Naito, H., Funayama, Y., and Matsuno, S. (1999). Colonization of microflora in mice: mucosal defense against luminal bacteria. J Gastroenterol *34*, 54-60.

Garrett, W.S., Gordon, J.I., and Glimcher, L.H. (2010). Homeostasis and inflammation in the intestine. Cell *140*, 859-870.

Gerke, V., Creutz, C.E., and Moss, S.E. (2005). Annexins: linking Ca2+ signalling to membrane dynamics. Nat Rev Mol Cell Biol *6*, 449-461.

Gersemann, M., Stange, E.F., and Wehkamp, J. (2011). From intestinal stem cells to inflammatory bowel diseases. World J Gastroenterol *17*, 3198-3203.

Gersemann, M., Wehkamp, J., and Stange, E.F. (2012). Innate immune dysfunction in inflammatory bowel disease. J Intern Med *271*, 421-428.

Ghosh, S., and Hayden, M.S. (2008). New regulators of NF-kappaB in inflammation. Nat Rev Immunol *8*, 837-848.

Gill, S.R., Pop, M., Deboy, R.T., Eckburg, P.B., Turnbaugh, P.J., Samuel, B.S., Gordon, J.I., Relman, D.A., Fraser-Liggett, C.M., and Nelson, K.E. (2006). Metagenomic analysis of the human distal gut microbiome. Science *312*, 1355-1359.

Giusti, I., D'Ascenzo, S., Millimaggi, D., Taraboletti, G., Carta, G., Franceschini, N., Pavan, A., and Dolo, V. (2008). Cathepsin B mediates the pH-dependent proinvasive activity of tumor-shed microvesicles. Neoplasia *10*, 481-488.

Goldberg, R.F., Austen, W.G., Jr., Zhang, X., Munene, G., Mostafa, G., Biswas, S., McCormack, M., Eberlin, K.R., Nguyen, J.T., Tatlidede, H.S., Warren, H.S., Narisawa, S., Millan, J.L., and Hodin, R.A. (2008). Intestinal alkaline phosphatase is a gut mucosal defense factor maintained by enteral nutrition. Proc Natl Acad Sci U S A *105*, 3551-3556.

Golub, E.E. (2009). Role of matrix vesicles in biomineralization. Biochim Biophys Acta *1790*, 1592-1598.

Golub, E.E. (2011). Biomineralization and matrix vesicles in biology and pathology. Semin Immunopathol *33*, 409-417.

Goosney, D.L., Gruenheid, S., and Finlay, B.B. (2000). Gut feelings: enteropathogenic E. coli (EPEC) interactions with the host. Annu Rev Cell Dev Biol *16*, 173-189.

Graner, M.W. (2011). Brain Tumor Exosomes and Microvesicles: Pleiotropic Effects from Tiny Cellular Surrogates. In: Molecular Targets of CNS Tumors, ed. M. Garami: InTech.

Grimm-Gunter, E.M., Revenu, C., Ramos, S., Hurbain, I., Smyth, N., Ferrary, E., Louvard, D., Robine, S., and Rivero, F. (2009). Plastin 1 binds to keratin and is required for terminal web assembly in the intestinal epithelium. Mol Biol Cell *20*, 2549-2562.

Gross, J.C., Chaudhary, V., Bartscherer, K., and Boutros, M. (2012). Active Wnt proteins are secreted on exosomes. Nat Cell Biol *14*, 1036-1045.

Guillou, H., Depraz-Depland, A., Planus, E., Vianay, B., Chaussy, J., Grichine, A., Albiges-Rizo, C., and Block, M.R. (2008). Lamellipodia nucleation by filopodia depends on integrin occupancy and downstream Rac1 signaling. Exp Cell Res *314*, 478-488.

Gupta, S., and Knowlton, A.A. (2007). HSP60 trafficking in adult cardiac myocytes: role of the exosomal pathway. Am J Physiol Heart Circ Physiol *292*, H3052-3056.

Guttman, J.A., and Finlay, B.B. (2009). Tight junctions as targets of infectious agents. Biochimica et biophysica acta *1788*, 832-841.

Harris, H. (1990). The human alkaline phosphatases: what we know and what we don't know. Clin Chim Acta *186*, 133-150.

Hausmann, M. (2010). How bacteria-induced apoptosis of intestinal epithelial cells contributes to mucosal inflammation. Int J Inflam *2010*, 574568.

Henne, W.M., Buchkovich, N.J., and Emr, S.D. (2011). The ESCRT pathway. Dev Cell *21*, 77-91.

Hicks, S., Frankel, G., Kaper, J.B., Dougan, G., and Phillips, A.D. (1998). Role of intimin and bundle-forming pili in enteropathogenic Escherichia coli adhesion to pediatric intestinal tissue in vitro. Infect Immun *66*, 1570-1578.

Higginbotham, J.N., Demory Beckler, M., Gephart, J.D., Franklin, J.L., Bogatcheva, G., Kremers, G.J., Piston, D.W., Ayers, G.D., McConnell, R.E., Tyska, M.J., and Coffey, R.J. (2011). Amphiregulin exosomes increase cancer cell invasion. Curr Biol *21*, 779-786.

Hirohashi, T., Suzuki, H., Chu, X.Y., Tamai, I., Tsuji, A., and Sugiyama, Y. (2000). Function and expression of multidrug resistance-associated protein family in human colon adenocarcinoma cells (Caco-2). J Pharmacol Exp Ther *292*, 265-270.

Hong, B.S., Cho, J.H., Kim, H., Choi, E.J., Rho, S., Kim, J., Kim, J.H., Choi, D.S., Kim, Y.K., Hwang, D., and Gho, Y.S. (2009). Colorectal cancer cell-derived microvesicles are enriched in cell cycle-related mRNAs that promote proliferation of endothelial cells. BMC Genomics *10*, 556.

Hood, J.L., Pan, H., Lanza, G.M., and Wickline, S.A. (2009). Paracrine induction of endothelium by tumor exosomes. Lab Invest *89*, 1317-1328.

Hood, J.L., San, R.S., and Wickline, S.A. (2011). Exosomes released by melanoma cells prepare sentinel lymph nodes for tumor metastasis. Cancer Res *71*, 3792-3801.

Hooper, L.V., Bry, L., Falk, P.G., and Gordon, J.I. (1998). Host-microbial symbiosis in the mammalian intestine: exploring an internal ecosystem. Bioessays *20*, 336-343.

Howard, J. (2001). Mechanics of motor proteins and the cytoskeleton. Sinauer associates, inc.: New York.

Hoylaerts, M.F., Manes, T., and Millan, J.L. (1997). Mammalian alkaline phosphatases are allosteric enzymes. J Biol Chem *272*, 22781-22787.

Hsu, C., Morohashi, Y., Yoshimura, S., Manrique-Hoyos, N., Jung, S., Lauterbach, M.A., Bakhti, M., Gronborg, M., Mobius, W., Rhee, J., Barr, F.A., and Simons, M. (2010). Regulation of exosome secretion by Rab35 and its GTPase-activating proteins TBC1D10A-C. J Cell Biol *189*, 223-232.

Hurley, J.H., and Odorizzi, G. (2012). Get on the exosome bus with ALIX. Nat Cell Biol *14*, 654-655.

Iglesias, D.M., El-Kares, R., Taranta, A., Bellomo, F., Emma, F., Besouw, M., Levtchenko, E., Toelen, J., van den Heuvel, L., Chu, L., Zhao, J., Young, Y.K., Eliopoulos, N., and Goodyer, P. (2012). Stem cell microvesicles transfer

cystinosin to human cystinotic cells and reduce cystine accumulation in vitro. PLoS One *7*, e42840.

Ivanov, II, Atarashi, K., Manel, N., Brodie, E.L., Shima, T., Karaoz, U., Wei, D., Goldfarb, K.C., Santee, C.A., Lynch, S.V., Tanoue, T., Imaoka, A., Itoh, K., Takeda, K., Umesaki, Y., Honda, K., and Littman, D.R. (2009). Induction of intestinal Th17 cells by segmented filamentous bacteria. Cell *139*, 485-498.

Jin, X., Zimmers, T.A., Zhang, Z., Pierce, R.H., and Koniaris, L.G. (2010). Interleukin-6 is an important in vivo inhibitor of intestinal epithelial cell death in mice. Gut *59*, 186-196.

Johansson, M.E., Larsson, J.M., and Hansson, G.C. (2011). The two mucus layers of colon are organized by the MUC2 mucin, whereas the outer layer is a legislator of host-microbial interactions. Proc Natl Acad Sci U S A *108 Suppl 1*, 4659-4665.

Johansson, M.E., Phillipson, M., Petersson, J., Velcich, A., Holm, L., and Hansson, G.C. (2008). The inner of the two Muc2 mucin-dependent mucus layers in colon is devoid of bacteria. Proc Natl Acad Sci U S A *105*, 15064-15069.

Kandori, H., Hirayama, K., Takeda, M., and Doi, K. (1996). Histochemical, lectin-histochemical and morphometrical characteristics of intestinal goblet cells of germfree and conventional mice. Exp Anim *45*, 155-160.

Karnovsky, M.J., Kleinfeld, A.M., Hoover, R.L., and Klausner, R.D. (1982). The concept of lipid domains in membranes. The J Cell Biol *94*, 1-6.

Kenny, B. (1999). Phosphorylation of tyrosine 474 of the enteropathogenic Escherichia coli (EPEC) Tir receptor molecule is essential for actin nucleating activity and is preceded by additional host modifications. Mol Microbiol *31*, 1229-1241.

Khurana, S., and George, S.P. (2008). Regulation of cell structure and function by actin-binding proteins: villin's perspective. FEBS Lett *582*, 2128-2139.

Koyama, I., Matsunaga, T., Harada, T., Hokari, S., and Komoda, T. (2002). Alkaline phosphatases reduce toxicity of lipopolysaccharides in vivo and in vitro through dephosphorylation. Clin Biochem *35*, 455-461.

Kuehn, M.J., and Kesty, N.C. (2005). Bacterial outer membrane vesicles and the host-pathogen interaction. Genes Dev *19*, 2645-2655.

Laakso, J.M., Lewis, J.H., Shuman, H., and Ostap, E.M. (2008). Myosin I can act as a molecular force sensor. Science *321*, 133-136.

Lachenal, G., Pernet-Gallay, K., Chivet, M., Hemming, F.J., Belly, A., Bodon, G., Blot, B., Haase, G., Goldberg, Y., and Sadoul, R. (2011). Release of exosomes from

differentiated neurons and its regulation by synaptic glutamatergic activity. Mol Cell Neurosci *46*, 409-418.

Lee, T.H., D'Asti, E., Magnus, N., Al-Nedawi, K., Meehan, B., and Rak, J. (2011). Microvesicles as mediators of intercellular communication in cancer--the emerging science of cellular 'debris'. Semin Immunopathol *33*, 455-467.

Lee, Y., El Andaloussi, S., and Wood, M.J. (2012). Exosomes and microvesicles: extracellular vesicles for genetic information transfer and gene therapy. Hum Mol Genet *21*, R125-134.

Ley, R.E., Backhed, F., Turnbaugh, P., Lozupone, C.A., Knight, R.D., and Gordon, J.I. (2005). Obesity alters gut microbial ecology. Proc Natl Acad Sci U S A *102*, 11070-11075.

Ley, R.E., Hamady, M., Lozupone, C., Turnbaugh, P.J., Ramey, R.R., Bircher, J.S., Schlegel, M.L., Tucker, T.A., Schrenzel, M.D., Knight, R., and Gordon, J.I. (2008). Evolution of mammals and their gut microbes. Science *320*, 1647-1651.

Li, Q., and Verma, I.M. (2002). NF-kappaB regulation in the immune system. Nat Rev Immunol *2*, 725-734.

Liu, H., Magoun, L., Luperchio, S., Schauer, D.B., and Leong, J.M. (1999). The Tir-binding region of enterohaemorrhagic Escherichia coli intimin is sufficient to trigger actin condensation after bacterial-induced host cell signalling. Mol Microbiol *34*, 67-81.

Liu, Y., Xiang, X., Zhuang, X., Zhang, S., Liu, C., Cheng, Z., Michalek, S., Grizzle, W., and Zhang, H.G. (2010). Contribution of MyD88 to the tumor exosome-mediated induction of myeloid derived suppressor cells. Am J Pathol *176*, 2490-2499.

Loomis, P.A., Zheng, L., Sekerkova, G., Changyaleket, B., Mugnaini, E., and Bartles, J.R. (2003). Espin cross-links cause the elongation of microvillus-type parallel actin bundles in vivo. J Cell Biol *163*, 1045-1055.

Louvard, D., Kedinger, M., and Hauri, H.P. (1992). The differentiating intestinal epithelial cell: establishment and maintenance of functions through interactions between cellular structures. Annu Rev Cell Biol *8*, 157-195.

Lowe, M., Strauss, A.W., Alpers, R., Seetharam, S., and Alpers, D.H. (1990). Molecular cloning and expression of a cDNA encoding the membrane-associated rat intestinal alkaline phosphatase. Biochim Biophys Acta *1037*, 170-177.

Lozupone, C.A., Stombaugh, J.I., Gordon, J.I., Jansson, J.K., and Knight, R. (2012). Diversity, stability and resilience of the human gut microbiota. Nature *489*, 220-230.

Luga, V., Zhang, L., Viloria-Petit, A.M., Ogunjimi, A.A., Inanlou, M.R., Chiu, E., Buchanan, M., Hosein, A.N., Basik, M., and Wrana, J.L. (2012). Exosomes Mediate Stromal Mobilization of Autocrine Wnt-PCP Signaling in Breast Cancer Cell Migration. Cell *151*, 1542-1556.

Lupp, C., Robertson, M.L., Wickham, M.E., Sekirov, I., Champion, O.L., Gaynor, E.C., and Finlay, B.B. (2007). Host-mediated inflammation disrupts the intestinal microbiota and promotes the overgrowth of Enterobacteriaceae. Cell Host Microbe *2*, 119-129.

Macconkey, A. (1905). Lactose-Fermenting Bacteria in Faeces. J Hyg (Lond) *5*, 333-379.

Malo, M.S., Alam, S.N., Mostafa, G., Zeller, S.J., Johnson, P.V., Mohammad, N., Chen, K.T., Moss, A.K., Ramasamy, S., Faruqui, A., Hodin, S., Malo, P.S., Ebrahimi, F., Biswas, B., Narisawa, S., Millan, J.L., Warren, H.S., Kaplan, J.B., Kitts, C.L., Hohmann, E.L., and Hodin, R.A. (2010). Intestinal alkaline phosphatase preserves the normal homeostasis of gut microbiota. Gut *59*, 1476-1484.

Mangeot, P.E., Dollet, S., Girard, M., Ciancia, C., Joly, S., Peschanski, M., and Lotteau, V. (2011). Protein transfer into human cells by VSV-G-induced nanovesicles. Mol Ther *19*, 1656-1666.

Massey-Harroche, D., Mayran, N., and Maroux, S. (1998). Polarized localizations of annexins I, II, VI and XIII in epithelial cells of intestinal, hepatic and pancreatic tissues. J Cell Sci *111 (Pt 20)*, 3007-3015.

Mathivanan, S., Ji, H., and Simpson, R.J. (2010). Exosomes: extracellular organelles important in intercellular communication. J Proteomics *73*, 1907-1920.

Matsudaira, P.T., and Burgess, D.R. (1979). Identification and organization of the components in the isolated microvillus cytoskeleton. J Cell Biol *83*, 667-673.

Mattila, P.K., and Lappalainen, P. (2008). Filopodia: molecular architecture and cellular functions. Nat Rev Mol Cell Biol *9*, 446-454.

Mause, S.F., and Weber, C. (2010). Microparticles: protagonists of a novel communication network for intercellular information exchange. Circ Res *107*, 1047-1057.

Mazmanian, S.K., Round, J.L., and Kasper, D.L. (2008). A microbial symbiosis factor prevents intestinal inflammatory disease. Nature *453*, 620-625.

McConnell, R.E., Benesh, A.E., Mao, S., Tabb, D.L., and Tyska, M.J. (2011). Proteomic analysis of the enterocyte brush border. Am J Physiol Gastrointest Liver Physiol *300*, G914-926.

McConnell, R.E., Higginbotham, J.N., Shifrin, D.A., Jr., Tabb, D.L., Coffey, R.J., and Tyska, M.J. (2009). The enterocyte microvillus is a vesicle-generating organelle. J Cell Biol *185*, 1285-1298.

McConnell, R.E., and Tyska, M.J. (2007). Myosin-1a powers the sliding of apical membrane along microvillar actin bundles. J Cell Biol *177*, 671-681.

McGuckin, M.A., Linden, S.K., Sutton, P., and Florin, T.H. (2011). Mucin dynamics and enteric pathogens. Nat Rev Microbiol *9*, 265-278.

McKenna, M.J., Hamilton, T.A., and Sussman, H.H. (1979). Comparison of human alkaline phosphatase isoenzymes. Structural evidence for three protein classes. Biochem J *181*, 67-73.

Meyer-Hoffert, U., Hornef, M.W., Henriques-Normark, B., Axelsson, L.G., Midtvedt, T., Putsep, K., and Andersson, M. (2008). Secreted enteric antimicrobial activity localises to the mucus surface layer. Gut *57*, 764-771.

Millan, J.L. (2006). Alkaline Phosphatases : Structure, substrate specificity and functional relatedness to other members of a large superfamily of enzymes. Purinergic Signal *2*, 335-341.

Mineo, M., Garfield, S.H., Taverna, S., Flugy, A., De Leo, G., Alessandro, R., and Kohn, E.C. (2012). Exosomes released by K562 chronic myeloid leukemia cells promote angiogenesis in a Src-dependent fashion. Angiogenesis *15*, 33-45.

Mooseker, M.S. (1985). Organization, chemistry, and assembly of the cytoskeletal apparatus of the intestinal brush border. Annu Rev Cell Biol *1*, 209-241.

Mooseker, M.S., and Cheney, R.E. (1995). Unconventional myosins. Annu Rev Cell Dev Biol *11:633-75*, 633-675.

Mooseker, M.S., and Tilney, L.G. (1975). Organization of an actin filament-membrane complex. Filament polarity and membrane attachment in the microvilli of intestinal epithelial cells. J Cell Biol *67*, 725-743.

Muralidharan-Chari, V., Clancy, J.W., Sedgwick, A., and D'Souza-Schorey, C. (2010). Microvesicles: mediators of extracellular communication during cancer progression. J Cell Sci *123*, 1603-1611.

Nabhan, J.F., Hu, R., Oh, R.S., Cohen, S.N., and Lu, Q. (2012). Formation and release of arrestin domain-containing protein 1-mediated microvesicles (ARMMs) at plasma membrane by recruitment of TSG101 protein. Proc Natl Acad Sci U S A *109*, 4146-4151.

Nambiar, R., McConnell, R.E., and Tyska, M.J. (2009). Control of cell membrane tension by myosin-I. Proc Natl Acad Sci U S A.

Nolen, B.J., Tomasevic, N., Russell, A., Pierce, D.W., Jia, Z., McCormick, C.D., Hartman, J., Sakowicz, R., and Pollard, T.D. (2009). Characterization of two classes of small molecule inhibitors of Arp2/3 complex. Nature *460*, 1031-1034.

O'Boyle, C.J., MacFie, J., Mitchell, C.J., Johnstone, D., Sagar, P.M., and Sedman, P.C. (1998). Microbiology of bacterial translocation in humans. Gut *42*, 29-35.

Ostrowski, M., Carmo, N.B., Krumeich, S., Fanget, I., Raposo, G., Savina, A., Moita, C.F., Schauer, K., Hume, A.N., Freitas, R.P., Goud, B., Benaroch, P., Hacohen, N., Fukuda, M., Desnos, C., Seabra, M.C., Darchen, F., Amigorena, S., Moita, L.F., and Thery, C. (2010). Rab27a and Rab27b control different steps of the exosome secretion pathway. Nat Cell Biol *12*, 19-30; sup pp 11-13.

Ouellette, A.J. (1999). IV. Paneth cell antimicrobial peptides and the biology of the mucosal barrier. Am J Physiol *277*, G257-261.

Packey, C.D., and Sartor, R.B. (2009). Commensal bacteria, traditional and opportunistic pathogens, dysbiosis and bacterial killing in inflammatory bowel diseases. Curr Opin Infect Dis *22*, 292-301.

Pang, W., Wang, H., Shi, L., Sun, Y., Wang, X., Wang, M., Li, J., and Shi, G. (2013). Immunomodulatory Effects of Escherichia coli ATCC 25922 on Allergic Airway Inflammation in a Mouse Model. PLoS ONE *8*, e59174.

Park, B.S., Song, D.H., Kim, H.M., Choi, B.S., Lee, H., and Lee, J.O. (2009). The structural basis of lipopolysaccharide recognition by the TLR4-MD-2 complex. Nature *458*, 1191-1195.

Paulick, M.G., and Bertozzi, C.R. (2008). The glycosylphosphatidylinositol anchor: a complex membrane-anchoring structure for proteins. Biochemistry *47*, 6991-7000.

Peinado, H., Aleckovic, M., Lavotshkin, S., Matei, I., Costa-Silva, B., Moreno-Bueno, G., Hergueta-Redondo, M., Williams, C., Garcia-Santos, G., Ghajar, C., Nitadori-Hoshino, A., Hoffman, C., Badal, K., Garcia, B.A., Callahan, M.K., Yuan, J., Martins, V.R., Skog, J., Kaplan, R.N., Brady, M.S., Wolchok, J.D., Chapman, P.B., Kang, Y., Bromberg, J., and Lyden, D. (2012). Melanoma exosomes educate bone marrow progenitor cells toward a pro-metastatic phenotype through MET. Nat Med *18*, 883-891.

Peralta-Ramirez, J., Hernandez, J.M., Manning-Cela, R., Luna-Munoz, J., Garcia-Tovar, C., Nougayrede, J.P., Oswald, E., and Navarro-Garcia, F. (2008). EspF Interacts with nucleation-promoting factors to recruit junctional proteins into pedestals for

pedestal maturation and disruption of paracellular permeability. Infect Immun *76*, 3854-3868.

Petersen, C.P., and Reddien, P.W. (2009). Wnt signaling and the polarity of the primary body axis. Cell *139*, 1056-1068.

Peterson, D.A., Frank, D.N., Pace, N.R., and Gordon, J.I. (2008). Metagenomic approaches for defining the pathogenesis of inflammatory bowel diseases. Cell Host Microbe *3*, 417-427.

Peterson, M.D., Bement, W.M., and Mooseker, M.S. (1993). An in vitro model for the analysis of intestinal brush border assembly. II. Changes in expression and localization of brush border proteins during cell contact-induced brush border assembly in Caco-2BBe cells. J Cell Sci *105*, 461-472.

Peterson, M.D., and Mooseker, M.S. (1992). Characterization of the enterocyte-like brush border cytoskeleton of the C2BBe clones of the human intestinal cell line, Caco-2. J Cell Sci *102*, 581-600.

Peterson, M.D., and Mooseker, M.S. (1993). An in vitro model for the analysis of intestinal brush border assembly. I. Ultrastructural analysis of cell contact-induced brush border assembly in Caco-2BBe cells. J Cell Sci *105*, 445-460.

Phillips, A.D., Giron, J., Hicks, S., Dougan, G., and Frankel, G. (2000). Intimin from enteropathogenic Escherichia coli mediates remodelling of the eukaryotic cell surface. Microbiology *146 (Pt 6)*, 1333-1344.

Pisetsky, D.S., Gauley, J., and Ullal, A.J. (2011). Microparticles as a source of extracellular DNA. Immunol Res *49*, 227-234.

Poelstra, K., Bakker, W.W., Klok, P.A., Kamps, J.A., Hardonk, M.J., and Meijer, D.K. (1997). Dephosphorylation of endotoxin by alkaline phosphatase in vivo. Am J Pathol *151*, 1163-1169.

Poltorak, A., He, X., Smirnova, I., Liu, M.Y., Van Huffel, C., Du, X., Birdwell, D., Alejos, E., Silva, M., Galanos, C., Freudenberg, M., Ricciardi-Castagnoli, P., Layton, B., and Beutler, B. (1998). Defective LPS signaling in C3H/HeJ and C57BL/10ScCr mice: mutations in Tlr4 gene. Science *282*, 2085-2088.

Pollard, T.D., Blanchoin, L., and Mullins, R.D. (2000). Molecular mechanisms controlling actin filament dynamics in nonmuscle cells. Annu Rev Biophys Biomol Struct *29*, 545-576.

Pollard, T.D., and Mooseker, M.S. (1981). Direct measurement of actin polymerization rate constants by electron microscopy of actin filaments nucleated by isolated microvillus cores. J Cell Biol *88*, 654-659.

Poste, G., and Nicolson, G.L. (1980). Arrest and metastasis of blood-borne tumor cells are modified by fusion of plasma membrane vesicles from highly metastatic cells. Proc Natl Acad Sci U S A *77*, 399-403.

Putz, U., Howitt, J., Doan, A., Goh, C.P., Low, L.H., Silke, J., and Tan, S.S. (2012). The tumor suppressor PTEN is exported in exosomes and has phosphatase activity in recipient cells. Sci Signal *5*, ra70.

Qin, J., Li, R., Raes, J., Arumugam, M., Burgdorf, K.S., Manichanh, C., Nielsen, T., Pons, N., Levenez, F., Yamada, T., Mende, D.R., Li, J., Xu, J., Li, S., Li, D., Cao, J., Wang, B., Liang, H., Zheng, H., Xie, Y., Tap, J., Lepage, P., Bertalan, M., Batto, J.M., Hansen, T., Le Paslier, D., Linneberg, A., Nielsen, H.B., Pelletier, E., Renault, P., Sicheritz-Ponten, T., Turner, K., Zhu, H., Yu, C., Jian, M., Zhou, Y., Li, Y., Zhang, X., Qin, N., Yang, H., Wang, J., Brunak, S., Dore, J., Guarner, F., Kristiansen, K., Pedersen, O., Parkhill, J., Weissenbach, J., Bork, P., and Ehrlich, S.D. (2010). A human gut microbial gene catalogue established by metagenomic sequencing. Nature *464*, 59-65.

Raiborg, C., and Stenmark, H. (2009). The ESCRT machinery in endosomal sorting of ubiquitylated membrane proteins. Nature *458*, 445-452.

Ramasamy, S., Nguyen, D.D., Eston, M.A., Nasrin Alam, S., Moss, A.K., Ebrahimi, F., Biswas, B., Mostafa, G., Chen, K.T., Kaliannan, K., Yammine, H., Narisawa, S., Millan, J.L., Warren, H.S., Hohmann, E.L., Mizoguchi, E., Reinecker, H.C., Bhan, A.K., Snapper, S.B., Malo, M.S., and Hodin, R.A. (2010). Intestinal alkaline phosphatase has beneficial effects in mouse models of chronic colitis. Inflamm Bowel Dis *17*, 532-542.

Rao, J.N., and Wang, J.Y. (2010). In: Regulation of Gastrointestinal Mucosal Growth, San Rafael (CA).

Rescher, U., Ruhe, D., Ludwig, C., Zobiack, N., and Gerke, V. (2004). Annexin 2 is a phosphatidylinositol (4,5)-bisphosphate binding protein recruited to actin assembly sites at cellular membranes. J Cell Sci *117*, 3473-3480.

Rescigno, M., Urbano, M., Valzasina, B., Francolini, M., Rotta, G., Bonasio, R., Granucci, F., Kraehenbuhl, J.P., and Ricciardi-Castagnoli, P. (2001). Dendritic cells express tight junction proteins and penetrate gut epithelial monolayers to sample bacteria. Nat Immunol *2*, 361-367.

Rietschel, E.T., Kirikae, T., Schade, F.U., Mamat, U., Schmidt, G., Loppnow, H., Ulmer, A.J., Zahringer, U., Seydel, U., Di Padova, F., and et al. (1994). Bacterial endotoxin: molecular relationships of structure to activity and function. FASEB J *8*, 217-225.

Round, J.L., and Mazmanian, S.K. (2009). The gut microbiota shapes intestinal immune responses during health and disease. Nat Rev Immunol *9*, 313-323.

Ruetz, T., Cornick, S., and Guttman, J.A. (2011). The spectrin cytoskeleton is crucial for adherent and invasive bacterial pathogenesis. PLoS One *6*, e19940.

Ruetz, T.J., Vogl, A.W., and Guttman, J.A. (2012). Detailed examination of cytoskeletal networks within enteropathogenic Escherichia coli pedestals. Anat Rec (Hoboken) *295*, 201-207.

Salzman, N.H., Hung, K., Haribhai, D., Chu, H., Karlsson-Sjoberg, J., Amir, E., Teggatz, P., Barman, M., Hayward, M., Eastwood, D., Stoel, M., Zhou, Y., Sodergren, E., Weinstock, G.M., Bevins, C.L., Williams, C.B., and Bos, N.A. (2010). Enteric defensins are essential regulators of intestinal microbial ecology. Nat Immunol *11*, 76-83.

Sartor, R.B. (2008). Microbial influences in inflammatory bowel diseases. Gastroenterology *134*, 577-594.

Sato, N., Funayama, N., Nagafuchi, A., Yonemura, S., and Tsukita, S. (1992). A gene family consisting of ezrin, radixin and moesin. Its specific localization at actin filament/plasma membrane association sites. J Cell Sci *103 (Pt 1)*, 131-143.

Savage, D.C. (1977). Microbial ecology of the gastrointestinal tract. Annu Rev Microbiol *31*, 107-133.

Scaletsky, I.C., Silva, M.L., and Trabulsi, L.R. (1984). Distinctive patterns of adherence of enteropathogenic Escherichia coli to HeLa cells. Infect Immun *45*, 534-536.

Schiera, G., Proia, P., Alberti, C., Mineo, M., Savettieri, G., and Di Liegro, I. (2007). Neurons produce FGF2 and VEGF and secrete them at least in part by shedding extracellular vesicles. J Cell Mol Med *11*, 1384-1394.

Schmidt, T.M., and Relman, D.A. (1994). Phylogenetic identification of uncultured pathogens using ribosomal RNA sequences. Methods Enzymol *235*, 205-222.

Schroeder, G.N., and Hilbi, H. (2008). Molecular pathogenesis of Shigella spp.: controlling host cell signaling, invasion, and death by type III secretion. Clin Microbiol Rev *21*, 134-156.

Sharma, R., Tesfay, S., Tomson, F.L., Kanteti, R.P., Viswanathan, V.K., and Hecht, G. (2006). Balance of bacterial pro- and anti-inflammatory mediators dictates net effect of enteropathogenic Escherichia coli on intestinal epithelial cells. Am J Physiol Gastrointest Liver Physiol *290*, G685-694.

Sharma, R., Young, C., and Neu, J. (2010). Molecular modulation of intestinal epithelial barrier: contribution of microbiota. J Biomed Biotechnol *2010*, 305879.

Shaw, R.K., Cleary, J., Murphy, M.S., Frankel, G., and Knutton, S. (2005). Interaction of enteropathogenic Escherichia coli with human intestinal mucosa: role of effector proteins in brush border remodeling and formation of attaching and effacing lesions. Infect Immun *73*, 1243-1251.

Shifrin, D.A., Jr., McConnell, R.E., Nambiar, R., Higginbotham, J.N., Coffey, R.J., and Tyska, M.J. (2012). Enterocyte microvillus-derived vesicles detoxify bacterial products and regulate epithelial-microbial interactions. Curr Biol *22*, 627-631.

Shifrin, D.A., Jr., and Tyska, M.J. (2012). Ready...aim...fire into the lumen: a new role for enterocyte microvilli in gut host defense. Gut Microbes *3*, 460-462.

Simopoulos, T.T., and Jencks, W.P. (1994). Alkaline phosphatase is an almost perfect enzyme. Biochemistry *33*, 10375-10380.

Skog, J., Wurdinger, T., van Rijn, S., Meijer, D.H., Gainche, L., Sena-Esteves, M., Curry, W.T., Jr., Carter, B.S., Krichevsky, A.M., and Breakefield, X.O. (2008). Glioblastoma microvesicles transport RNA and proteins that promote tumour growth and provide diagnostic biomarkers. Nat Cell Biol *10*, 1470-1476.

Soleti, R., and Martinez, M.C. (2012). Sonic Hedgehog on microparticles and neovascularization. Vitam Horm *88*, 395-438.

Sommer, F., and Backhed, F. (2013). The gut microbiota - masters of host development and physiology. Nat Rev Microbiol *11*, 227-238.

Stevens, J.M., Galyov, E.E., and Stevens, M.P. (2006). Actin-dependent movement of bacterial pathogens. Nat Rev Microbiol *4*, 91-101.

Tamai, K., Tanaka, N., Nakano, T., Kakazu, E., Kondo, Y., Inoue, J., Shiina, M., Fukushima, K., Hoshino, T., Sano, K., Ueno, Y., Shimosegawa, T., and Sugamura, K. (2010). Exosome secretion of dendritic cells is regulated by Hrs, an ESCRT-0 protein. Biochem Biophys Res Commun *399*, 384-390.

Tapping, R.I., Akashi, S., Miyake, K., Godowski, P.J., and Tobias, P.S. (2000). Toll-like receptor 4, but not toll-like receptor 2, is a signaling receptor for Escherichia and Salmonella lipopolysaccharides. J Immunol *165*, 5780-5787.

Thery, C., Boussac, M., Veron, P., Ricciardi-Castagnoli, P., Raposo, G., Garin, J., and Amigorena, S. (2001). Proteomic analysis of dendritic cell-derived exosomes: a secreted subcellular compartment distinct from apoptotic vesicles. J Immunol *166*, 7309-7318.

Thery, C., Ostrowski, M., and Segura, E. (2009). Membrane vesicles as conveyors of immune responses. Nat Rev Immunol *9*, 581-593.

Thery, C., Zitvogel, L., and Amigorena, S. (2002). Exosomes: composition, biogenesis and function. Nat Rev Immunol *2*, 569-579.

Thomas, L.M., and Salter, R.D. (2010). Activation of macrophages by P2X7-induced microvesicles from myeloid cells is mediated by phospholipids and is partially dependent on TLR4. J Immunol *185*, 3740-3749.

Tisoncik, J.R., Korth, M.J., Simmons, C.P., Farrar, J., Martin, T.R., and Katze, M.G. (2012). Into the eye of the cytokine storm. Microbiol Mol Biol Rev *76*, 16-32.

Trajkovic, K., Hsu, C., Chiantia, S., Rajendran, L., Wenzel, D., Wieland, F., Schwille, P., Brugger, B., and Simons, M. (2008). Ceramide triggers budding of exosome vesicles into multivesicular endosomes. Science *319*, 1244-1247.

Tuin, A., Poelstra, K., de Jager-Krikken, A., Bok, L., Raaben, W., Velders, M.P., and Dijkstra, G. (2009). Role of alkaline phosphatase in colitis in man and rats. Gut *58*, 379-387.

Turnbaugh, P.J., Hamady, M., Yatsunenko, T., Cantarel, B.L., Duncan, A., Ley, R.E., Sogin, M.L., Jones, W.J., Roe, B.A., Affourtit, J.P., Egholm, M., Henrissat, B., Heath, A.C., Knight, R., and Gordon, J.I. (2009). A core gut microbiome in obese and lean twins. Nature *457*, 480-484.

Turola, E., Furlan, R., Bianco, F., Matteoli, M., and Verderio, C. (2012). Microglial microvesicle secretion and intercellular signaling. Front Physiol *3*, 149.

Tyska, M.J., Mackey, A.T., Huang, J.D., Copeland, N.G., Jenkins, N.A., and Mooseker, M.S. (2005). Myosin-1a is critical for normal brush border structure and composition. Mol Biol Cell *16*, 2443-2457.

Tyska, M.J., and Mooseker, M.S. (2002). MYO1A (brush border myosin I) dynamics in the brush border of LLC-PK1-CL4 cells. Biophys J *82*, 1869-1883.

Tyska, M.J., and Mooseker, M.S. (2004). A role for myosin-1A in the localization of a brush border disaccharidase. J Cell Biol *165*, 395-405.

Valadi, H., Ekstrom, K., Bossios, A., Sjostrand, M., Lee, J.J., and Lotvall, J.O. (2007). Exosome-mediated transfer of mRNAs and microRNAs is a novel mechanism of genetic exchange between cells. Nat Cell Biol *9*, 654-659.

Vallance, B.A., and Finlay, B.B. (2000). Exploitation of host cells by enteropathogenic Escherichia coli. Proc Natl Acad Sci U S A *97*, 8799-8806.

van den Brink, G.R. (2007). Hedgehog signaling in development and homeostasis of the gastrointestinal tract. Physiol Rev *87*, 1343-1375.

van der Pol, E., Boing, A.N., Harrison, P., Sturk, A., and Nieuwland, R. (2012). Classification, functions, and clinical relevance of extracellular vesicles. Pharmacol Rev *64*, 676-705.

van Niel, G., Porto-Carreiro, I., Simoes, S., and Raposo, G. (2006). Exosomes: a common pathway for a specialized function. J Biochem *140*, 13-21.

van Veen, S.Q., van Vliet, A.K., Wulferink, M., Brands, R., Boermeester, M.A., and van Gulik, T.M. (2005). Bovine intestinal alkaline phosphatase attenuates the inflammatory response in secondary peritonitis in mice. Infect Immun *73*, 4309-4314.

Vanlandingham, P.A., and Ceresa, B.P. (2009). Rab7 regulates late endocytic trafficking downstream of multivesicular body biogenesis and cargo sequestration. J Biol Chem *284*, 12110-12124.

Veigel, C., Coluccio, L.M., Jontes, J.D., Sparrow, J.C., Milligan, R.A., and Molloy, J.E. (1999). The motor protein myosin-I produces its working stroke in two steps. Nature *398*, 530-533.

Verderio, C., Muzio, L., Turola, E., Bergami, A., Novellino, L., Ruffini, F., Riganti, L., Corradini, I., Francolini, M., Garzetti, L., Maiorino, C., Servida, F., Vercelli, A., Rocca, M., Dalla Libera, D., Martinelli, V., Comi, G., Martino, G., Matteoli, M., and Furlan, R. (2012). Myeloid microvesicles are a marker and therapeutic target for neuroinflammation. Ann Neurol *72*, 610-624.

Viswanathan, V.K., Hodges, K., and Hecht, G. (2009). Enteric infection meets intestinal function: how bacterial pathogens cause diarrhoea. Nat Rev Microbiol *7*, 110-119.

Von Bartheld, C.S., and Altick, A.L. (2011). Multivesicular bodies in neurons: distribution, protein content, and trafficking functions. Prog Neurobiol *93*, 313-340.

Waldenstrom, A., Genneback, N., Hellman, U., and Ronquist, G. (2012). Cardiomyocyte microvesicles contain DNA/RNA and convey biological messages to target cells. PLoS One *7*, e34653.

Wang, Q., Garrity, G.M., Tiedje, J.M., and Cole, J.R. (2007). Naive Bayesian classifier for rapid assignment of rRNA sequences into the new bacterial taxonomy. Appl Environ Microbiol *73*, 5261-5267.

Weflen, A.W., Alto, N.M., and Hecht, G.A. (2009). Tight junctions and enteropathogenic E. coli. Ann N Y Acad Sci *1165*, 169-174.

Wen, L., Ley, R.E., Volchkov, P.Y., Stranges, P.B., Avanesyan, L., Stonebraker, A.C., Hu, C., Wong, F.S., Szot, G.L., Bluestone, J.A., Gordon, J.I., and Chervonsky, A.V. (2008). Innate immunity and intestinal microbiota in the development of Type 1 diabetes. Nature *455*, 1109-1113.

Wexler, H.M. (2007). Bacteroides: the good, the bad, and the nitty-gritty. Clin Microbiol Rev *20*, 593-621.

Wlodarska, M., Willing, B., Keeney, K.M., Menendez, A., Bergstrom, K.S., Gill, N., Russell, S.L., Vallance, B.A., and Finlay, B.B. (2011). Antibiotic treatment alters the colonic mucus layer and predisposes the host to exacerbated Citrobacter rodentium-induced colitis. Infect Immun *79*, 1536-1545.

Wolfers, J., Lozier, A., Raposo, G., Regnault, A., Thery, C., Masurier, C., Flament, C., Pouzieux, S., Faure, F., Tursz, T., Angevin, E., Amigorena, S., and Zitvogel, L. (2001). Tumor-derived exosomes are a source of shared tumor rejection antigens for CTL cross-priming. Nat Med *7*, 297-303.

Wong, A.R., Pearson, J.S., Bright, M.D., Munera, D., Robinson, K.S., Lee, S.F., Frankel, G., and Hartland, E.L. (2011). Enteropathogenic and enterohaemorrhagic Escherichia coli: even more subversive elements. Mol Microbiol *80*, 1420-1438.

Woodruff, S.A., Masterson, J.C., Fillon, S., Robinson, Z.D., and Furuta, G.T. (2011). Role of eosinophils in inflammatory bowel and gastrointestinal diseases. J Pediatr Gastroenterol Nutr *52*, 650-661.

Wullaert, A., Bonnet, M.C., and Pasparakis, M. (2011). NF-kappaB in the regulation of epithelial homeostasis and inflammation. Cell Res *21*, 146-158.

Yuhan, R., Koutsouris, A., Savkovic, S.D., and Hecht, G. (1997). Enteropathogenic Escherichia coli-induced myosin light chain phosphorylation alters intestinal epithelial permeability. Gastroenterology *113*, 1873-1882.

Zahavi, E.E., Lieberman, J.A., Donnenberg, M.S., Nitzan, M., Baruch, K., Rosenshine, I., Turner, J.R., Melamed-Book, N., Feinstein, N., Zlotkin-Rivkin, E., and Aroeti, B. (2011). Bundle-forming pilus retraction enhances enteropathogenic Escherichia coli infectivity. Mol Biol Cell *22*, 2436-2447.

Zobiack, N., Rescher, U., Laarmann, S., Michgehl, S., Schmidt, M.A., and Gerke, V. (2002). Cell-surface attachment of pedestal-forming enteropathogenic E. coli induces a clustering of raft components and a recruitment of annexin 2. J Cell Sci *115*, 91-98.

Zwaenepoel, I., Naba, A., Da Cunha, M.M., Del Maestro, L., Formstecher, E., Louvard, D., and Arpin, M. (2012). Ezrin regulates microvillus morphogenesis by promoting distinct activities of Eps8 proteins. Mol Biol Cell *23*, 1080-1094.

Zwicker, J.I., Trenor, C.C., 3rd, Furie, B.C., and Furie, B. (2011). Tissue factor-bearing microparticles and thrombus formation. Arterioscler Thromb Vasc Biol *31*, 728-733.